Unsteady Natural Convection in Open Ended Vertical Concentric Annuli

by

Muhsen Ali Al-Attas

A Thesis Presented to the

FACULTY OF THE COLLEGE OF GRADUATE STUDIES

KING FAHD UNIVERSITY OF PETROLEUM & MINERALS

DHAHRAN, SAUDI ARABIA

In Partial Fulfillment of the
Requirements for the Degree of

MASTER OF SCIENCE

In

MECHANICAL ENGINEERING

January, 1992

Order Number 1354080

Unsteady natural convection in open ended vertical concentric annuli

Al-Attas, Muhsen Ali, M.S.

King Fahd University of Petroleum and Minerals (Saudi Arabia), 1992

U·M·I
300 N. Zeeb Rd.
Ann Arbor, MI 48106

UNSTEADY NATURAL CONVECTION IN OPEN ENDED VERTICAL CONCENTRIC ANNULI

BY

MUHSEN ALI AL-ATTAS

A Thesis Presented to the

FACULTY OF THE COLLEGE OF GRADUATE STUDIES

KING FAHD UNIVERSITY OF PETROLEUM & MINERALS

DHAHRAN, SAUDI ARABIA

In Partial Fulfillment of the
Requirements for the Degree of

MASTER OF SCIENCE

In

MECHANICAL ENGINEERING

January, 1992

KING FAHD UNIVERSITY OF PETROLEUM & MINERALS

DHAHRAN, SAUDI ARABIA

This thesis, written by **MUHSEN ALI AL-ATTAS** *under the direction of his thesis committee, and approved by all the members, has been presented to and accepted by the Dean, College of Graduate Studies, in partial fulfillment of the requirements for the degree of*

MASTER OF SCIENCE IN MECHANICAL ENGINEERING

Thesis Committee

Jan. 15, 1992
Chairman (Dr. M.A.I. El-Shaarawi)

15/1/92
Member (Dr.-Ing. W.H. Stahl)

15/1/92
Member (Dr. A.Z.Sahin)

15/2/92
Dr. M.O. Budair
Department Chairman

Dr. Ala H. Rabeh
Dean College of Graduate Studies

Date : 15.2.92

بِسْمِ اللَّهِ الرَّحْمَٰنِ الرَّحِيمِ

In the name of God, Most Gracious, Most Merciful

TO MY PARENTS

ACKNOWLEDGEMENT

Acknowledgement is due to King Fahad University of Petroleum and Minerals for the support provided to carry out this research.

I wish to express my deep thanks and appreciation to my thesis advisor Professor Maged A.I. El-Shaarawi for his supervision and continuous encouragement throughout this research.He was generous in time and thought.He gave many weekends and evenings in revising the draft of this thesis. I also extend thanks to other members of my Thesis Committee Dr. W.H. Stahl and Dr. Ahmet Z. Sahin .

Thanks are also due to Dr.Mohammed O. Budair,Chairman of Mechanical Engineering Department,for his cooperation and support in using the research facilities .

Finally,other faculty and staff of Mechanical Engineering Department also deserve appreciation for their encouragement throughout the period which I spent among them.

CONTENTS

Page

THESIS ABSTRACT

NAME OF STUDENT : **MUHSEN ALI AL-ATTAS**

TITLE OF STUDY : **Unsteady Natural Convection in Open Ended Vertical Concentric Annuli**

MAJOR FIELD : **Mechanical ENGINEERING**

DATE OF DEGREE : **JANUARY, 1992**

The problem of transient laminar free convection in the developing region of a vertical concentric annulus is investigated using an iterative implicit finite difference scheme.The following two cases are considered :

Case (I) : In which a step-temperature change occurs at the inner wall while the outer wall is kept adiabatic.

Case (O) : In which a step-temperature change occurs at the outer wall while the inner wall is kept adiabatic.

The investigation is based on the boundary layer theory. The range of Grashaf number considered is $4 \leq Gr^{*} \leq 100{,}000$ while the Prandtl number (Pr) is held constant at a value of 0.7 .

Results are presented for the variation of the temperature and velocity profiles with time and location. Furthermore, variations of the total heat absorbed by the fluid ,the pressure distribution and the fluid flow rate with time are presented.

The adequacy of the present solution is checked by comparing the time variation of the fluid flow rate with the available results for the vertical parallel plate channel as a limiting case. Moreover, the obtained results at large values of time are compared with the available steady state results. Finally, the fully developed results are compared with the available analytical solutions for the same geometry.

MASTER OF SCIENCE

KING FAHD UNIVERSITY OF PETROLEUM & MINERALS

Dhahran, Saudi Arabia

ملخص الرسالة

إســـم الطـالـــب : محسن علي العطاس
عنوان الرســالـــة : الحمل الحراري الحر الغير مستقر في منطقة التطور بين إسطوانتين مركزيتين رأسيتين .
التـخـــصـص : الهندسه الميكانيكية .

لقد تمت دراسة الحمل الحراري الحر الغير مستقر في منطقة التطور بين إسطوانتين مركزيتين رأسيتين باستخدام طريقة الفروق المحدودة العددية وذلك للحالتين الآتيتين : ـ
الحالة الأولى : ويتم فيها رفع درجة حرارة الجدار الداخلي فجأة إلى قيمة ثابتة بينما يكون الجدار الخارجي معزولا حرارياً .
الحالة الثانية : ويتم فيها رفع درجة حرارة الجدار الخارجي فجأة إلى قيمة ثابتة بينما يكون الجدار الداخلي معزولا حرارياً .
وتعتمد هذه الدراسة على قوانين حفظ المادة ، وكمية الحركة ، والطاقة بعد تبسيطها باستخدام نظرية الطبقة المتاخمة وافتراض ثبات جميع خصائص المائع الفيزيائية وعدم إعتمادها على درجة الحرارة ماعدا الكثافة ، ويتراوح رقم جراشوف في هذه الدراسة ما بين ٤ ، ٠٠٠ر١٠٠ أما رقم براندتل فإنه ثابت ويساوي ٧ر٠ .

وتوضح النتائج تفاصيل تغير درجات الحرارة ومركبات السرعة مع كل من الزمن والمسافة التي يقطعها المائع من المدخل كما تعطي النتائج أيضا تغير كمية الحرارة المنتقلة الى المائع مع الزمن وتطور كمية المائع المنساب إلى داخل الحيز الحلقي مع الزمن . ولإثبات دقة النتائج فقد تم مقارنه تغير كمية المائع الداخل مع الزمن مع النتائج الخاصة بمثل هذه الدراسة ولكن لشكل صفيحتين متقابلتين رأسيتين وذلك لكونها حالة خاصة من الحالة قيد البحث . كما تم أيضا مقارنة النتائج التي تم الحصول عليها بعد فترة زمنية طويلة من بدء التغير مع تلك المناظرة لها في حالة الإنسياب المستقر (الغير متغير من الزمن) وتم أيضا مقارنة النتائج الخاصة بالجزء المتطور تماماً من الحيز الحلقي بتلك المناظرة لها .

درجة الماجستير في العلوم
جامعة الملك فهد للبترول والمعادن
الظهران ـ المملكه العربية السعودية
يناير ١٩٩٢ م

LIST OF FIGURES

LIST OF TABLES

NOMENCLATURE

a	local heat transfer coefficient based on the area of the heat transfer surface, $q/(T_w - T_o)$
$\bar{a}$	average heat transfer coefficient over the annulus height, $\bar{h}/\pi D_w l(T_w - T_o) = \int_o^l a\,dz/l$
b	annular gap width, $(r_2 - r_1)$
c_p	specific heat of fluid at constant pressure
D	equivalent (hydraulic) diameter of annulus, $2b$
D_w	diameter of heat transfer boundary, $2r_1$ in case(I) or $2r_2$ in case(O)
f	volumetric flow rate, $\int_{r_1}^{r_2} 2\pi r u\,dr = \pi(r_2^2 - r_1^2)u_o$
f_{ss}	steady state value of f
F	dimensionless volumetric flow rate, $f/(\pi l \nu Gr^*) = (1-N^2)U_o$
F_{ss}	steady-state value of F , $(1-N^2)U_{oss}$
F_{fd}	steady-state fully developed value of F
g	gravitational body force per unit mass (acceleration)
Gr	Grashof number, $g\beta(T_w - T_o)D^3/\nu^2$
Gr^*	modified Grashof number, $Gr\ D/l$
h	heat gained by fluid from the entrance up to a particular elevation in the annulus, $\rho_o f C_p(T_m - T_o)$
$\bar{h}$	heat gained by fluid from the entrance up to the annulus

	exit,i.e. value of h at z = l, $\rho f c_p(\overline{T}_m - T_o)$
H	dimensionless heat absorbed from the entrance up to any particular elevation , $h/[\pi\rho_o C_p l\gamma Gr^*(T_w - T_o)] = F\,\theta_m = 2\int_N^1 UR\theta dR$
$\overline{H}$	dimensionless heat absorbed from the entrance up to the annulus exit; i.e. value of H at Z = L, $\overline{h}/[\pi\rho_o C_p l\gamma Gr^*(T_w - T_o)] = F\,\overline{\theta_m} = 2\int_N^1 UR\bar{\theta} dR$
H_{fd}	steady state fully-developed value of $\overline{H}$
K	number of time increments needed to reach steady state conditions
l	height of annulus
L	dimensionless height of annulus, l/Gr^*
m	number of axial steps in the numerical grid
n	number of radial steps in the numerical grid
N	annulus radius ratio, r_1/r_2
Nu	local Nusselt number, aD/κ
$\overline{NU}$	average Nusselt number based on the area of the heat transfer surface over the whole annulus height, $\bar{a}D/\kappa$
p	pressure of the fluid inside the channel at any cross station
p′	pressure defect at any point, $p-p_s$
p_o	pressure of fluid at the annulus entrance, $-\rho_o u_o^2/2$
p_s	hydrostatic pressure, $-\rho_o gz$
P	dimensionless pressure defect at any point $p' r_2^4/\rho_o l^2\gamma^2 Gr^{*2}$

P_o	dimensionless pressure defect at annulus entrance, $p_o r_2^4/\rho_o l^2 \gamma^2 Gr^{*2} = -U_o^2/2$
Pr	Prandtl number, $\mu C_p/\kappa = \gamma/\alpha$
q	heat flux at the heat transfer surface, $q = \pm\kappa(\partial T/\partial r)_w$ where the minus and plus signs are for case(I) and case(O),respectively
r	radial coordinate
r_1	inner radius of annulus
r_2	outer radius of annulus
R	dimensionless radial coordinate, r/r_2
Ra	Rayleigh number, Gr Pr
Ra^*	modified Rayleigh number, $Gr^* pr$
t	dimensionless time , $\tau v/r_2^2$
t_{ss}	dimensionless steady state time, $\tau_{ss} v/r_2^2$
T	fluid temperature at any point
T_{ad}	adiabatic wall temperature
T_m	mixing cup temperature over any cross-section, $\int_{r_1}^{r_2} rut\ dr / \int_{r_1}^{r_2} ru\ dr$
$\overline{T}_m$	mixing cup temperature at exit cross-section,i.e. value of T_m at Z = L
T_o	fluid temperature at annulus entrance
T_w	temperature of heat transfer boundary
u	axial velocity component at any point
u_{ss}	steady state (independent of time) value of the axial velocity component at any point

u_o	entrance axial velocity , $\int_{r_1}^{r_2} 2\pi r u dr / [\pi(r_2^2 - r_1^2)]$
u_{oss}	steady-state (independent of time) value of the entrance axial velocity
U	dimensionless axial velocity component at any point, $ur_2^2/l\gamma Gr^*$
U_o	dimensionless axial velocity at annulus entrance $u_o r_2^2/l\gamma Gr^*$
U_{ofd}	steady-state fully-developed value of U_o
U_{oss}	steady-state value of U_o, $u_{oss} r_2^2/l\gamma Gr^*$
v	radial velocity component at any point
V	dimensionless radial velocity component vr_2/γ
w	tangential velocity component
z	axial coordinate
Z	dimensionless axial coordinate z/lGr^*

Greek Symbols:

α	fluid thermal diffusivity, $\kappa/\rho_o C_p$
β	volumetric coefficient of thermal expansion
Δ	difference
θ	dimensionless temperature at any point, $(T - T_o)/(T_w - T_o)$
θ_{ad}	dimensionless adiabatic wall temperature
θ_{fd}	steady-state fully developed value of θ.
θ_m	dimensionless mixing cup temperature at any cross section, $(T_m - T_o)/(T_w - T_o)$

$\bar{\theta}_m$	dimensionless mixing cup temperature at exit cross section,i.e. value of θ_m at $Z = L$
θ_{ss}	steady-state value of θ
μ	dynamic fluid viscosity
ν	kinematic fluid viscosity, μ/ρ_o
κ	thermal conductivity of fluid
ρ	fluid density at temperature T,$\rho_o[1-\beta(T-T_o)]$
ρ_o	fluid density at inlet fluid temperature T_o
τ	time
τ_{ss}	steady-state time

CHAPTER ONE

INTRODUCTION

In many practical engineering applications , transient convection heat transfer is of great importance in the design of control systems for modern convection heat exchange devices. Despite the practical importance of the unsteady natural convection heat transfer encountered in many engineering systems, which can be modeled as vertical channel or vertical open-ended annulus , it has not received as much attention as it's steady state counterpart.

Considerable interest has been shown recently in the problem of natural convection heat transfer to fluids in heated, vertical, open-ended annuli. Such systems are of practical importance in the field of double pipe heat exchangers. A typical application is that of gas cooled nuclear reactors, in which cylindrical fissionable fuel elements are placed axially in vertical coolant channels within the graphite moderator; the cooling gas is flowing along the channels parallel to the fuel elements. In such a system laminar free convection may provide the sole means of the necessary cooling during the shut-down or accident periods.

Practical importance of this problem and the lack of either experimental or theoretical data concerning transient laminar natural convection in open-ended

vertical concentric annuli motivated the present work. In the present work an implicit finite-difference scheme has been developed to study the transient natural convection flow inside a vertical concentric annulus. The following two initial conditions are investigated .

Case (I) : In which a step-temperature change occurs at the inner wall while the outer wall is kept adiabatic.

Case (O) : In which a step-temperature change occurs at the outer wall while the inner wall is kept adiabatic.

The literature review is presented in Chapter Two while the problem formulation and the initial and boundary conditions are presented in Chapter Three. In Chapter Four, the numerical methodology of solution is given in detail. The results are given and discussed in Chapter Five. Finally, conclusions are reported in Chapter Six.

CHAPTER TWO

LITERATURE REVIEW

The unsteady laminar free convection in the vicinity of a vertical flat plate, which is subjected to a step change in wall temperature or wall heat flux, has been investigated by many research workers [1-11]. Siegel [1] studied the problem of unsteady laminar free convection for a semi-infinite plate. Sparrow and Gregg [2] investigated the nearly quasi-steady free convection heat transfer in gases from a flat plate with time dependent surface temperature. They assumed quasi-steady conditions which mean that at each and every instant, an instantaneous steady state exists and, as a consequence, the steady heat-transfer relationships may be applied instantaneously.

In addition to the vertical plate geometry,Chung and Anderson [3] analyzed the unsteady laminar free convection boundary layer from a horizontal circular geometry. Using an integral method of analysis ,Gebhart [4] analyzed the transient natural convection from a vertical plate. Hellums and Churchill [5] demonstrated that the partial differential equations describing natural convection can be solved by finite difference methods. Using such methods , they [6] studied transient natural convection from an isothermal vertical plate

and inside a horizontal cylinder. They found that the computed values for temperatures and local heat transfer coefficients for short times agree very well with the analytical solution for conduction heat transfer which is the dominant mode at this stage. Moreover, the limiting values for long time agree well with those of steady state.

Schetz and Eichhorn [7], using Laplace transforms, studied the case of unsteady natural convection in the vicinity of a doubly infinite vertical plate whose temperature or heat flux is an arbitrary function of time. Exact asymptotic solutions for unsteady laminar free convection from a vertical plate whose surface temperature or heat flux varies arbitrarily with time were presented by Menold and Yang [8], for various values of Prantdl number. Gebhart and Adams [9] compared their experimental measurements of transient natural convection in air and water with the results of the integral analysis presented by Gebhart [4]. Analytical and experimental investigations related to transient free convection heat transfer on vertical surfaces and in vertical cylinders have been reviewed by Ede [10]. Nanbu [11] gave the limit of pure conduction for unsteady free convection from a vertical plate. He found the critical time afterwhich leading-effect begins and convection heat transfer mode dominates .

Nanda and Sharma [12] and Yang et al. [13] investigated the same case but with oscillatory surface temperature. Yang et al. [13] used an explicit finite difference method to study the effect of the amplitude and the frequency of

oscillation on the instantaneous and the time average Nusselt number, temperature and velocity profiles. They found that the timewise variation of the fluid temperature in the inner region adjacent to the surface produces back heat flow at high amplitude, high frequency, and at high local Grashof number.

Kawase and Ulbrecht [14] proposed a model for laminar natural convection from an isothermal vertical plate to a power-law fluid.They avoid the difficulty caused by the fact that the momentum and energy equations are coupled by introducing an approximation based on the partial similarity between the velocity fields for forced and natural convection. Recently,Haq et al. [15] investigated the case of transient free convection of a non-Newtonian fluid along a vertical flat plate.

Natural convection in vertical channels formed by two parallel plates has been investigated by many authors [16-23]. Steady-state developing and fully developed flow solutions for natural convection in a channel formed by two isothermal vertical parallel plates were presented by Bodoia and Osterle [16]. Kettleborough [17] considered the transient laminar free convection between heated vertical plates with constant wall temperature including entrance effects. He used both alternating direction implicit and the simple explicit finite difference methods. He assumed that Boussinesq approximation is valid and that all thermodynamic properties,except the density , are independent of temperature . Furthermore, the compressibility as well as dissipation effects

were neglected. He found that as Grashof number increases the time taken to reach steady state conditions decreases and the value of Nusselt number increases.

Lee et al. [18] studied the natural convection in a vertical channel with opposing buoyancy forces experimentally and theoretically via finite difference solution of the time dependent boundary layer equations. The measured profiles of temperature and concentrations showed close agreement with the theoretical predictions. Sparrow et al. [19] studied the steady case with one wall maintained at a uniform temperature and the other unheated. They studied the case experimentally and numerically via a parabolic finite difference scheme. The Nusselt numbers computed were in good agreement with those of the experiment. Burch et al. [20] studied the laminar natural convection between finitely conducting vertical plates.They found that conduction has significant influence on the natural convection heat transfer , particularly at high Grashof numbers.

Azevedo and Sparrow [21] carried out heat transfer and flow visualization experiments in water to investigate the effect of inclination on natural convection in a parallel walled channel. Nusselt number correlations were found for the following three heating modes: both walls heated and maintained at the same uniform temperature, heating only from above, and heating only from below.

Johsi [22] studied the same case but with different boundary conditions, namely: uniform but different wall temperatures (UWT) and uniform but different wall heat fluxes (UHF) . He used a finite difference method to develop simple correlations to predict the minimum heat transfer for UWT and the maximum plate temperature for UHF, during the transient period. It is found that for the UWT case the ratio of the minimum heat transfer to the steady state heat transfer decreases with length of the channel.For the UHF case, the maximum transient temperature has a maximum of about 9% over the steady state temperature. Chang and Lin [23] studied the transient buoyancy induced flow through a heated, vertical channel of finite height numerically. Both the inlet and exit effects are included in the analysis. They found ,at early time stages, a temperature overshoot which is caused by the fact that conduction dominates at such early stages,and hence the local Nusselt number decreases. Correlation equations are proposed for the average Nusselt number and the amount of air drawn into the channel at steady state.

Of particular interest to the present investigation is the case of natural convection flow inside vertical concentric annuli. A survey of the literature shows that transient natural convection in an open-ended vertical annulus has not been investigated analytically or experimentally.Only steady state natural convection has been considered in the literature [24-30]

El-Shaarawi and Sarhan [24-25] and Sarhan [26] studied numerically the developing laminar free convection in a heated vertical open ended concentric

annulus. They considered the case of one wall being isothermal while the other is adiabatic. Keyhani et al. [27] studied experimentally free convection in a vertical annulus with constant heat flux on the inner wall while the outer cylinder is at constant temperature. Overall data are corrected for thermal radiation in the annulus. The results of the study provide data relevant to the design and performance assessment of spent fuel packages as part of a waste terminal storage program for nuclear waste isolation. This model can serve to form a limiting case correlation for heat transfer from a nuclear fuel rod bundle to the interior of its container in either storage or disposal. Littlefield and Desai [28] examined the natural steady convection motion in a vertical cylindrical annulus of large aspect ratio analytically. Constant heat flux at the inner wall was considered, while the outer wall was either isothermal or at constant heat flux .

Al-Arabi et al. [29] used an implicit finite difference method to study the natural convection flow through vertical annuli with one wall uniformly heated and the other wall being adiabatic. They also, studied the case experimentally and found good agreement between the theoretical and experimental values. Three radius ratios (0.26,0.5 and 0.9) were investigated. El-Shaarawi and Al-Nimr [30] presented analytical solutions for the fully developed natural convection in open-ended vertical concentric annuli . Four fundamental boundary conditions have been investigated. These boundary conditions are obtained by combining each of the two conditions of having one boundary

maintained at uniform heat flux or at uniform wall temperature with each of the conditions that the opposite boundary is kept isothermal at the inlet fluid temperature or adiabatic. Expressions for flow and heat transfer parameters are given for each case.

To the best of the writer's knowledge, transient natural convection heat transfer in open ended vertical concentric annuli has not been investigated yet.

CHAPTER THREE

PROBLEM FORMULATION

In this chapter, the governing equations which describe the case under consideration are given and the boundary conditions are stated. Since the governing equations are elliptic, nonlinear and strongly coupled partial differential equations, the following assumptions are imposed to facilitate the solution of the problem under consideration. Firstly, some assumptions related to the fluid and the flow are imposed on Navier-Stokes and the energy equations . Secondly, the boundary layer approximations will be used to neglect the second derivative of the axial velocity component in the streamwise direction, the streamwise diffusion of heat , and the entire momentum equation in the transverse direction. This is done by an order of magnitude analysis . Finally, the boundary layer equations are normalized, using nondimensional parameters, to have the least possible number of computer runs and the most general numerical results.

3.1 GOVERNING EQUATIONS

Figure 1 depicts the geometry and coordinate system. The geometry considered in this study is a vertical annulus of finite length,open at both ends

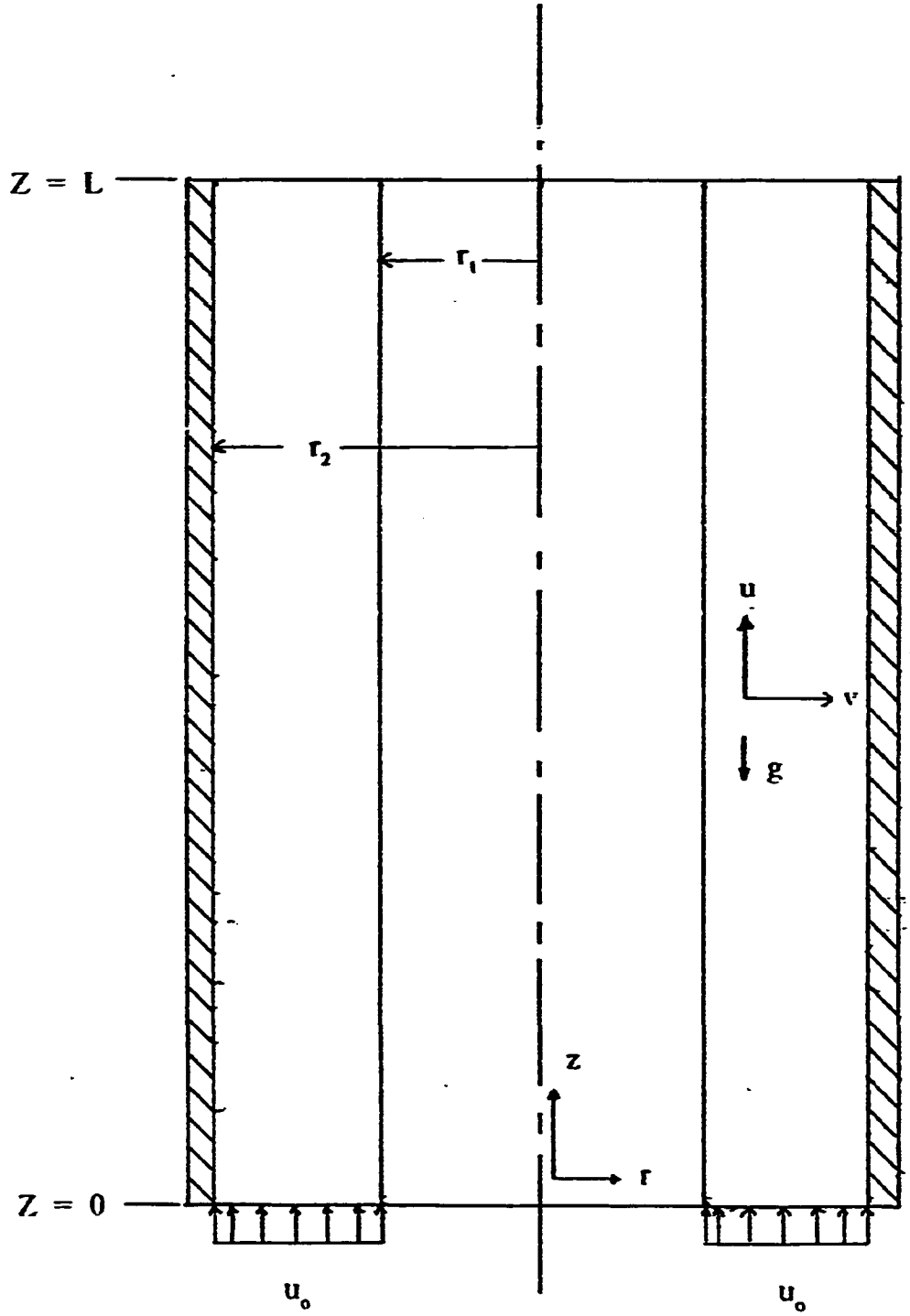

FIG. 1 Schematic diagram of the annulus

and immersed in a fluid of infinite extent maintained at a constant temperature T_o. After the step rise in the temperature of either wall, fluid rises in the annular gab between the cylindrical walls by natural convection .It is assumed that the time dependent entrance velocity has a uniform profile. The following assumptions, related to the geometry, physical properties of the fluid, and flow conditions, are imposed.

1. Fluid is Newtonian.

2. The flow is axisymetric ($\frac{\partial}{\partial \varphi} = 0$).

3. The tangential (azimuthal,in φ -direction) velocity component is zero everywhere ($w = 0$) .

4. There are no internal heat generation and no radiation heat flux .

5. Viscous dissipation and radial and tangential body forces are neglected.

6. The fluid physical properties (C_p , ρ , μ and κ) are constants but Boussinesq approximation is valid according to which the density varies in only the buoyancy term in the momentum equation.

Applying the above assumptions give the following governing equations.

Continuity

$$\frac{1}{r}\frac{\partial}{\partial r}(rv)+\frac{\partial u}{\partial z}=0 \qquad (1)$$

Momentum (radial)

$$\rho_o\left[\frac{\partial v}{\partial \tau}+v\frac{\partial v}{\partial r}+u\frac{\partial v}{\partial z}\right]=-\frac{\partial p}{\partial r}+\mu\left[\frac{\partial}{\partial r}\left(\frac{1}{r}\frac{\partial}{\partial r}(rv)\right)+\frac{\partial^2 v}{\partial z^2}\right] \qquad (2)$$

Momentum (axial)

$$\rho_o\left[\frac{\partial u}{\partial \tau}+v\frac{\partial u}{\partial r}+u\frac{\partial u}{\partial z}\right]=F_z-\frac{\partial p}{\partial z}+\mu\left[\frac{1}{r}\frac{\partial}{\partial r}\left(r\frac{\partial u}{\partial r}\right)+\frac{\partial^2 u}{\partial z^2}\right] \qquad (3)$$

Energy

$$\frac{\partial T}{\partial \tau}+v\frac{\partial T}{\partial r}+u\frac{\partial T}{\partial z}=\alpha\left[\frac{1}{r}\frac{\partial}{\partial r}\left(r\frac{\partial T}{\partial r}\right)+\frac{\partial^2 T}{\partial z^2}\right] \qquad (4)$$

As the flow is natural and confined, the pressure p within the annulus, will be less than the hydrostatic ambient pressure, at the same elevation. The difference between the two pressures is known as the pressure defect (p'). Noting that $F_z=-\rho g$, $\rho=\rho_o\left[1-\beta(T-T_0)\right]$,and $p=p'+\rho_o gz$, the axial

momentum equation can be rewritten in terms of the coefficient of thermal expansion (β) and the pressure defect (p') as follows.

$$\frac{\partial u}{\partial t}+v\frac{\partial u}{\partial r}+u\frac{\partial u}{\partial z}=-\frac{1}{\rho_o}\frac{\partial p'}{\partial z}+g\beta(T-T_o)+\nu\left[\frac{1}{r}\frac{\partial}{\partial r}\left(r\frac{\partial u}{\partial r}\right)+\frac{\partial^2 u}{\partial z^2}\right] \qquad (5)$$

Boundary conditions:

The problem in hand is solved under the following conditions.

For $\tau=0$

$u = 0$, $v = 0$,and $T = T_o$ everywhere

For $\tau>0$

At $z=0$ and $r_1<r<r_2$

$u=u_o(t)$, $v = 0$,and $T=T_o$

At $z>0$ and $r=r_1$

$u = 0$, $v = 0$,and $T=T_w$ for case(I)

or $\frac{\partial T}{\partial r}=0$ for case(O)

At $z>0$ and $r=r_2$

$u = 0$, $v = 0$,and $\frac{\partial T}{\partial r}=0$ for case(I)

or $T=T_w$ for case(O)

3.2 BOUNDARY LAYER EQUATIONS

To obtain the boundary layer equations, equations (1),(2),(4),(5) are transformed to nondimensional forms, then an order of magnitude analysis is made .The procedure is presented in Appendix (I). The resulting boundary-layer equations are as follows .

Continuity

$$\frac{1}{r}\frac{\partial}{\partial r}(rv)+(\frac{\partial u}{\partial z})=0 \qquad (6)$$

Momentum (axial)

$$\frac{\partial u}{\partial \tau}+v\frac{\partial u}{\partial r}+u\frac{\partial u}{\partial z}=-\frac{1}{\rho_o}\frac{\partial p}{\partial z}+g\beta(T-T_\infty)+\frac{\nu}{r}\frac{\partial}{\partial r}(r\frac{\partial u}{\partial r}) \qquad (7)$$

Energy

$$\frac{\partial T}{\partial \tau}+v\frac{\partial T}{\partial r}+u\frac{\partial T}{\partial z}=\frac{\alpha}{r}\frac{\partial}{\partial r}(r\frac{\partial T}{\partial r}) \qquad (8)$$

3.3 DIMENSIONLESS BOUNDARY LAYER EQUATIONS

To reduce the computational effort and time required for the numerical solution of the above boundary layer equations, these equations (with their boundary conditions) should be put in nondimensional forms in a way that the least number of nondimensional numbers appear in the final forms. This makes

the solution as general as possible and prevent the need for computer runs corresponding to specific values of these numbers. The nondimensional forms of equations (6-8) which are presented in Appendix 1 are not good enough because they contain the Reynolds, Grashof and Prandtl numbers ; this will make a restriction on the solution (from each computer run) to be for only one value of each of these numbers . Therefore ,the following group of dimensionless parameters are used.

$$R=\frac{r}{r_2} \quad , \quad Z=\frac{z}{lGr^{\cdot}}$$

$$V=\frac{vr_2}{\nu} \quad , \quad U=\frac{ur_2^2}{l\nu Gr^{\cdot}}$$

$$P=\frac{p'r_2^4}{\rho_o l^2\nu^2(Gr^{\cdot})^2} \quad , \quad F=\frac{f}{\pi l\nu Gr^{\cdot}} \text{ , and}$$

$$\theta=\frac{T-T_o}{T_w-T_o}$$

Inserting these parameters in equations (6-8) and rearranging the terms give the following dimensionless forms of the boundary-layer equations .

Continuity

$$\frac{V}{R}+\frac{\partial V}{\partial R}+\frac{\partial U}{\partial Z}=0 \qquad (9)$$

Momentum (axial)

$$\frac{\partial U}{\partial t}+V\frac{\partial U}{\partial R}+U\frac{\partial U}{\partial Z}=-\frac{\partial P}{\partial Z}+\frac{\theta}{16(1-N)^4}+\frac{1}{R}\frac{\partial}{\partial R}(R\frac{\partial U}{\partial R}) \qquad (10)$$

Energy

$$\frac{\partial \theta}{\partial t}+V\frac{\partial \theta}{\partial R}+U\frac{\partial \theta}{\partial Z}=\frac{1}{Pr}\frac{1}{R}\frac{\partial}{\partial R}(R\frac{\partial \theta}{\partial R}) \qquad (11)$$

Since the momentum equation in r-direction has been eliminated due to the boundary layer simplifications another equation is needed to obtain the four unknowns V,U,P and θ.

The volumetric flow rate can be written in terms of u_o (which is a function of time in the present case) as:

$$f=\int_{r_1}^{r_2} 2\pi r.dr.u=\pi(r_2^2-r_1^2)u_o .$$

When the dimensionless variables are substituted into this equation , the dimensionless volumetric flow rate becomes:

$$F=\frac{f}{\pi l Gr^{*}\nu}=2\int_{N}^{1} R.U.dR=(1-N^2)U_o \qquad (12)$$

This equation together with equations (9-11) will be used to obtain numerical solutions for the natural convection fluid flow in a concentric vertical annulus.

Nondimensional Initial and Boundary Conditions

The conditions given in Section 3.1 are rewritten hereunder in dimensionless forms.

For $t = 0$

$$U = 0 \quad , \quad V = 0 \quad , \text{and} \quad \theta = 0$$

For $t > 0$

At $Z = 0$ and $N < R < 1$

$$U = U_o(t), \quad V = 0 \quad , \text{and} \quad \theta = 0$$

At $Z > 0$ and $R = N$

$$U = 0 \quad , \quad V = 0 \quad , \text{and} \quad \theta = 1 \qquad \text{for case(I)}$$

$$\text{or} \quad \left(\frac{\partial \theta}{\partial R}\right) = 0 \qquad \text{for case(O)}$$

At $Z > 0$ and $R = 1$

$$U = 0 \quad , \quad V = 0 \quad , \text{and} \quad \theta = 1 \qquad \text{for case(O)}$$

$$\text{or} \quad \left(\frac{\partial \theta}{\partial R}\right) = 0 \qquad \text{for case(I)}$$

CHAPTER FOUR

NUMERICAL METHODOLOGY

Recent advances in computer technology made it possible to numerically solve the conservation equations describing flow and heat transfer for many problems of engineering interest. Several numerical methods such as finite element and finite difference techniques are used to solve the conservation equations. The restrictions and simplifying assumptions are minimized when using finite difference techniques.

To solve the problem under consideration by a finite difference technique, the governing partial differential equations are converted into their corresponding finite difference equations, which form a set of algebraic equations applied to the nodes of the grid. The grid size affects the accuracy of the numerical solution. However, there is a practical limitation on the grid size, since the computational time and hence the cost required to obtain a numerical solution, is directly proportional to the number of grid points.

The present numerical technique may be considered as an indirect extension of the original work of Bodoia and Osterele [16] and that of El-Shaarawi and Sarhan [24] to include the unsteady terms. In this research, an

implicit method is used to convert the differential equations into finite difference equations. Thus , the unknown values at a grid point are not only a function of previous values, but also a function of unknown values at the same step. This requires solution of a set of simultaneous algebraic equations that result when the difference equations are written for all interior grid points.

In most cases, implicit finite difference techniques tend to be numerically stable .For this reason,it was decided to use an implicit method in this investigation . Even though implicit techniques permit large steps, the cost per step is high and storage requirements tend to increase rapidly with decreasing the size of the mesh.

4.1 The Finite Difference Domain

In the present work, there are three independent variables; R,Z and t. A three dimensional parallelepiped grid in R,Z and t is imposed on half of the annular flow field; only half of the channel is needed due to the symmetry about the Z-axis. Thus, a rectangular grid ,as shown in Fig. 2 ,is superimposed on half of the annulus flow field in the R-Z plane; this grid represents the solution domain for a given t. For other values of t, there are other identical parallel plane-grids, i.e. the nondimensional time is simulated as a third coordinate normal to R-Z plane . Mesh points are numbered consecutively from the arbitrary origin (on the inner wall at entrance) with the i progressing in the radial direction, with $i = 1$ (at the inner wall), 2,3,..., and $n + 1$ (at the outer

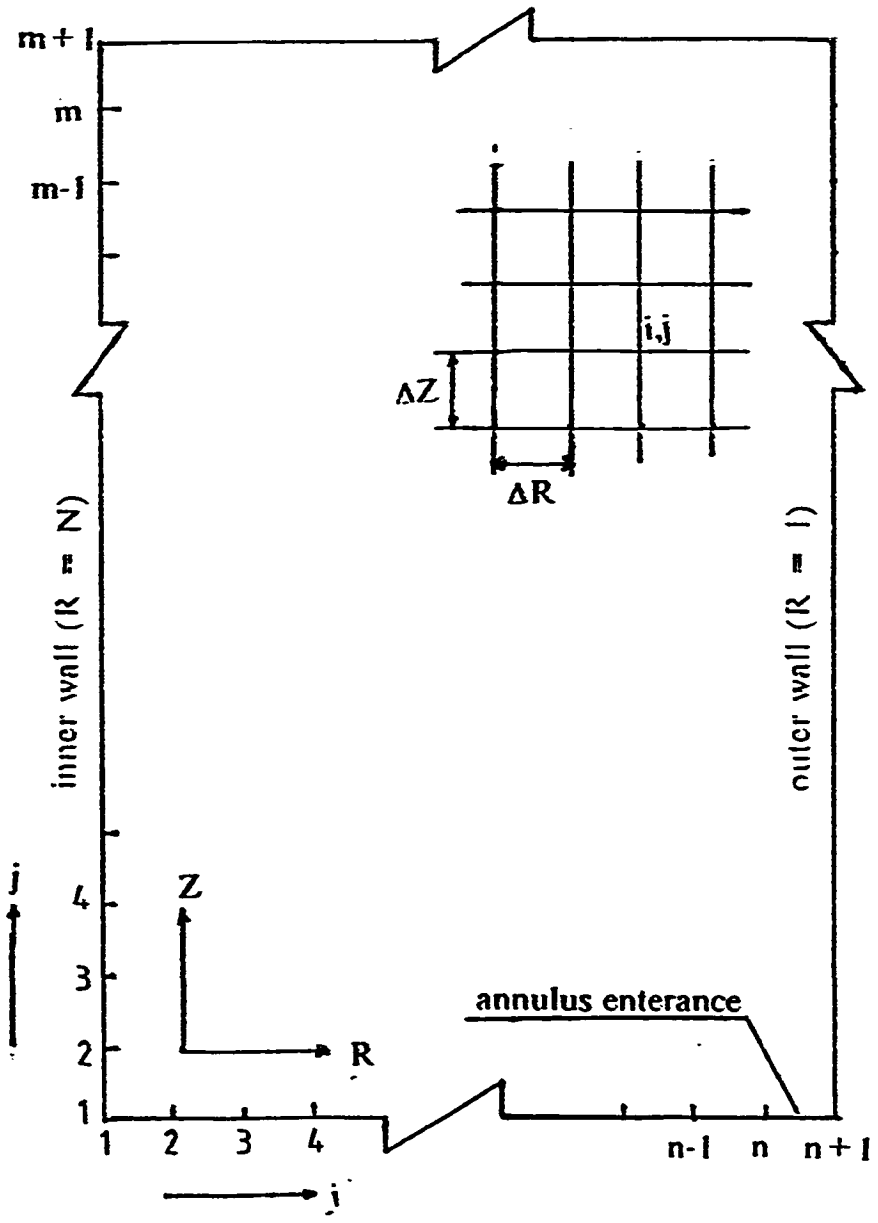

FIG. 2 Mesh network for finite difference representation at a given time (t).

wall), the j progressing in the axial flow direction, with j=1 (at inlet cross section), 2,3,....., and m+1 (at the final cross section), and the k progressing in the imaginary time direction, with k=1 (the initial state), 2,3,...., and K+1 (at the final steady state).

4.2 Finite Difference Formulation of the Continuity Equation

Considering the mesh network shown in Fig. 3.a , the continuity equation can be written in the following finite-difference form .

$$\frac{V_{i+1,j+1,k+1}-V_{i,j+1,k+1}}{\Delta R}+\frac{V_{i+1,j+1,k+1}+V_{i,j+1,k+1}}{2[N+(i-1/2)\Delta R]}+$$

$$\frac{U_{i+1,j+1,k+1}+U_{i,j+1,k+1}-U_{i+1,j,k+1}-U_{i,j,k+1}}{2\Delta Z}=0 \qquad (13)$$

Rearranging the terms, the equation will take the following form:

$$V_{i+1,j+1,k+1}=V_{i,j+1,k+1}[\frac{N+(i-1)\Delta R}{N+i\Delta R}]-[\frac{2N+(2i-1)\Delta R}{N+i\Delta R}]$$

$$[\frac{\Delta R}{4\Delta Z}][U_{i+1,j+1,k+1}+U_{i,j+1,k+1}-U_{i+1,j,k+1}-U_{i,j,k+1}] \qquad (14)$$

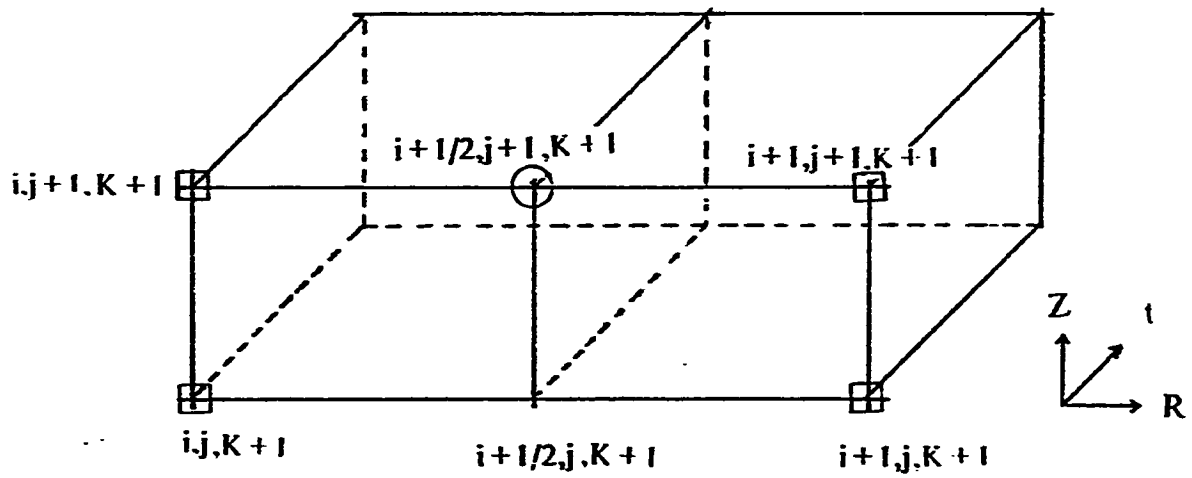

FIG. 3.a Three dimensional mesh network showing points invloved in the finite-difference representation of the continuity equation

4.3 Finite Difference Formulation of the Axial Momentum Equation

Considering the mesh network shown in Fig. 3.b , the axial momentum equation can be written in the following finite difference form.

$$\frac{U_{i,j+1,k+1}-U_{i,j+1,k}}{\Delta t}+V_{i,j,k}\frac{U_{i+1,j+1,k+1}-U_{i-1,j+1,k+1}}{2\Delta R}+U_{i,j,k}\frac{U_{i,j+1,k+1}-U_{i,j,k+1}}{\Delta Z}$$

$$=\frac{P_{j,k+1}-P_{j+1,k+1}}{\Delta Z}+\frac{\theta_{i,j+1,k+1}}{16(1-N)^4}+\frac{U_{i+1,j+1,k+1}-U_{i-1,j+1,k+1}}{2[N+(i-1)\Delta R]\Delta R}$$

$$+\frac{U_{i+1,j+1,k+1}-2U_{i,j+1,k+1}+U_{i-1,j+1,k+1}}{(\Delta R)^2} \qquad (15)$$

Rearranging the equation we get

$$U_{i,j+1,k+1}[\frac{1}{\Delta t}+\frac{U_{i,j,k}}{\Delta Z}+\frac{2}{(\Delta R^2)}]+U_{i+1,j+1,k+1}[\frac{V_{i,j,k}}{2\Delta R}-\frac{1}{2[N+(i-1)\Delta R]\Delta R}$$

$$-\frac{1}{(\Delta R)^2}]-U_{i-1,j+1,k+1}[\frac{V_{i,j,k}}{2\Delta R}-\frac{1}{2[N+(i-1)\Delta R]\Delta R}+\frac{1}{(\Delta R)^2}]$$

$$+\frac{P_{j+1,k+1}}{\Delta Z}=\frac{\theta_{i,j+1,k+1}}{16(1-N)^4}+\frac{U_{i,j+1,k}}{\Delta t}+\frac{(U_{i,j,k+1}*U_{i,j,k})}{\Delta Z}+\frac{P_{j,k+1}}{\Delta Z} \qquad (16)$$

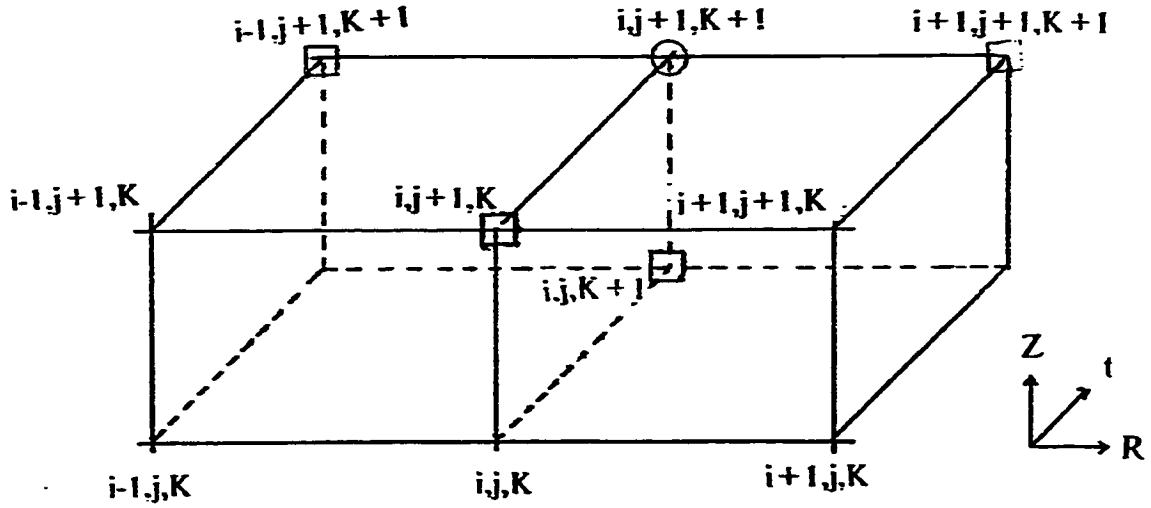

FIG. 3.b Three dimensional mesh network showing points invloved in the finite-difference representation of the axial momentum and energy equations

4.4 Finite Difference Formulation of the Energy Equation

Considering the mesh network shown in Fig. 3.b , the energy equation can be written in the following finite difference form:

$$\frac{\theta_{i,j+1,k+1}-\theta_{i,j+1,k}}{\Delta t}+V_{i,j,k}\frac{\theta_{i+1,j+1,k+1}-\theta_{i-1,j+1,k+1}}{2\Delta R}+U_{i,j,k}\frac{\theta_{i,j+1,k+1}-\theta_{i,j,k+1}}{\Delta Z}=$$

$$+\frac{1}{Pr}\left[\frac{1}{N+(i-1)\Delta R}\frac{\theta_{i+1,j+1,k+1}-\theta_{i-1,j+1,k+1}}{(2\Delta R)}+\frac{\theta_{i+1,j+1,k+1}-2\theta_{i,j+1,k+1}+\theta_{i-1,j+1,k+1}}{(\Delta R)^2}\right] \quad (17)$$

Rearranging the equation we get

$$\theta_{i,j+1,k+1}\left[\frac{1}{\Delta t}+\frac{U_{i,j,k}}{\Delta Z}+\frac{2}{(Pr)(\Delta R)^2}\right]+\theta_{i+1,j+1,k+1}\left[\frac{V_{i,j,k}}{2\Delta R}-\frac{1}{(2\Delta R)(Pr)[N+(i-1)\Delta R]}\right.$$

$$\left.-\frac{1}{(Pr)(\Delta R)^2}\right]+\theta_{i-1,j+1,k+1}\left[-\frac{V_{i,j,k}}{2\Delta R}+\frac{1}{(2\Delta R)(Pr)[N+(i-1)\Delta R]}-\frac{1}{(Pr)(\Delta R)^2}\right]$$

$$=\theta_{i,j,k+1}\left(\frac{U_{i,j,k}}{\Delta Z}\right)+\frac{\theta_{i,j+1,k}}{\Delta t} \quad (18)$$

It should be noted that the finite difference equations are linearized , i.e, if two unknowns are multiplied by each other, one of them is replaced by its value at the previous step. Also it is observed that some of the finite difference approximations are made in central difference forms and others in backward difference forms. This is done to enable the solutions of the equations in the

manner described later, and to ensure numerical stability of the numerical solution.

4.5 Numerical Representation of the Integral Form of the Continuity Equation

For a given instant of time, the integral form of the continuity equation is written as

$$2\int_{N}^{1} UR\ dR = (1-N^2)U_o$$

Using the trapezoidal rule for numerical integration, the above equation can be reduced to the following form:

$$\frac{\Delta R}{2}(NU_{1,j+1,k+1}+U_{n+1,j+1,k+1})+\Delta R\sum_{i=2}^{n}U_{i,j+1,k+1}[N+(i-1)\Delta R]=\frac{(1-N^2)U_o}{2} \qquad (19)$$

However the no slip boundary conditions are

$$U_{1,j+1,k+1}=U_{n+1,j+1,k+1}=0$$

Substituting these conditions in (19) leads to the following numerical representation of the integral continuity equation.

$$\Delta R\sum_{i=2}^{n} U_{i,j+1,k+1}[N+(i-1)\Delta R]=\frac{(1-N^2)U_o}{2} \qquad (20)$$

Initial and Boundary Conditions :

Initially,i.e.,at t = 0

$$U_{i,j,1}=V_{i,j,1}=\theta_{i,j,1}=0$$

For t > 0

At R = N and R = 1

$$U_{1,j,k}=V_{1,j,k}=U_{n+1,j,k}=V_{n+i,j,k}=0$$

At R = N

$\theta_{1,j,k}=1$ for case(I) and $\theta_{0,j,k}=\theta_{2,j,k}$ for case(O)

At R = 1

$\theta_{n,j,k}=\theta_{n+2,j,k}$ for case(I) and $\theta_{n+1,j,k}=1$ for case(O)

4.6 Method of Solution

In this work all the equations are coupled together but, at a given time, the developed numerical technique allows us to , first ,solve the energy equation (17) and get the dimensionless temperatures at a specified cross-section. This is because the linearization process has made the velocities involved in the equation as known values from the previous step (with respect to time and axial coordinate). Then, the axial momentum equation (15) together with the integral continuity equation (20) will be used to get the dimensionless axial velocities and dimensionless pressure defect. Next, the dimensionless radial velocities will be found through the solution of the continuity equation (13). Finally, the heat transfer parameters will be computed for the specified cross section and the given time.

4.6.1 Iteration process:

To obtain a numerical solution for the governing equations values of N, Pr, ΔR, ΔZ, Δt and Gr^* ,which are constants for each computer run , have to be selected . The axial and time steps are chosen in the following ranges.

$2 \times 10^{-7} \leq \Delta Z \leq 5 \times 10^{-3}$

$10^{-3} \leq \Delta t \leq 2 \times 10^{-2}$

For example , $\Delta Z = 2 \times 10^{-7}$ and $\Delta t = 10^{-3}$, were used in both cases (I) and (O) for $Gr^* = 100{,}000$. For $Gr^* = 1000$, $\Delta Z = 2 \times 10^{-5}$ and $\Delta t = 5 \times 10^{-3}$ were used in both cases (I) and (O) . The number of radial increments n was selected to be 40 in all the computer runs. The radial increment (ΔR) is given by

$$\Delta R = \frac{(1-N)}{n}$$

Thus the value of ΔR for the present annulus,where $N = 0.5$, is 0.0125 .

In the present work ,the numerical solutions are thus found for pre-chosen values of Gr^*, i.e. specific values of the dimensionless annulus height L . The value of the dimensionless pressure defect at the exit section should be zero or practically satisfies the following arbitrarily chosen criterion.

$$-10^{-15} \leq P_{i,m+1,k} \leq 10^{-15} \qquad (21)$$

To satisfy this condition ,iteration process is used for every time step as follows. First, the inlet axial velocity (U_o) is assumed and computations continue ,for this time step, till the exit-cross section dimensionless pressure defect $P_{i,m+1,k}$ is obtained.If it does not satisfy the above criterion , another value of the inlet axial velocity has to be assumed ,for the same time step,and it's corresponding exit dimensionless pressure defect has to be computed.Then, a linear interpolation is done between these two assumed values of U_o to get the

next trial value of the inlet axial velocity U_o corresponding to zero dimensionless pressure defect at the annulus exit.Such an interpolation process continues, for the same time step, till the dimensionless exit pressure defect satisfies the iteration criterion (21). The same process can then be repeated for each next time step till steady-state conditions are reached. The change in the total heat absorbed is used as a criterion for the achievement of steady-state conditions.Steady-state conditions are considered achieved if the following criterion is satisfied.

$$-10^{-6} \leq \frac{\overline{H}(k+1)-\overline{H}(k)}{\overline{H}(k+1)} \leq 10^{-6} \qquad (22)$$

4.6.2 Solution of the Temperature Field:

The numerical solution of the temperature field is obtained by starting with $k=1$ (i.e. $t=\Delta t$). At $j=1$ (entrance cross section), equation (17) is applied with $i=2,3,..n+1$ in case (I). This gives n equations in n unknowns, for the next cross section ($j = 2$).On the other hand,for case(O), equation (17) is applied with $i=1,2,3...n$ and similarly n equations in n unknowns are obtained. In a matrix form, these equations are written as follows.

For case (I), at a given j, we have

$$\begin{bmatrix} A_2 & B_2 & 0 & 0 & - & 0 \\ C_3 & A_3 & B_3 & 0 & - & 0 \\ 0 & C_4 & A_4 & B_4 & 0 & 0 \\ 0 & 0 & - & - & - & - \\ - & - & - & c_n & A_n & B_n \\ - & - & - & - & C_{n+1} & A_{n+1} \end{bmatrix} \quad X \quad \begin{bmatrix} \theta_{2j+1,k+1} \\ \theta_{3j+1,k+1} \\ \theta_{4j+1,k+1} \\ - \\ - \\ \theta_{n+1,j+1,k+1} \end{bmatrix} \quad = \quad \begin{bmatrix} D_2 \\ D_3 \\ D_4 \\ - \\ - \\ D_{n+1} \end{bmatrix}$$

and for case (O), at a given j, we have

$$\begin{bmatrix} A_1 & B_1 & 0 & 0 & - & 0 \\ C_2 & A_2 & B_2 & 0 & - & 0 \\ 0 & C_3 & A_3 & B_3 & 0 & 0 \\ - & - & - & - & - & - \\ - & - & - & C_{n-1} & A_{n-1} & B_{n-1} \\ - & - & - & - & C_n & A_n \end{bmatrix} \quad X \quad \begin{bmatrix} \theta_{1j+1,k+1} \\ \theta_{2j+1,k+1} \\ \theta_{3j+1,k+1} \\ - \\ - \\ \theta_{nj+1,k+1} \end{bmatrix} \quad = \quad \begin{bmatrix} D_1 \\ D_2 \\ D_3 \\ - \\ - \\ D_n \end{bmatrix}$$

where

$$A_i = \frac{U_{i,j,k}}{\Delta Z} + \frac{2}{Pr(\Delta R)^2} + \frac{1}{\Delta t} \ ,$$

$$B_i = \frac{V_{ijk}}{2\Delta R} - \frac{1}{2Pr[N+(i-1)\Delta R]\Delta R} - \frac{1}{Pr(\Delta R)^2} \quad ,$$

$$C_i = -\frac{V_{ijk}}{2\Delta R} + \frac{1}{2Pr[N+(i-1)\Delta R]\Delta R} - \frac{1}{Pr(\Delta R)^2} \quad , \text{ and}$$

$$D_i = \frac{\theta_{ijk+1} U_{ijk}}{\Delta Z} + \frac{\theta_{ij+1k}}{\Delta t}$$

It should be noted that the terms with simultaneous subscripts j+1 and k+1 are unknowns while those with one subscript k or j are known from either the previous time step or the previous axial step ,respectively. The coefficient matrix is tridiagonal .Therefore, Thomas method [33] ,which has the benefit of low required storage ,is used to solve this system of linear equations .

For the given time ($t=\Delta t$) ,having obtained the unknown temperatures at the second axial cross-section, the axial and radial velocities and the pressure are computed at this axial station as explained in the next section. Then ,the same procedure is repeated for the next value of j. Calculation will continue to obtain the temperature distribution all over the annulus at the specified time ($t=\Delta t$). After satisfying the iteration criterion (21), the next time step temperatures can be computed by repeating the whole procedure again. That wise the computation will continue till steady-state conditions are practically achieved.

4.6.3 Solution of the velocity field

Equations (13),(15) and (20) govern the velocity field. It should be known that the terms with a subscript j or k are knowns while those with simultaneous subscripts j+1 and k+1 are unknowns.

Starting with j=1 (annulus entrance cross-section) and at the first time step at k=1, applying equation (15) with i=2,3,...n and equation (20) with i=2,3,...n, we get n simultaneous linear algebraic equations in n unknowns $U_{2,2,2}$, $U_{3,2,2}$, $U_{4,2,2}$,....., $U_{n,2,2}$, $P_{2,2}$. These equations are solved by means of a special form of the Guass Jordan elimination scheme [34]. Now the radial velocity at the grid points of the second cross section can be obtained by applying equation (13) in a stepwise manner. This process will be repeated for each next j (cross section) after getting it's temperatures (as explained in the previous section).Thus the dimensionless axial velocity , dimensionless pressure defect and the radial velocity are obtained all over the domain of solution at a time step .

The above process is repeated till steady state conditions are reached. Equations (15) and (20) can be written, for a given cross section (j), in the following matrix form:

The matrix is given as

$$\begin{bmatrix} e_2 & e_3 & e_4 & 0 & - & e_n & 0 \\ A_2 & B_2 & 0 & 0 & - & - & 1 \\ C_3 & A_3 & B_3 & 0 & 0 & - & 1 \\ 0 & C_4 & A_4 & B_4 & 0 & 0 & 1 \\ 0 & & 0 & - & 0 & 0 & 1 \\ & & & 0 & C_{n-1} & A_{n-1} & 1 \\ & & & & & e_n & 1 \end{bmatrix} \quad X \quad \begin{bmatrix} U_{2,j+1,k+1} \\ U_{3,j+1,k+1} \\ U_{4,j+1,k+1} \\ - \\ - \\ U_{n,j+1,k+1} \\ P_{j+1,k+1} \end{bmatrix} \quad = \quad \begin{bmatrix} E \\ D_2 \\ D_3 \\ D_4 \\ - \\ D_{n-1} \\ D_n \end{bmatrix}$$

where

$e_i = N + (i-1)\Delta R$,

$$E = \frac{(1 - N^2)U_o}{2\Delta R} ,$$

$$A_i = \frac{\Delta Z}{\Delta t} + U_{i,j,k} + \frac{2\Delta Z}{\Delta R^2} ,$$

$$B_i = \frac{\Delta Z}{\Delta R}\left[\frac{V_{i,j,k}}{2} - \frac{1}{\Delta R} - \frac{1}{2[N + (i-1)\Delta R]}\right] ,$$

$$C_i = \frac{\Delta Z}{\Delta R}\left[\frac{1}{2[N + (i-1)\Delta R]} - \frac{V_{i,j,k}}{2} - \frac{1}{\Delta R}\right] , \text{ and}$$

$$D_i = U_{i,j+1,k}\frac{\Delta Z}{\Delta T} + U_{i,j,k+1} * U_{i,j,k} + P_{j,k+1} + \frac{\Delta Z}{16(1-N)^4}0_{i,j+1,k+1}$$

CHAPTER FIVE

RESULTS AND DISCUSSION

5.1 INTRODUCTION

In this chapter, we focus the light upon the main results of this research. The numerical solutions are carried out for one radius ratio (N = 0.5), one value of Prandtl number (Pr= 0.7) and a range of Grashof number ($4 \leq Gr^{*} \leq 100{,}000$).

Developing axial and radial velocities and temperature profiles along the annulus are presented for various selected values of time. The variation with time of the mid-height and top-exit axial and radial velocities and temperature profiles are also presented. Furthermore, the axial variation of pressure, mixing cup temperature, and adiabatic wall temperature are shown. Finally, the variation with time of the amount of flow and the total heat absorbed by fluid are presented as a function of Grashof number .

To check the adequacy of the present numerical technique and the obtained results, the following comparisons have been made.

I. The present results ,which are obtained after a long period of time

is elapsed, are compared with the steady-state results of El-Shaarawi and Sarhan [25] for the developing laminar free convection flow in vertical concentric annuli.

II. The present steady-state results at the top-exit cross section of a long annulus (large value of L , i.e. small value of Gr^*) are compared with the available fully developed laminar natural convection solution of the third kind [30].

III. A special computer run was made for an annulus of N = 0.99 with both walls subjected to equal step temperature changes. The obtained transient free convection results are compared with the corresponding results of Joshi [22] in a vertical parallel plates channel.

5.2 DEFINITIONS

Some of the parameters computed in this work are defined below:-

I. Mixing Cup Temperature (θ_m)

At a given instant, the mixing cup temperature at any given cross section is defined as

$$T_m = \frac{2\pi\rho_o c_p \int_{r_1}^{r_2} ruT\,dr}{2\pi\rho_o c_p \int_{r_1}^{r_2} ru\,dr} \quad ,$$

which can be written in the following dimensionless form

$$\theta_m = \frac{\int_N^1 RU\theta\,dR}{\int_N^1 RU\,dR} \tag{23}$$

Using the trapezoidal rule to evaluate the integrals , the numerical representation of Equation (19) (at cross section $Z=j\Delta Z$ and time $t=k\Delta t$) is :

$$\theta_m = \frac{\sum_{i=2}^{N} R_i U_{i,j,k} \theta_{i,j,k}}{\sum_{i=2}^{N} R_i U_{i,j,k}}$$

II. Heat Absorbed ($\overline{H}$)

At a given instant, the amount of heat absorbed by the fluid as it passes through the annulus , from the entrance to the exit , is given by

$$\overline{h} = 2\pi\rho_o c_p \int_{r_1}^{r_2} ru(\overline{T} - T_o)\,dr$$

Substituting the nondimensional parameters in this equation leads to the

following dimensionless form

$$\overline{H} = 2\int_{N}^{1} RU\bar{\theta}\,dR = 2\bar{\theta}_m \int_{N}^{1} U\ R\ dR = (\ 1-N^2\ )\ U_o\ \bar{\theta}_m = F\ \bar{\theta}_m$$

Using the trapezoidal rule to evaluate the above integral leads to the following numerical representation .

$$\overline{H} = 2\Delta R \sum_{i=2}^{N-1} R_i U_{i,1} \bar{\theta}_{i,1}$$

5.3 RESULTS

5.3.1 Axial Velocity

Figures 4 through 11 present the variation of the axial velocity profiles, at specific values of time, with Z for both cases (I) and (O). In all cases, the axial velocity profile is flat at the annulus entrance.As the fluid moves upward, two boundary-layers are formed on both annulus walls creating an asymmetrical axial velocity profile with it's peak shifted toward the heated wall, the outer wall in case (O) and the inner wall in case (I). Since for a given time the flow rate is constant ,then in view of the continuity concept , the value of the axial velocity on the unheated side of the curve must correspondingly decrease with axial distance as shown in these figures.

Backflow (reversed flow) occurs at very large Grashof numbers near the adiabatic wall as shown in Figs. 10 and 11 . Note that large values of Gr^* represent a short annulus with a large hydraulic diameter and a large temperature difference ($T_w - T_o$). The occurrence of the reversed flow can be attributed to the continuity principle as follows.For a given time,since the same amount of fluid is flowing across each cross section, the need for more fluid to flow near the heated wall is compensated by withdrawing it from regions close to the adiabatic wall.

For various values of Gr^* ,Figs. 12 through 21 present the mid-height axial velocity profiles at different values of time for both cases (I) and (O) . Generally, at any radial location, the axial velocity increases with time. Figures 20 and 21 show that there is a growth and decay of backflow near the adiabatic wall for case(I) and case(O)at modified Grashof numbers of 100,000 and 50,000, respectively.

Even though the stability analysis of the present numerical scheme,given in Appendix (2), requires a positive axial velocity value all over the domain of solution(i.e. no flow reversals), the program succeeded in obtaining numerical solutions for some cases where backflow effect is small. In other cases,especially with very large values of Gr^* ,the program failed in obtaining the solutions due to the occurrence of numerical instability.For example numerical instability occurred and numerical solution could not be obtained for case(O) with $Gr^* = 100{,}000$. However,in some other cases with very large values of Gr^* [as case(I) with $Gr^* = 10^5$], numerical disturbances in computing some of the parameters were observed near the separation point (in reversed flow region) but the solution could recover and such disturbances decay.

Figures 22 through 25 present examples of the exit axial velocity profiles for both cases (I) and (O). They show that ,for the given values of Gr^* , the axial velocity increases to a maximum and then decreases to a steady state profile. This overshoot in the velocity profiles is a direct result of the

temperature overshoot which will be discussed later.

Finally,it can be seen from all the previously mentioned axial-velocity profile figures that the maximum axial velocity decreases as Gr^* increases.This is because as Gr^* decreases the annulus height increases causing more buoyancy or chimney effect with more fluid being sucked.

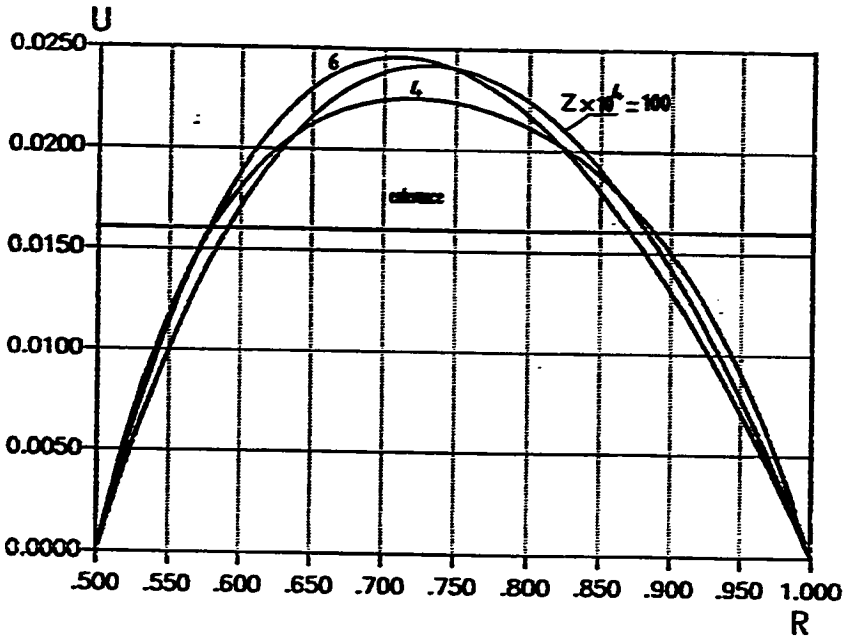

FIG. 4 U versus R for different Z's,at t = 0.2,case(i), N=0.5,G_r^*=100

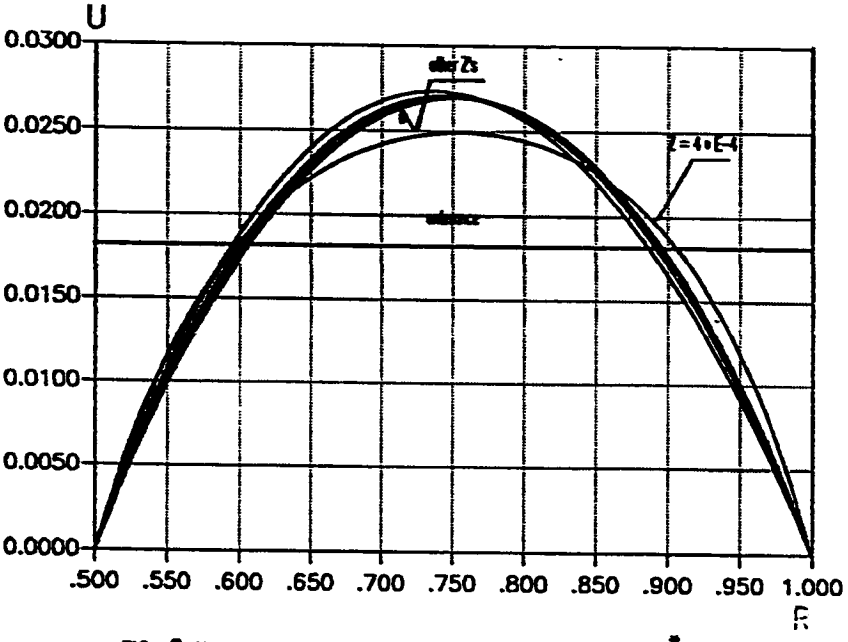

FIG. 5 U versus R for different Z's at t = 0.2,case(C) G_r^*=100,N=0.5

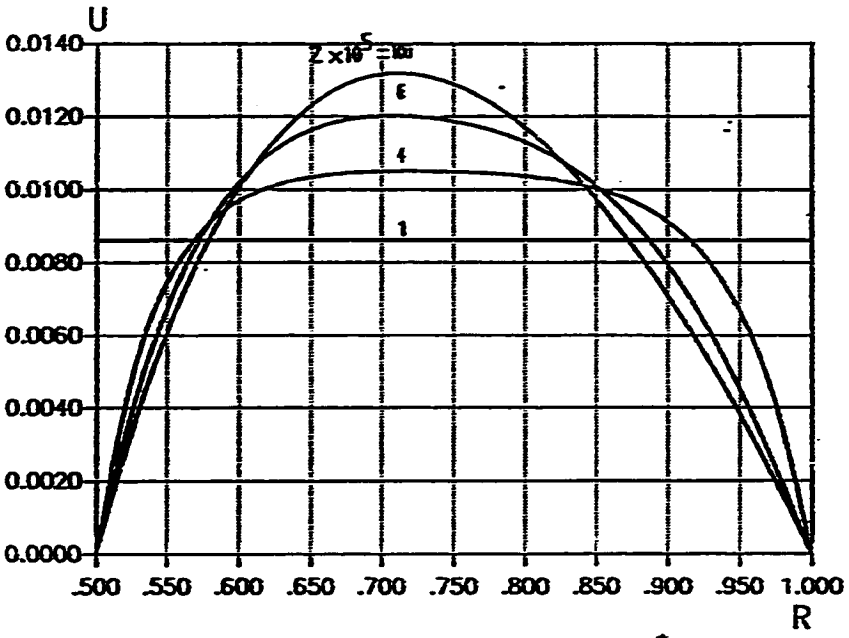

FIG. 6 U versus R for differentZ's ,at $\dagger$ = 0.1,case(i) ,$G\bar{r}$=1000,N=0.5

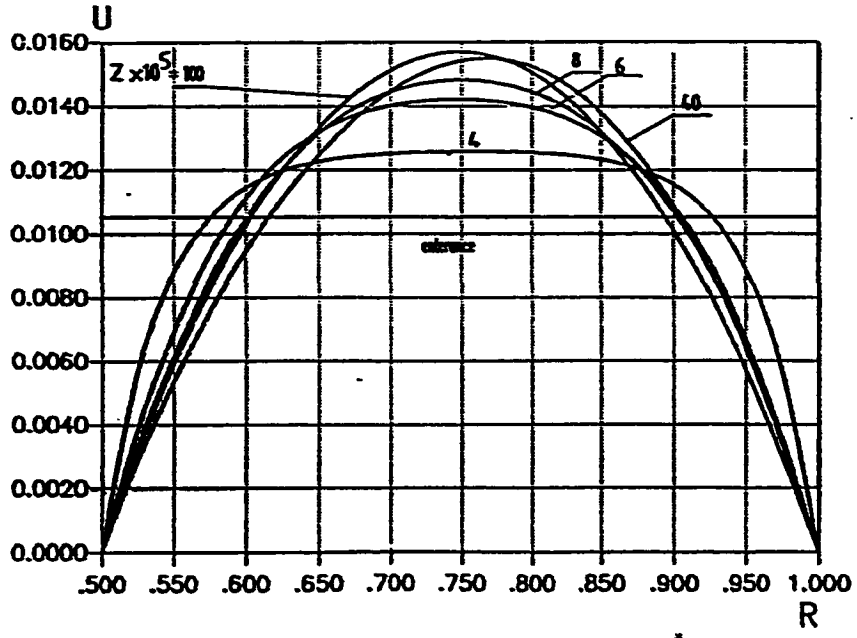

FIG. 7 U versus R for different Z's at t = 0.1,case(i) ,$G\bar{r}$=1000,N=0.5

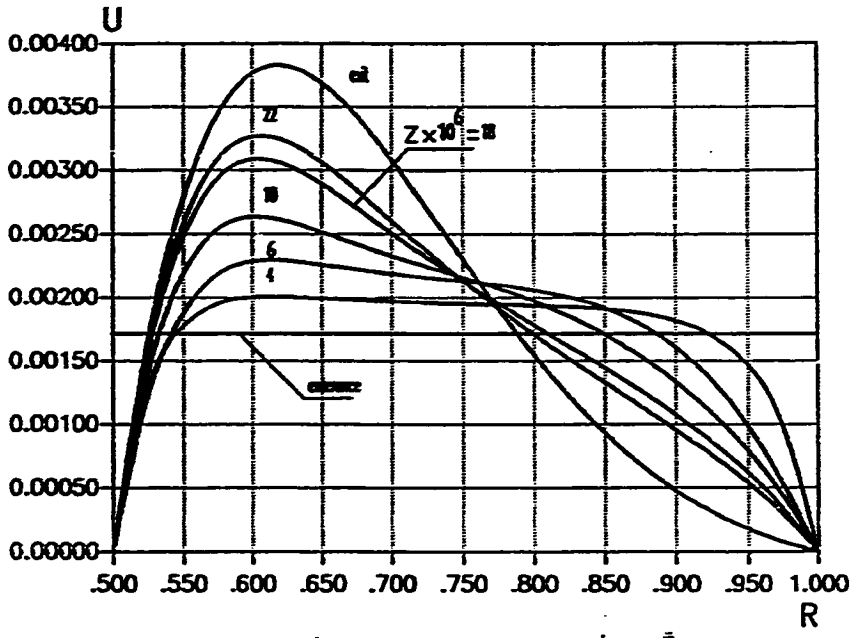

FIG. 8 U versus R for different Z's,at τ = 0.02,case(i) ,Gr=10,000,N=0.6

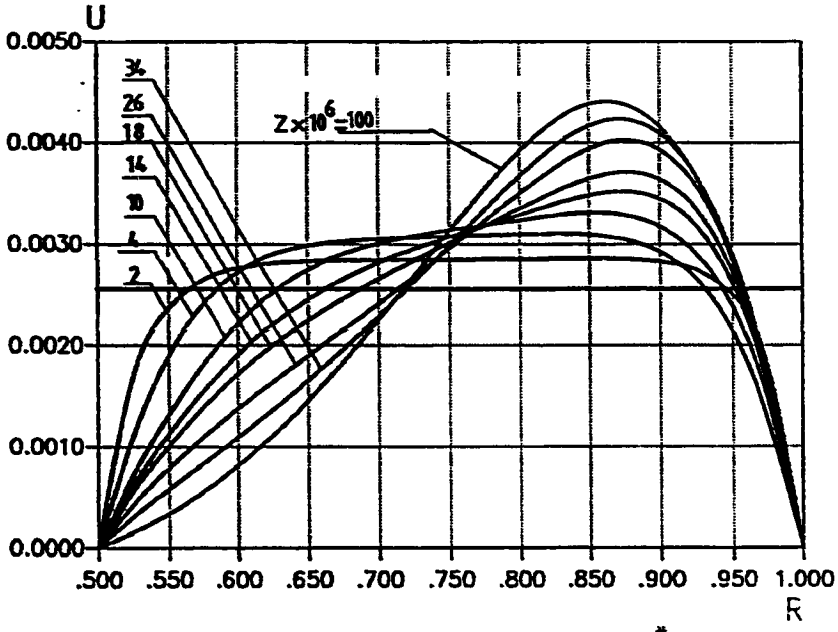

FIG. 9 U versus R for different Z's at t = 0.02 ,case(i) ,Gr=10,000,N=0.6

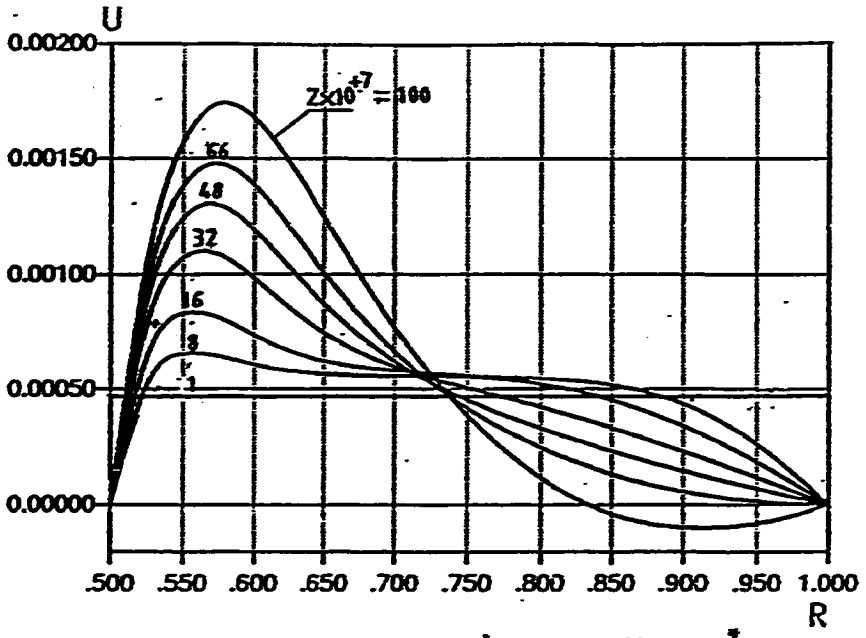

FIG. 10 U versus R at different Z points,at τ =0.02,case(I) , Gr^*=100,000,N=0.5.

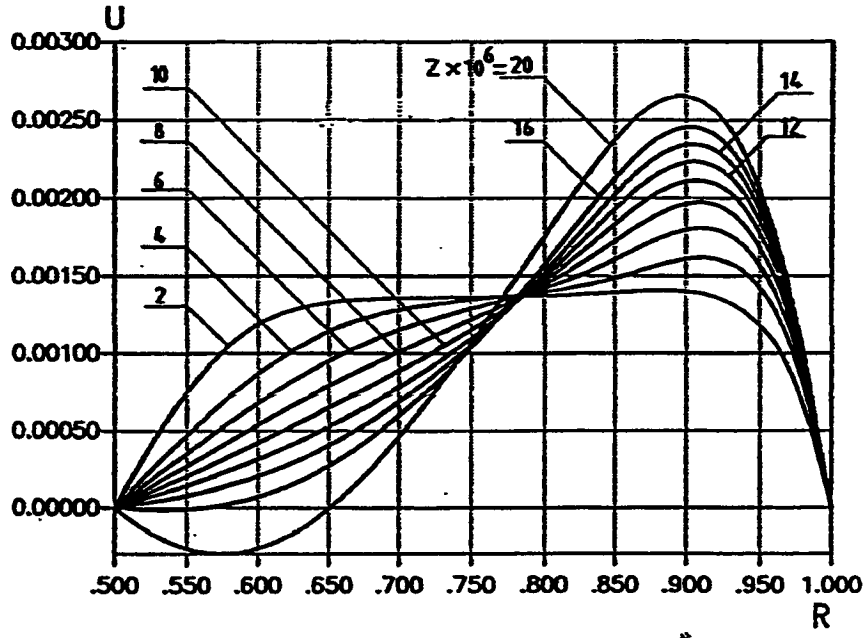

FIG. 11 U versus R for different Z's at t = 0.02,case(I) Gr^*=50,000,N=0.5

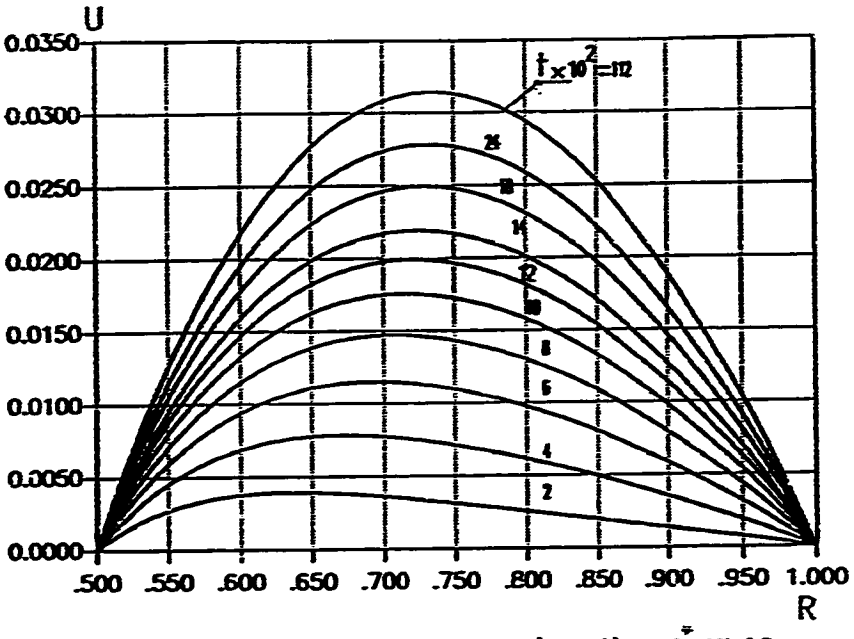

FIG. 12 Mid-height U verses R for different $\frac{t}{}$,case(i) ,Gr=4,N=0.5

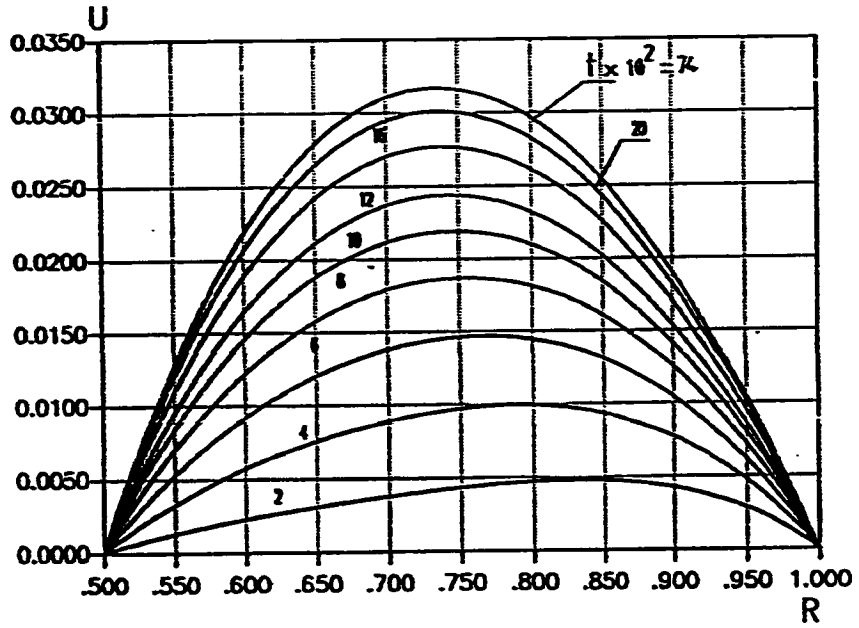

FIG. 13 Mid-height U versus R for different t ,case(i) - ,Gr=4,N=0.5

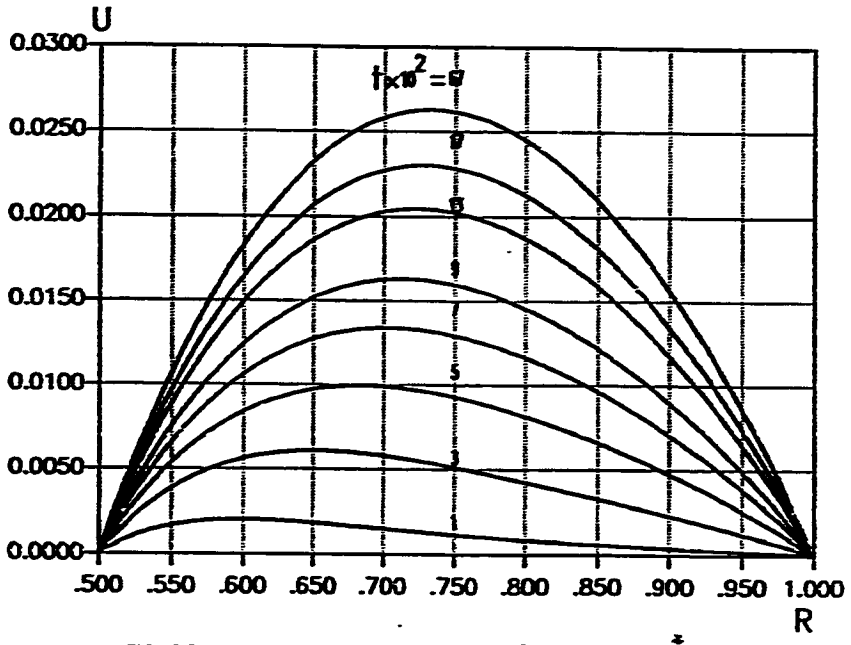

FIG. 14 Mid-height U versus R for different t^* ,case(I) ,Gr=100,N=0.5

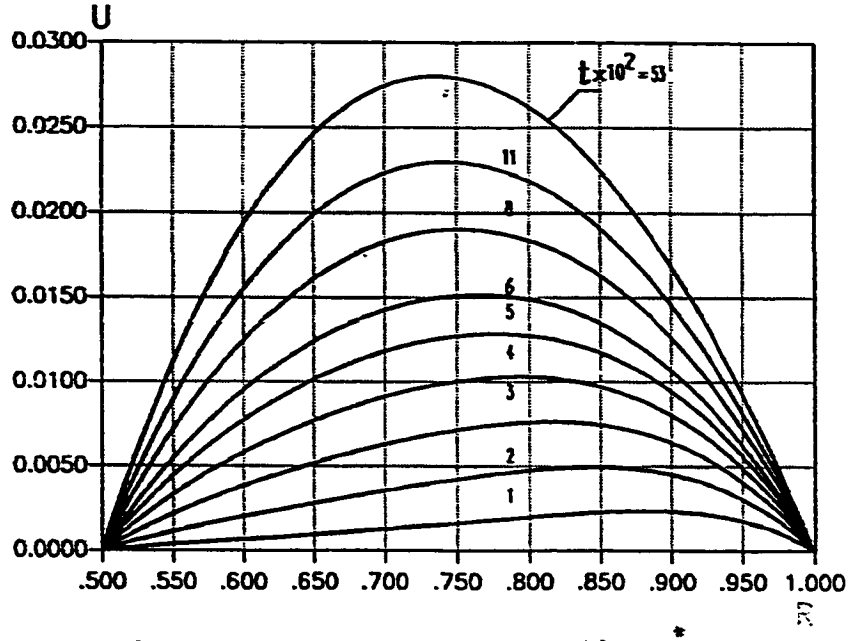

FIG. 15 Mid-height U versus R for different t^* ,case(I) ,Gr=100,N=0.5

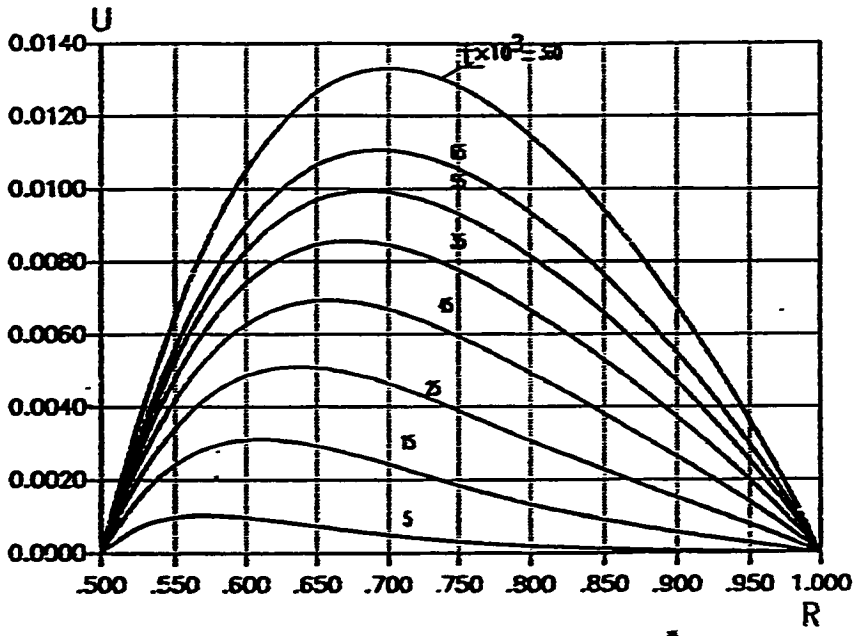

FIG. 16 Mid-height U versus R for different $\dagger$,case(I) ,$\tilde{Gr}$=1000,N=0.5

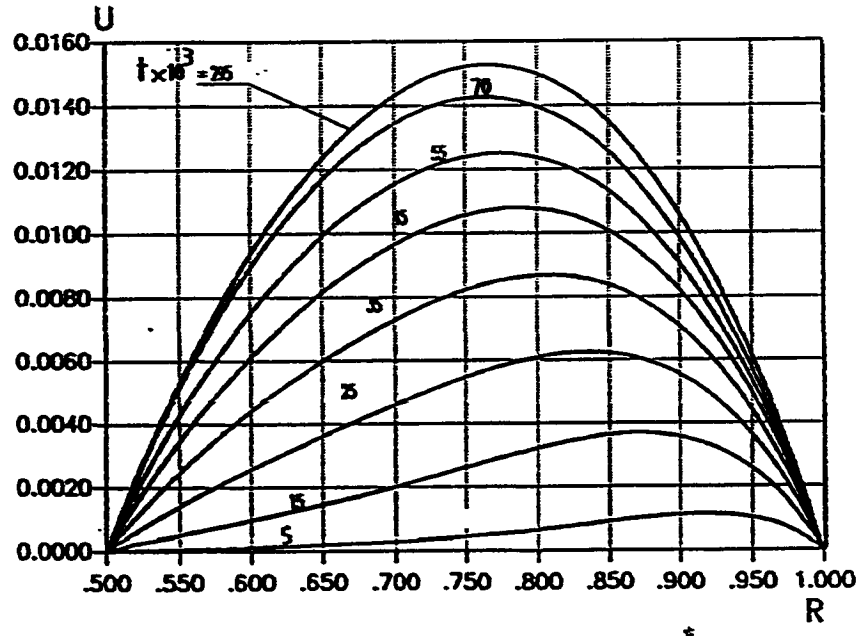

FIG. 17 Mid-height U versus R for different t ,case(I) ,$\tilde{Gr}$=1000,N=0.5

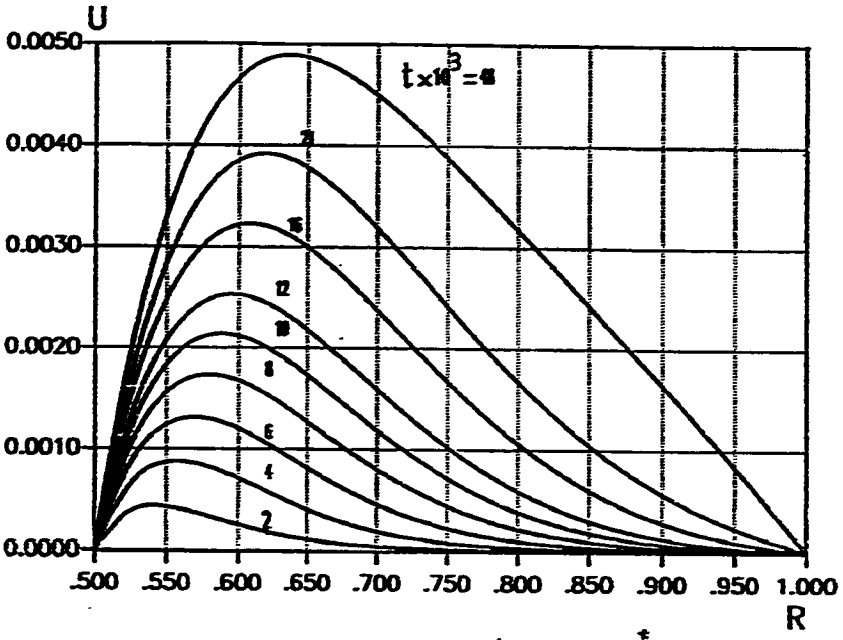

FIG. 18 Mid-height U versus R for different t^* ,case(I) ,Gr=10,000,N=0.5

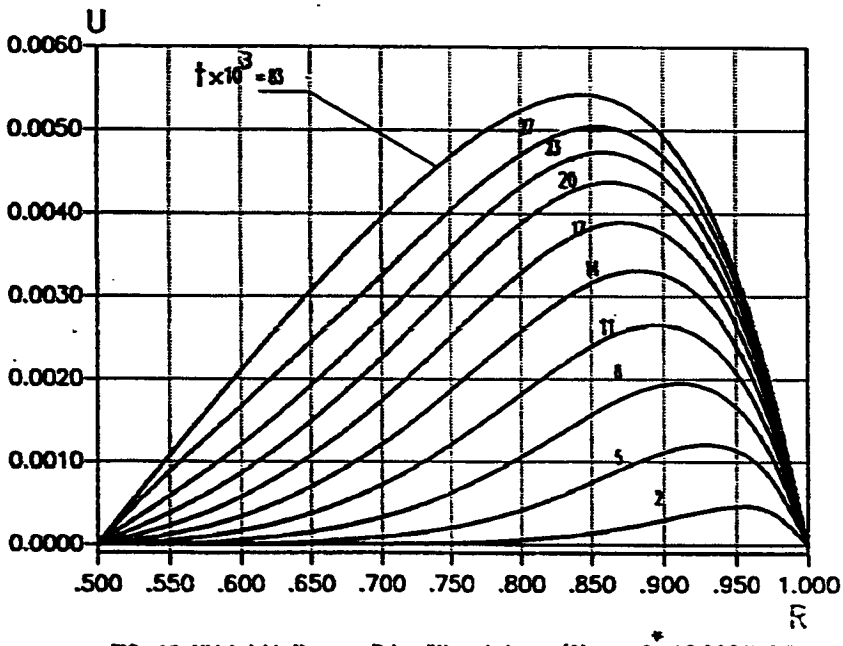

FIG. 19 Mid-height U versus R for different t^* ,case(I) ,Gr=10,000,N=0.5

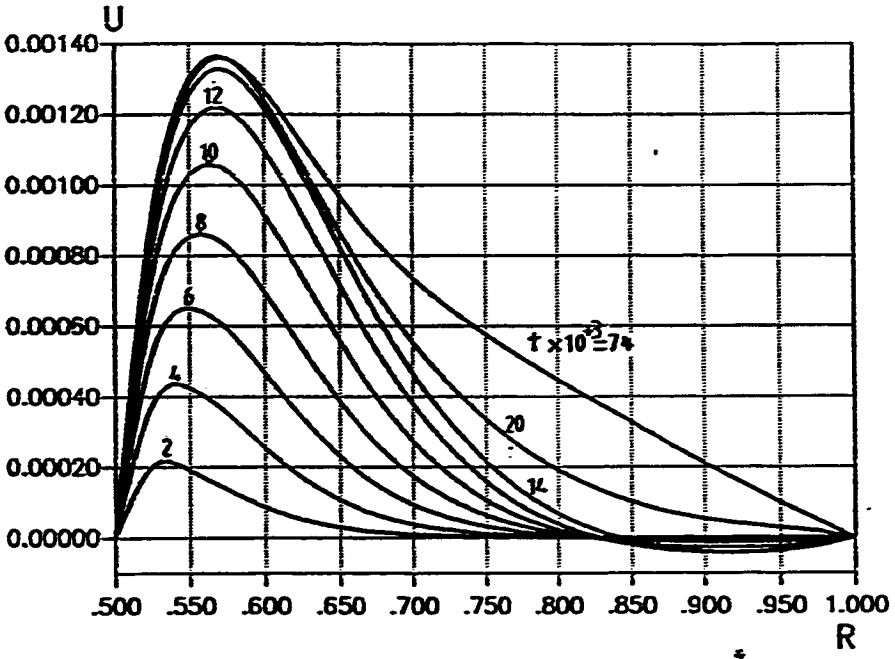

FIG. 20 Mid-height U versus R for different $\dagger$,case(I) ,Gr^{*}=100,000,N=0.5

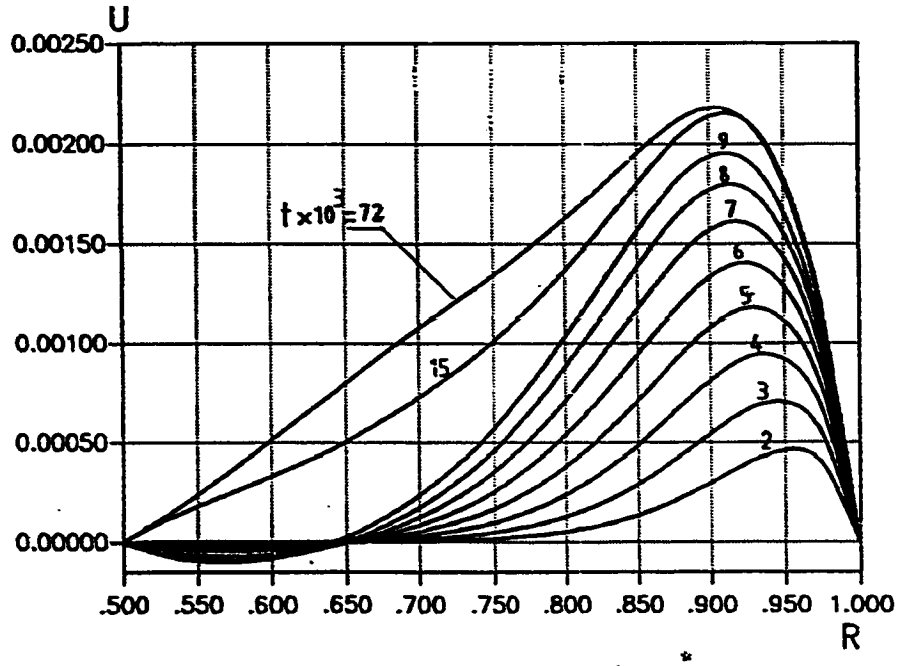

FIG. 21 Mid-height U versus R for different t,case(0) ,Gr^{*}=50,000,N=0.5

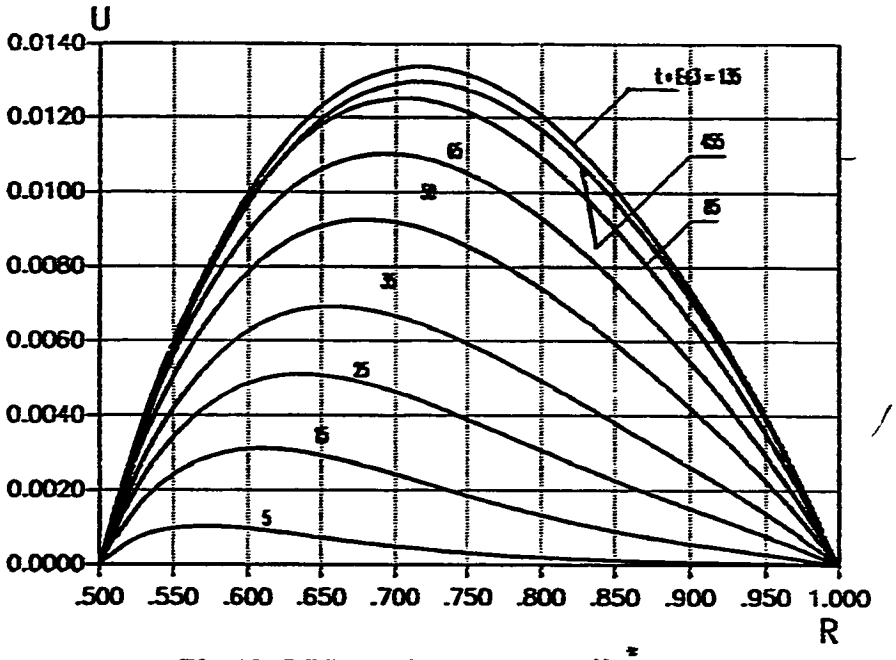

FIG. 22 Exit U versus R for different t,case(I),Gr^*=1000,N=0.5

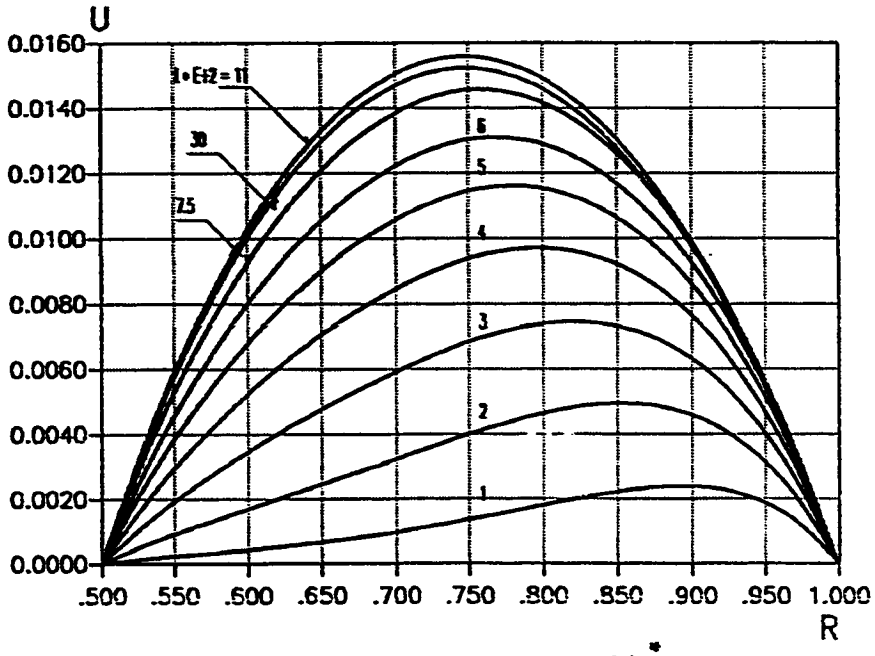

FIG. 23 Exit U versus R for different t,case(0),Gr^*=1000,N=0.5

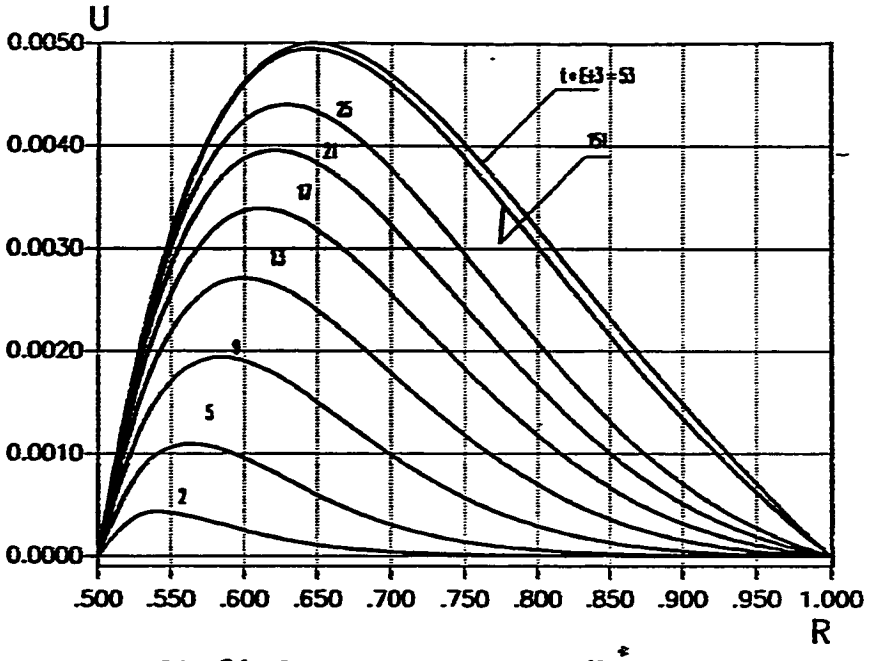

FIG. 24 Exit U versus R for different t,case(1),Gr=10,000,N=0.5

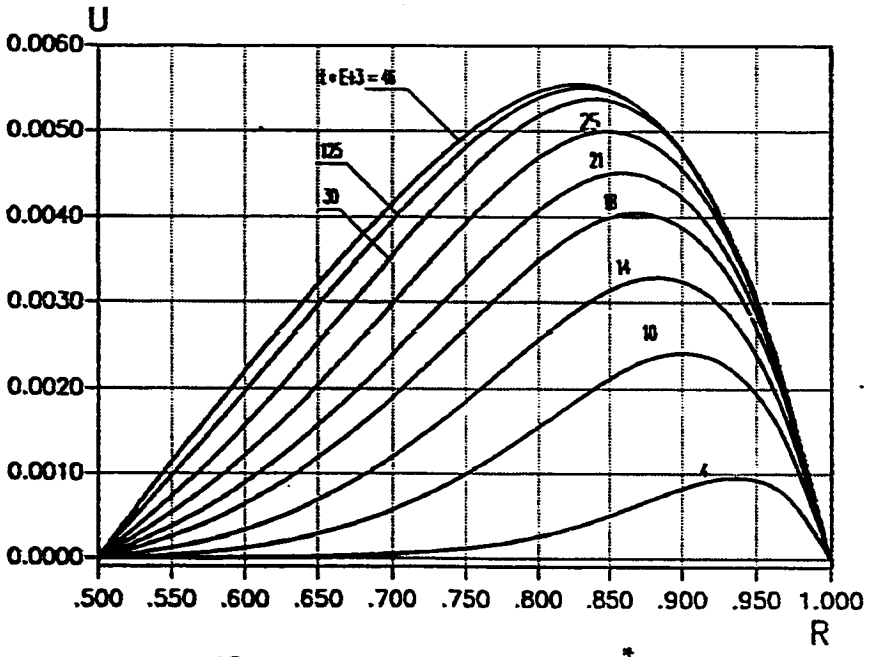

FIG. 25 Exit U versus R for different t ,case(0),Gr=10,000,N=0.5

5.3.2 Radial Velocity Profiles

Figures 26 through 33 show the dimensionless radial velocity profiles against the dimensionless radial coordinate for different dimensionless axial positions.These figures are for both cases (I) and (O) and each figure is for a specific instant of time. Thus each figure shows how the profiles would develop with axial distance if there were a time-freeze .

From these figures it can be seen that the radial velocity is decreasing with distance from the entrance. Figures 26 and 27 show that, for small values of Gr^* , the fluid is moving all over the annulus height from regions close to the heated surface towards the adiabatic wall ,at the specified time. In Figs. 28 and 29,which may represent a moderate value of Gr^*($Gr^* = 1000$) the fluid mainly moves towards the center of the annular gab. On the other hand ,the fluid mainly moves towards the heated wall for large values of Grashof number ($Gr^* \geq 10{,}000$) as can be seen from Figs. (30 - 33) . The irregularity in some of the radial velocity profiles at some values of Z, as shown in Figs. 32 and 33, is indeed due to the presence of flow reversals in such cases.

Figures 34 through 41 present the variation of the dimensionless mid-height radial velocity profiles with time. For $Gr^* = 1000$, Fig. 36 shows that the radial velocity is increasing with time and fluid is mainly transported from

regions close to the heated wall toward the adiabatic wall.For $Gr^* = 10{,}000$, Fig. 38 shows that the value of the radial velocity is increasing to a maximum and then it decreases to a steady state value.This phenomenon is related to the phenomenon of temperature overshoot which will be discussed later.

Figures 42 through 45 present the variation with time of the exit radial velocity profiles . For $Gr^* = 1000$, Figs. 42 and 43 shows clearly the overshoot phenomenon. In Fig. 42 the profile corresponding to $t = 200 \times 10^{-3}$ overshoot the steady-state profile corresponding to $t = 455 \times 10^{-3}$. Similarly in Fig. 43 the profile corresponding to $t = 150 \times 10^{-3}$ overshoots that corresponding to $t = 300 \times 10^{-3}$. On the other hand,Fig. 44 clarifies how the radial movement of fluid varies with time for case(I) with $Gr^* = 10{,}000$. It shows that,in this case,the fluid starts at early times to move toward the heated wall and after a while to the core region and then finally towards the adiabatic wall.However, Fig.45 shows that for case(O) the variation with time of the radial movement of fluid is opposite to that presented in Fig. 44.

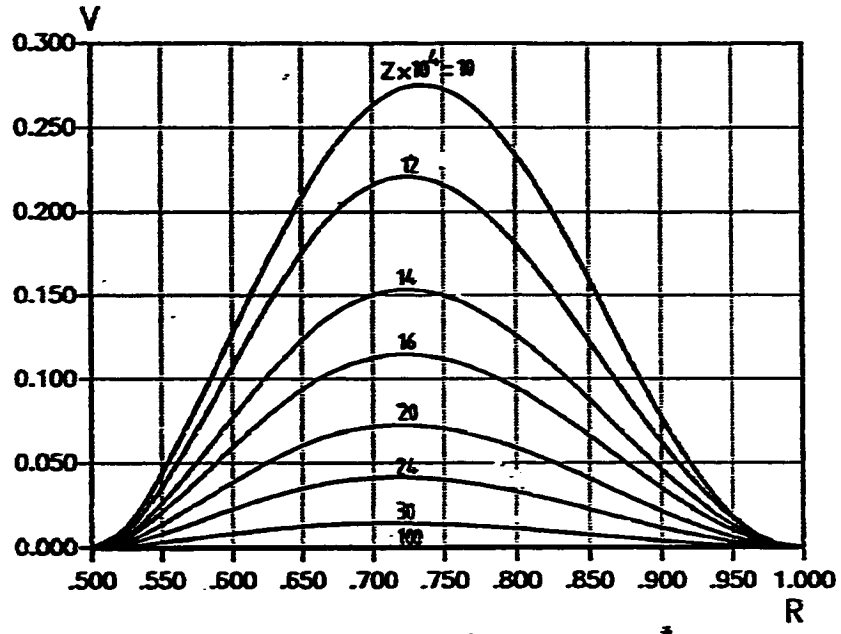

FIG. 26 V versus R for different Z's,at $\bar{t}$ = 0.2,case(I) ,G_r^*=100,N=0.5

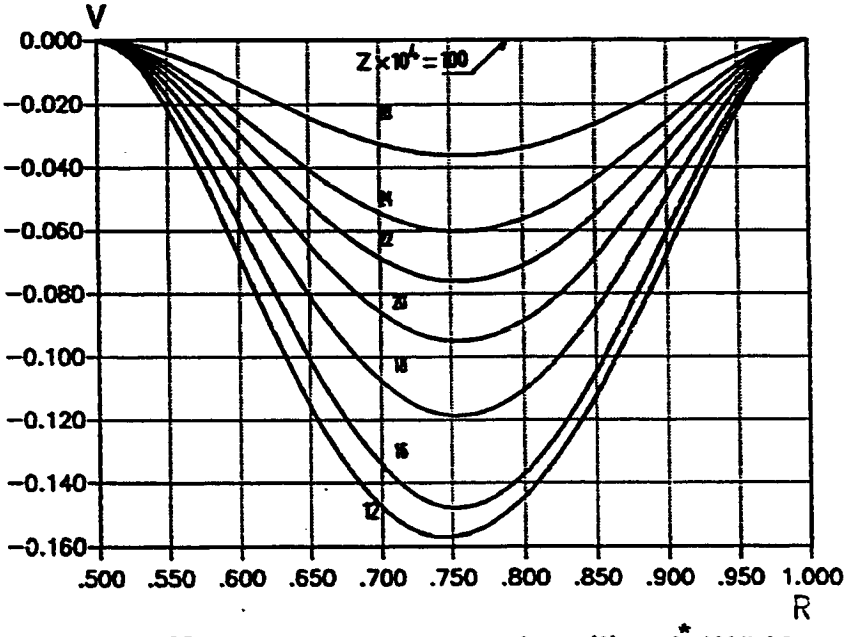

FIG. 27 V versus R for different Z's at t = 0.2,case(0) ,G_r^*=100,N=0.5

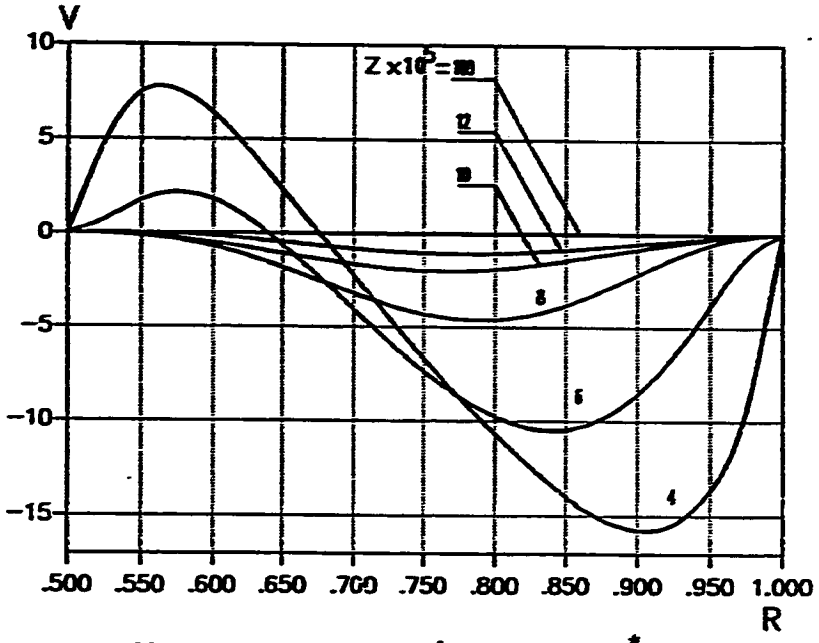

FIG. 28 V versus R for different Z's ,at τ = 0.1,case(1) ,G^*=1000,N=0.5

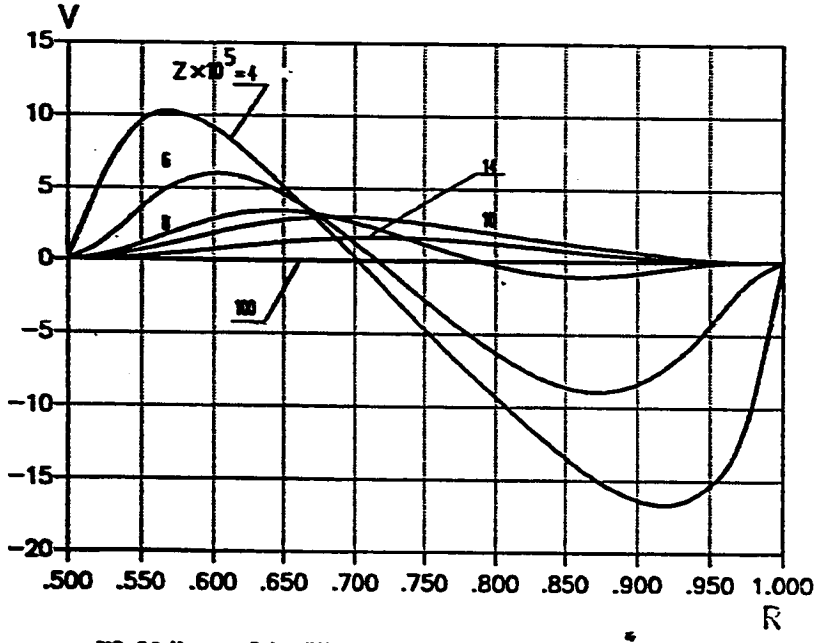

FIG. 29 V versus R for different Z's at t = 0.1,case(0) ,G^*=1000,N=0.5

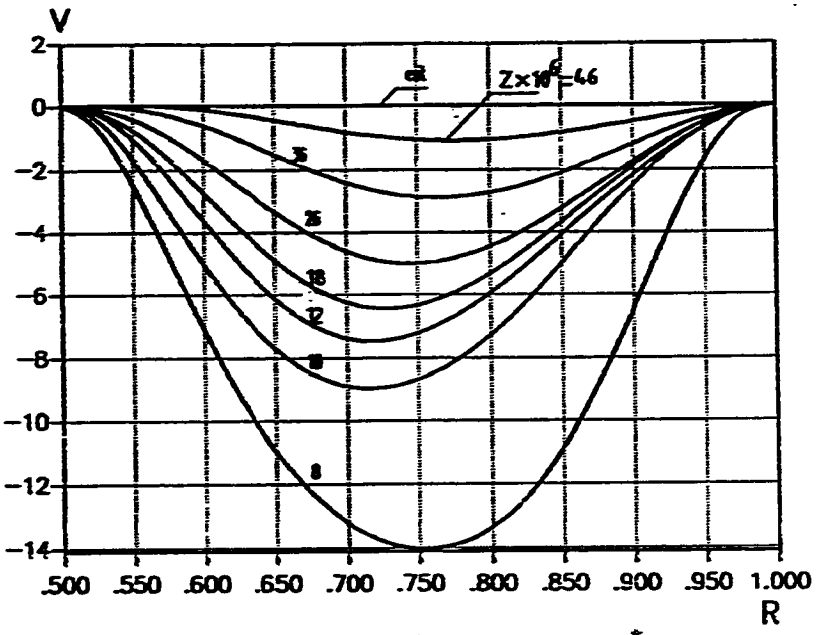

FIG. 30 V versus R for different Z's, at t = 0.02,case(0) , Gr=10,000,N=0.5

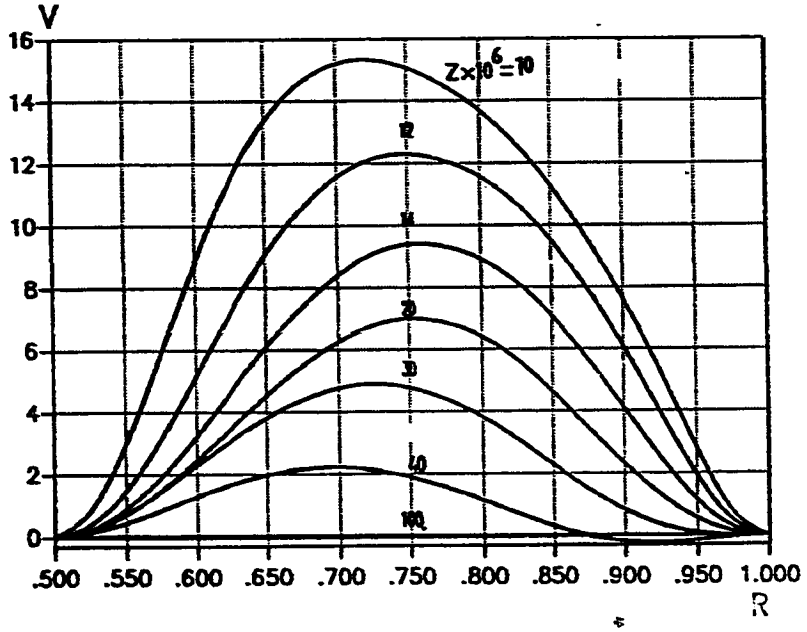

FIG. 31 V versus R for different Z's at t = 0.02,case(0) , Gr=10,000,N=0.5

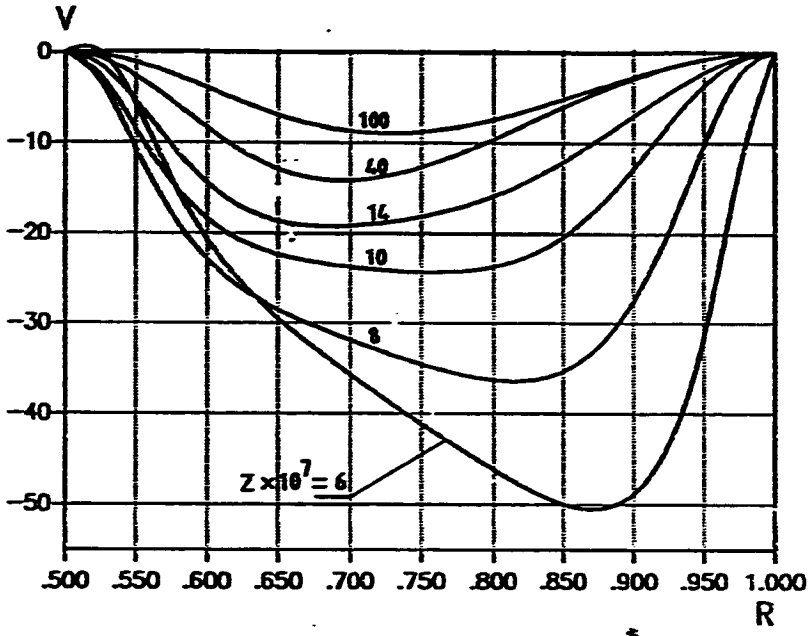

FIG. 32 V versus R at different Z positions,at t = 0.02,case(0) Gr^*=100,000,N=0.5

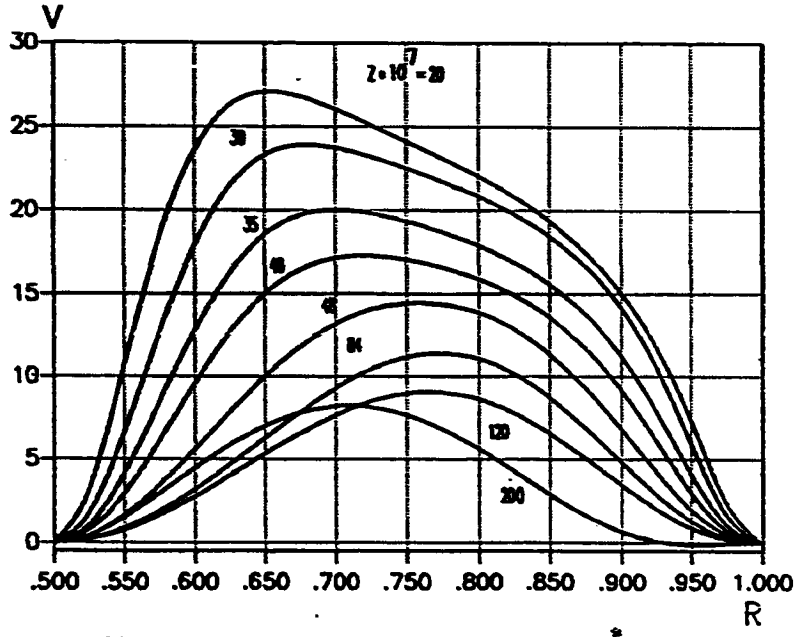

FIG.33 V versus R for different Z's at t = 0.02,case(0) Gr^*=50,000,N=0.5

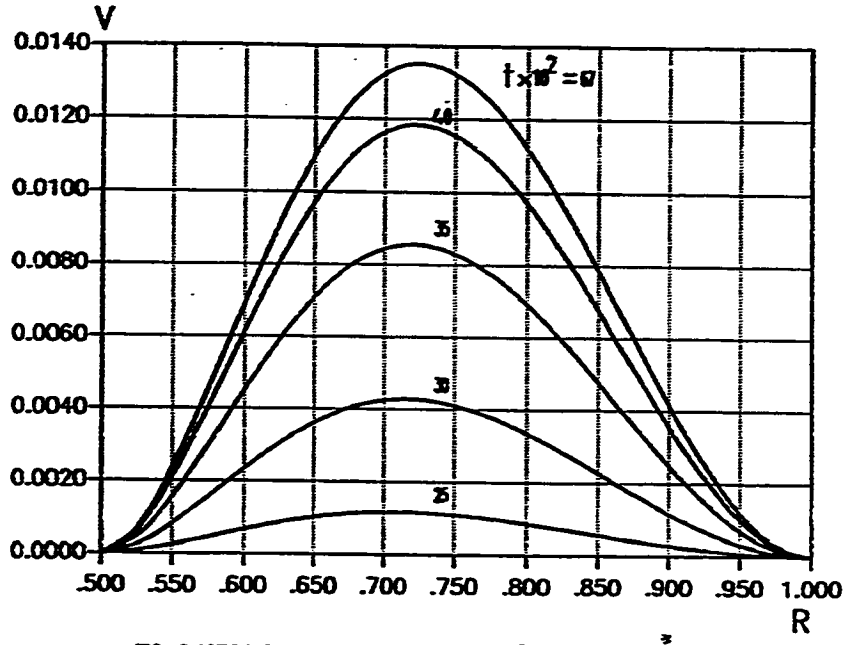

FIG. 34 Mid-height V versus R for different τ ,case(I) ,Gr^*=100,N=0.5

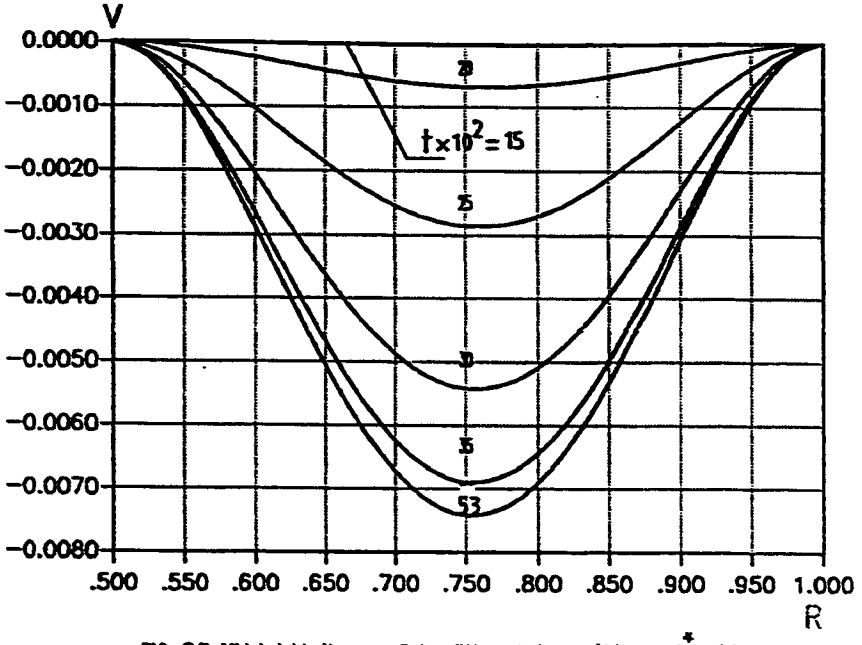

FIG. 35 Mid-height V versus R for different t ,case(O) ,Gr^*=100,N=0.5

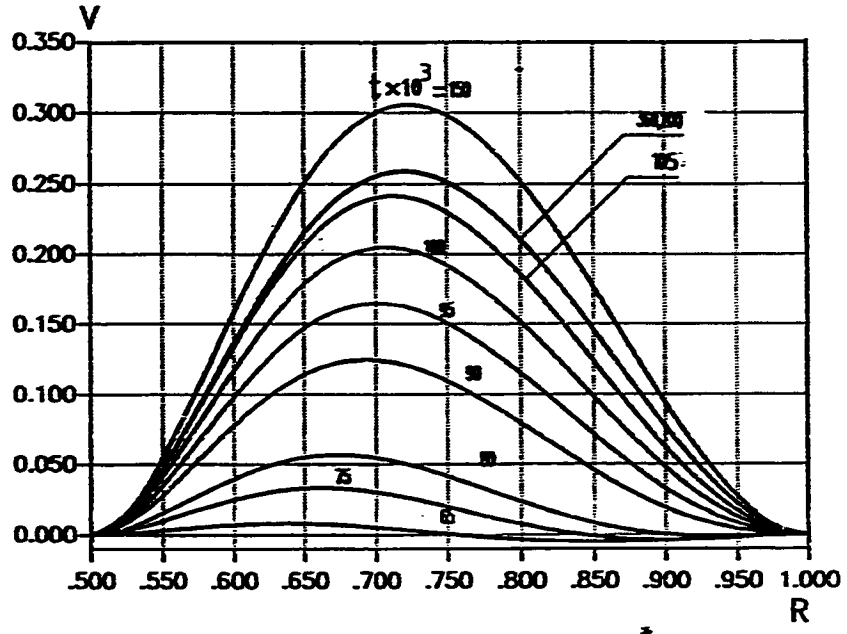

FIG. 36 Mid-height V versus R for different $\dagger$,case(i) ,$\overset{*}{Gr}$=1000,N=0.5

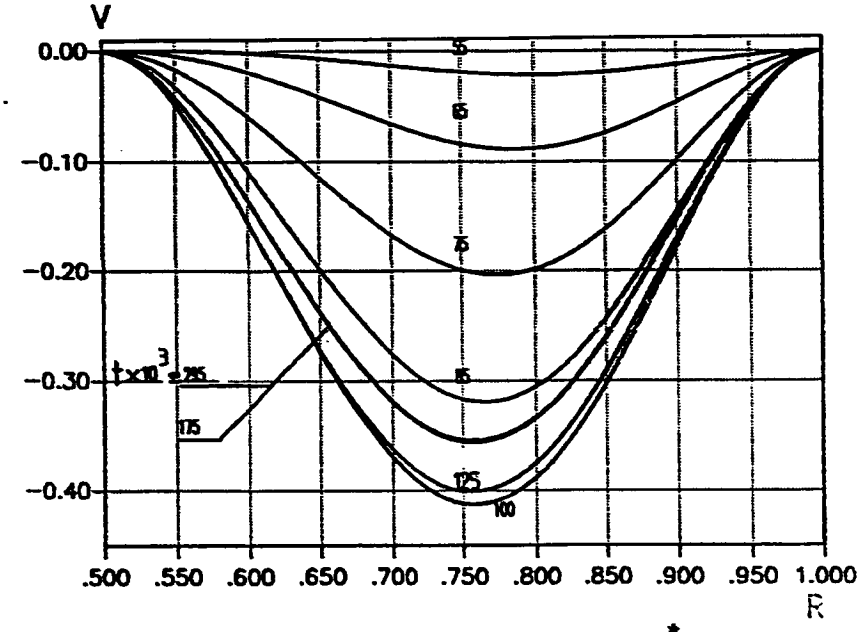

FIG. 37 Mid-height V versus R for different t ,case(ii) ,$\overset{*}{Gr}$=1000,N=0.5

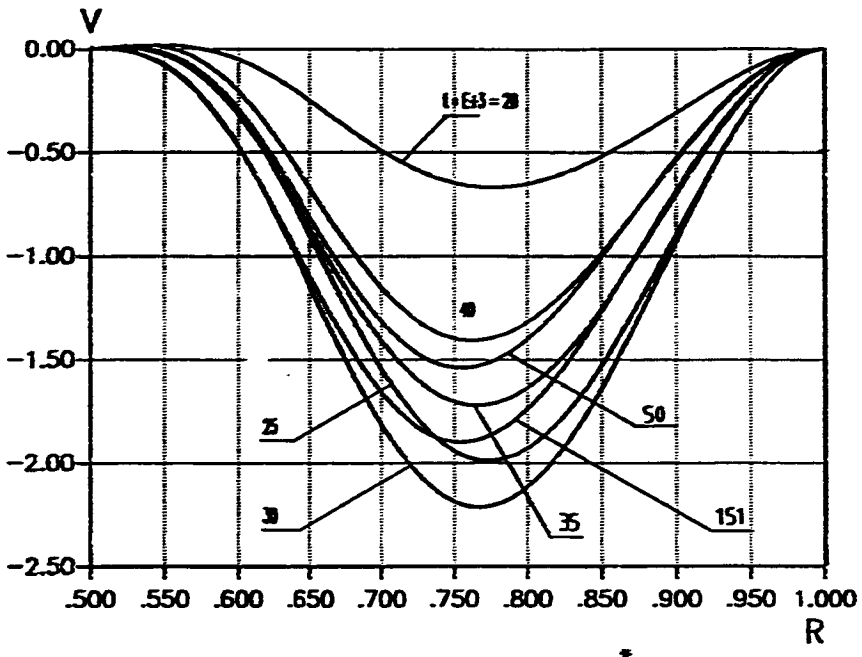

FIG. 38 Mid-height V versus R for different t,case(i),Gr*=10,000,N=0.5

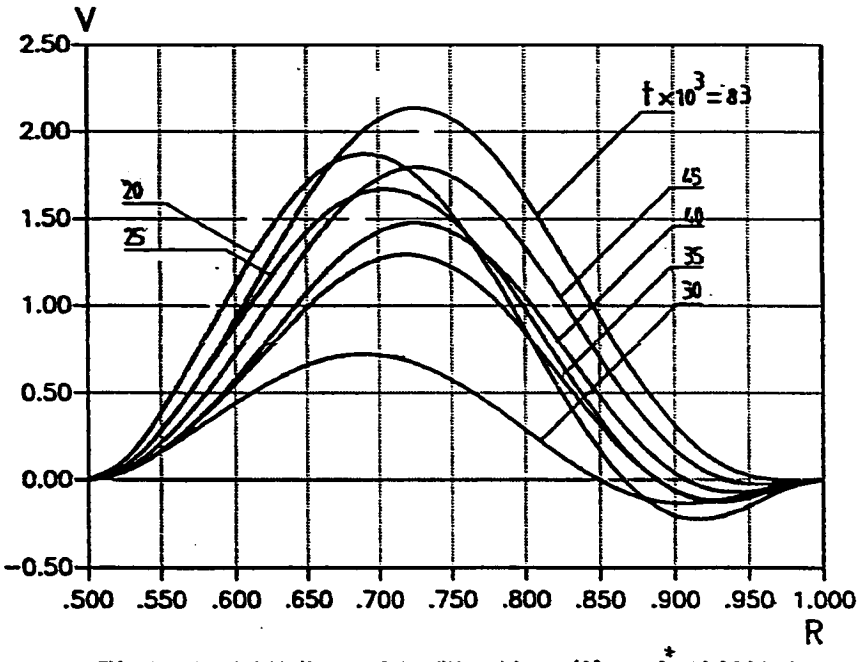

FIG. 39 Mid-height V versus R for different t ,case(i) , Gr*=10,000,N=0.5

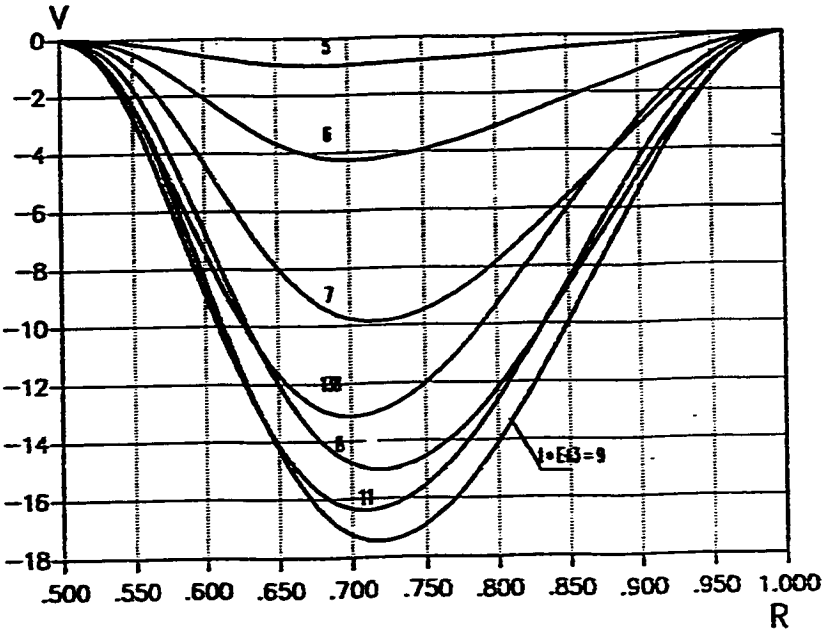

FIG. 40 Mid-height V verses R for different t,case(0),Gr^*=100,000,N=0.5

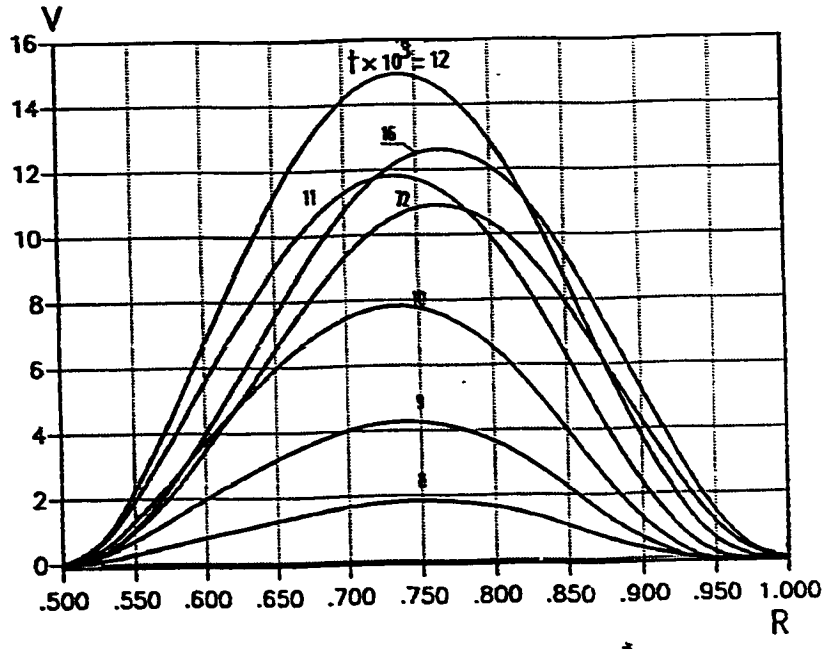

FIG.41 Mid-height V versus R for different t ,case(0) ,Gr^*=50,000,N=0.5

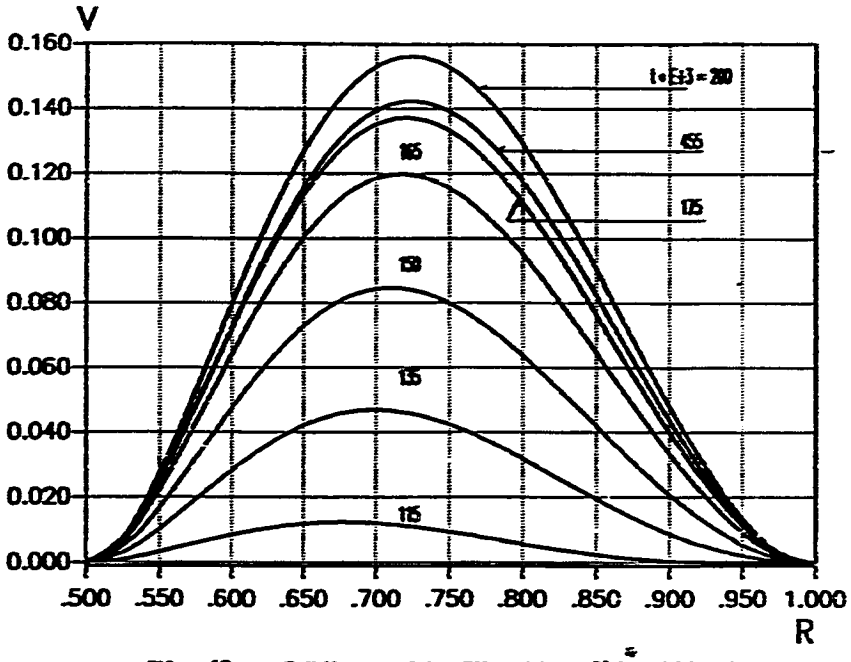

FIG. 42 Exit V versus R for different t,case(0),$\tilde{Gr}$=1000,N=0.5

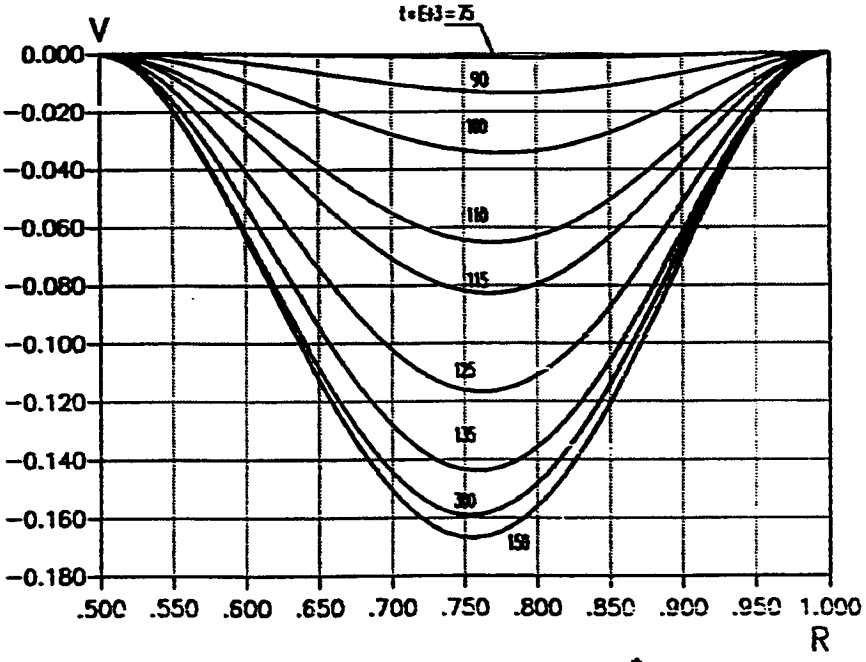

FIG. 43 Exit V versus R for different t,case(0),$\tilde{Gr}$=1000,N=0.5

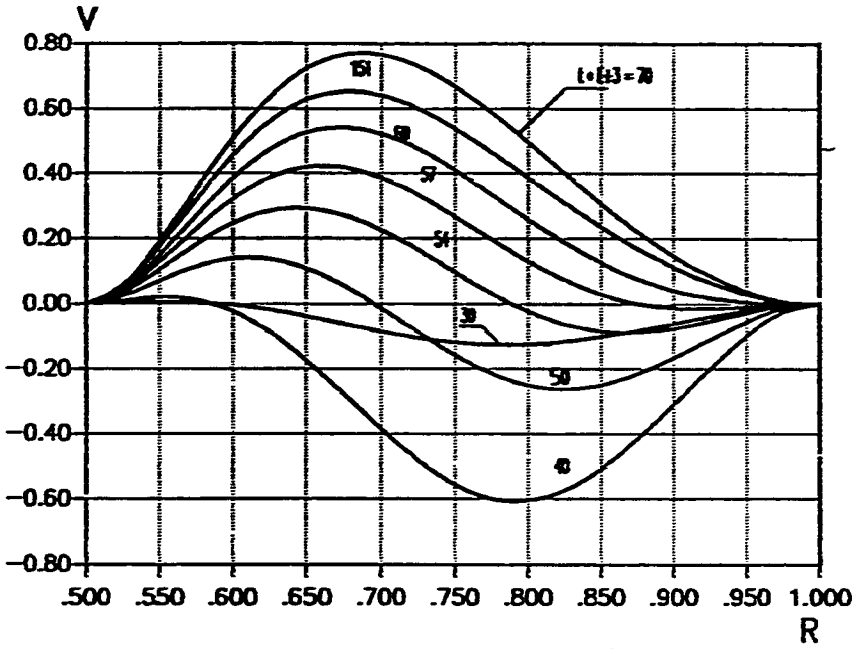

FIG. 44 Exit V versus R for different t,case(0),Gr=10,000,N=0.5

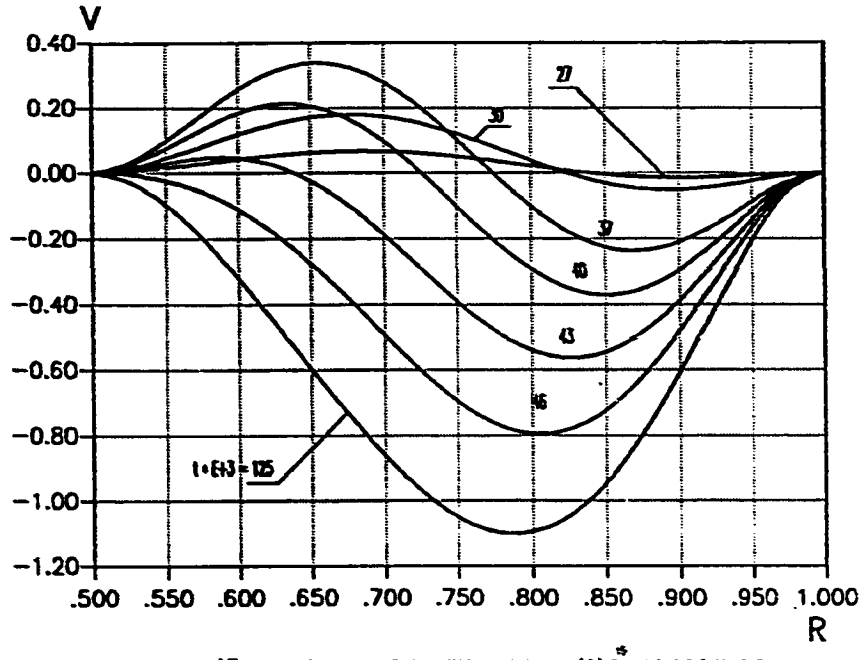

FIG. 45 Exit V versus R for different t,case(0),Gr=10,000,N=0.5

5.3.3 Temperature Profiles

For the five investigated values of Gr^* (4 , 100 , 1000 , 10,000 , 50,000 or 100,000), Figs. 46 through 53 present the dimensionless temperature profiles across the annular gab. Each figure is for a given time and the profiles are drawn for different values of the dimensionless axial distance. All these figures show that the value of the temperature (θ) , generally ,increases with height and decreases radially from a value of 1 at the heated wall to a minimum at the adiabatic wall. Steady state temperature profiles have larger values for smaller modified Grashof numbers (Gr^*) . This is because for lower values of Gr^* the flow has enough length, from the entrance till the exit, to gain more heat than in the case of higher Gr^* . The dimensionless temperature (θ) could reach the value of 1 over the entire gab width for $Gr^*=4$ in both cases (I) and (O). This is the case where hydrodynamic and thermal full development is achieved .

Figures 54 through 63 present the variation of the mid-height temperature profiles with time and Figs. 64 through 67 present such variation at the exit cross section for different values of Gr^*. Figures 62 and 63 show that mid-height temperature values increase to a maximum and then decrease to steady state values. This phenomenon is called the temperature overshoot and it is due to the domination of conduction at early times. Such a phenomenon is well known in the field of transient free convection [e.g.6,22and23]. In this case (at early times

) the diffusion terms on the RHS of the energy equation (11) are dominant and the convection terms on the LHS of this equation are negligible.The heat transfer process follows the conduction pattern and the heat transfer coefficient decreases accordingly with time to values lower than the steady state convection value.Thus ,the temperature becomes higher than the corresponding steady-state convection temperature .However,when the convection starts the heat transfer coefficient increases and the temperature therefore decreases until it reaches steady-state value.

The overlapping and intersections of the temperature profiles presented in Figs. 60 and 61 are due to the presence of backflow at the corresponding modified Grashof numbers.

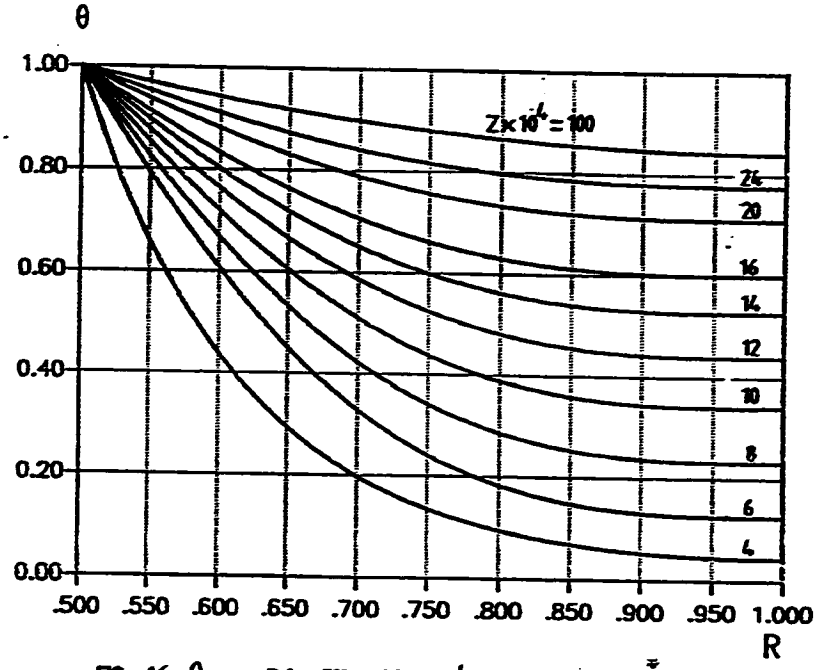

FIG. 46 θ versus R for different Z's,at $\dagger$ = 0.2,case(i) . ,Gr=100,N=0.6

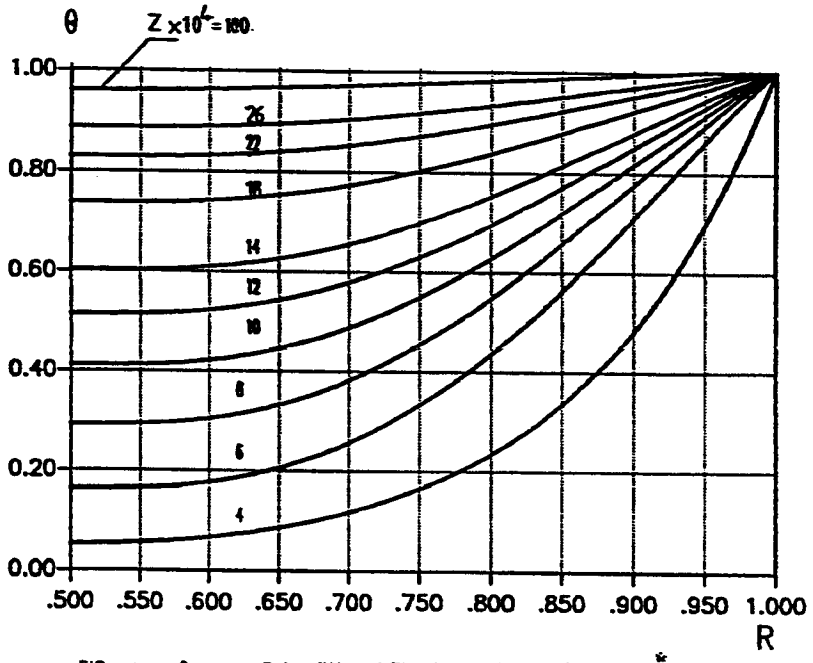

FIG. 47 θ versus R for different Z's at t = 0.2,case(0) ,Gr=100,N=0.6

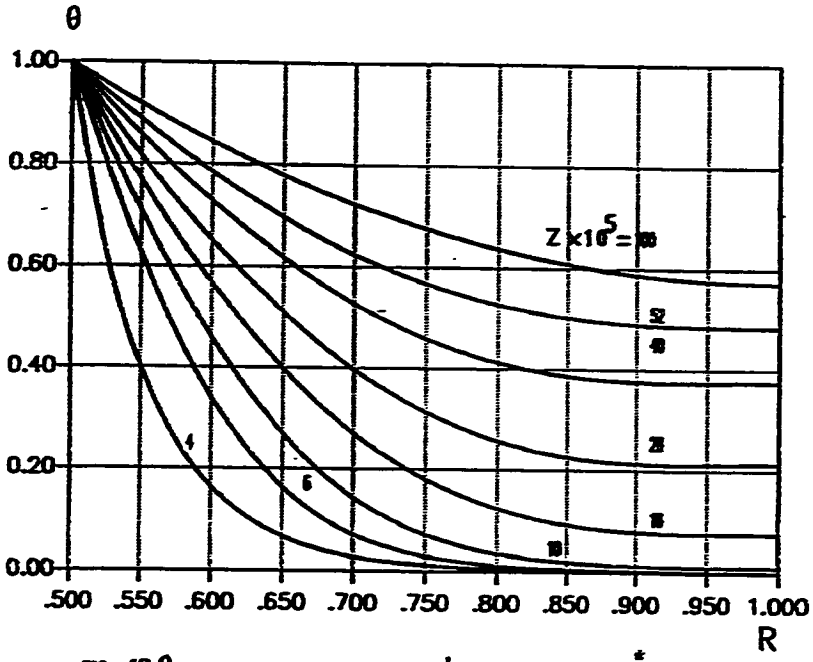

FIG. 48 θ versus R for different Z's,at $\dot{t}$ = 0.1,case(I) G_r^*=1000,N=0.5

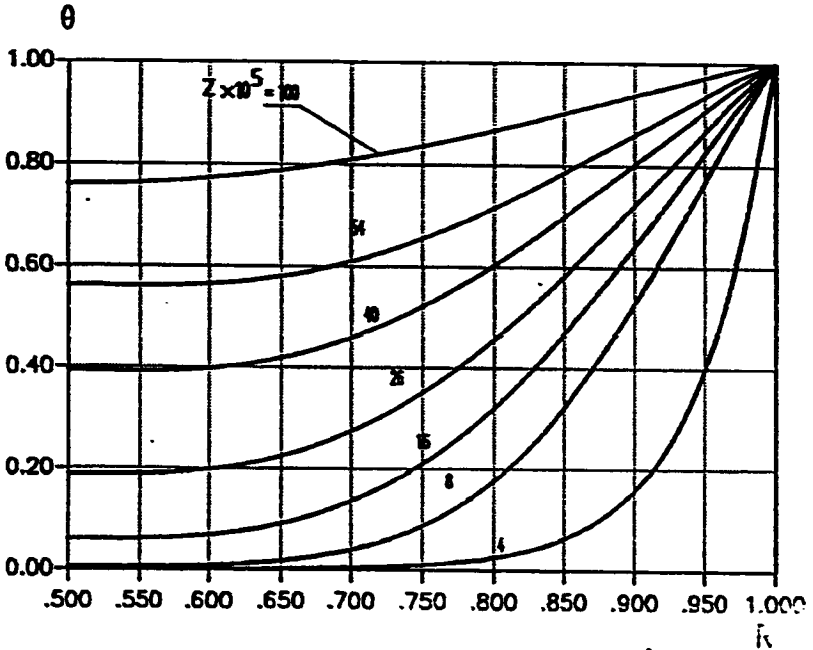

FIG. 49 θ versus R for different Z's at t = 0.1,case(0) G_r^*=1000,N=0.5

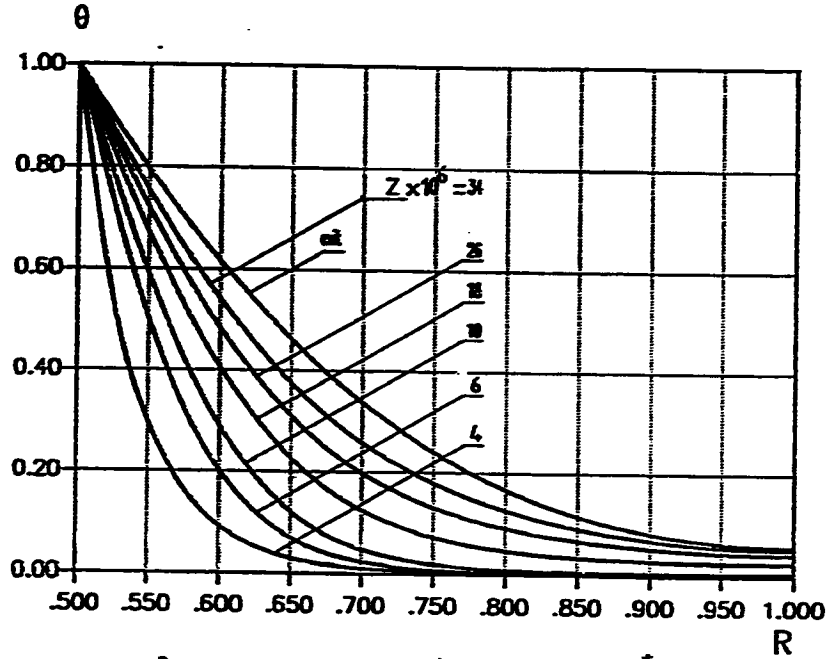

FIG. 50 θ versus R for different Z's, at t = 0.02,case(I) *,Gr=10,000,N=0.5

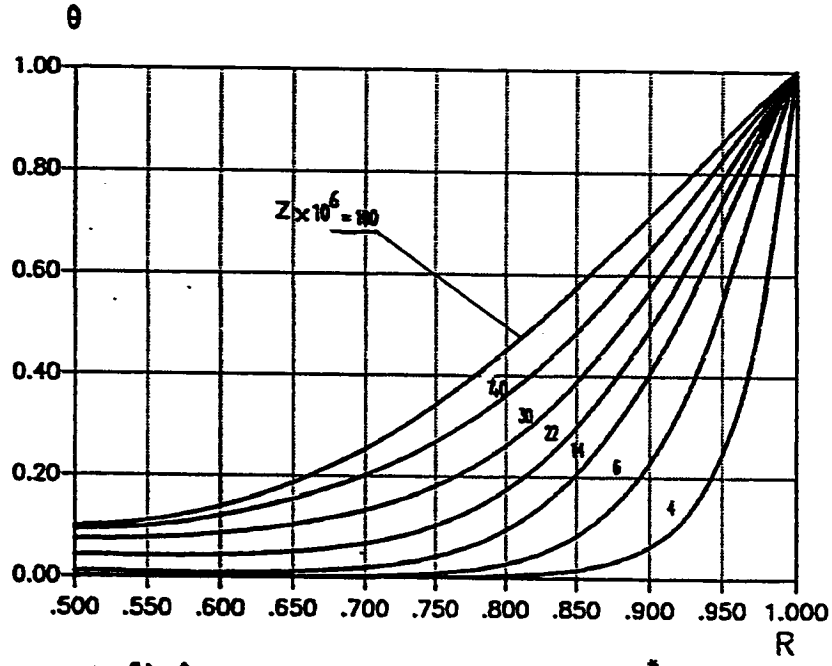

FIG. 51 θ versusR for different Z's at t = 0.02,case(0) *,Gr=10,000,N=0.5

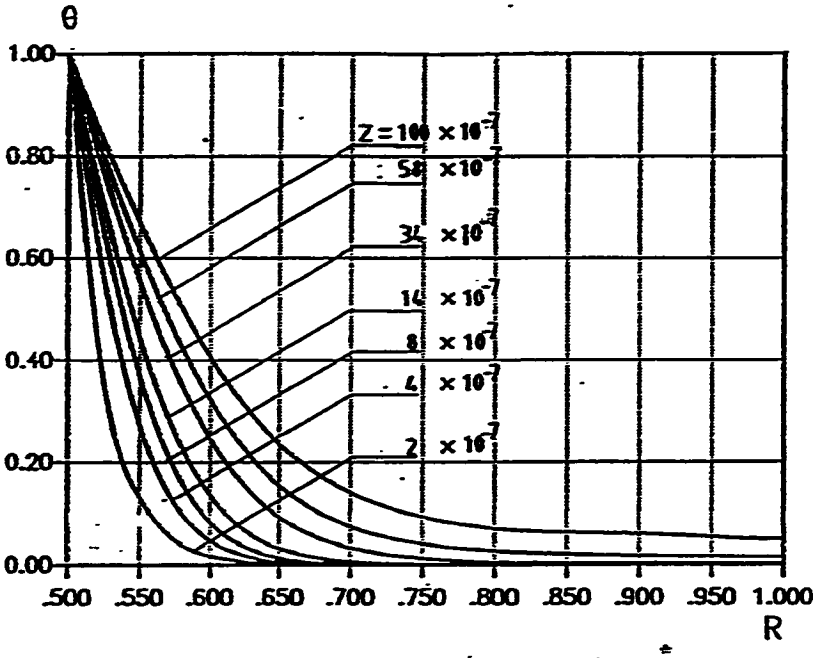

FIG. 52 θ versus R at different Z positions at $\bar{t}$ = 0.02,case(I) Gr=100,000,N=0.5

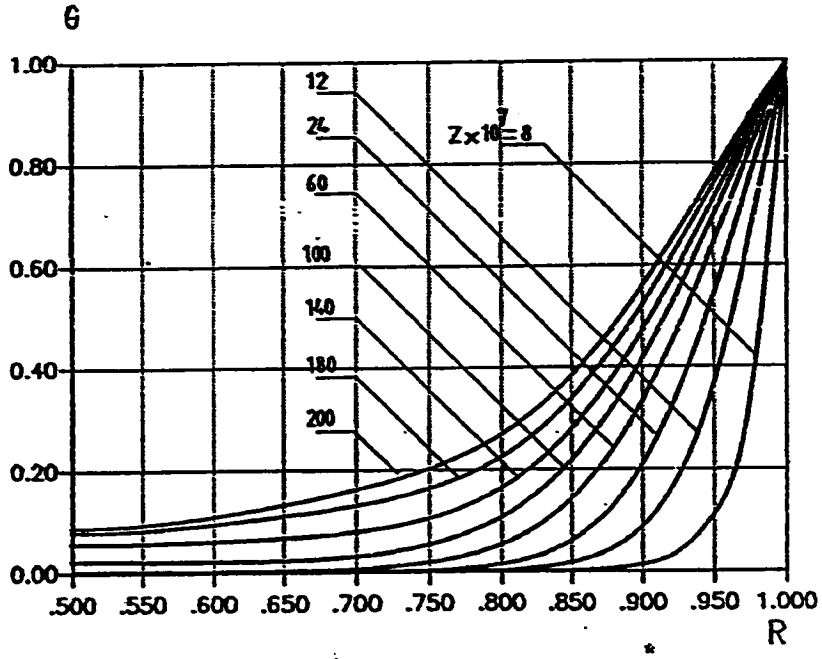

FIG. 53 θ versus R for different Z's at t = 0.02,case(0) Gr=50,000,N=0.5

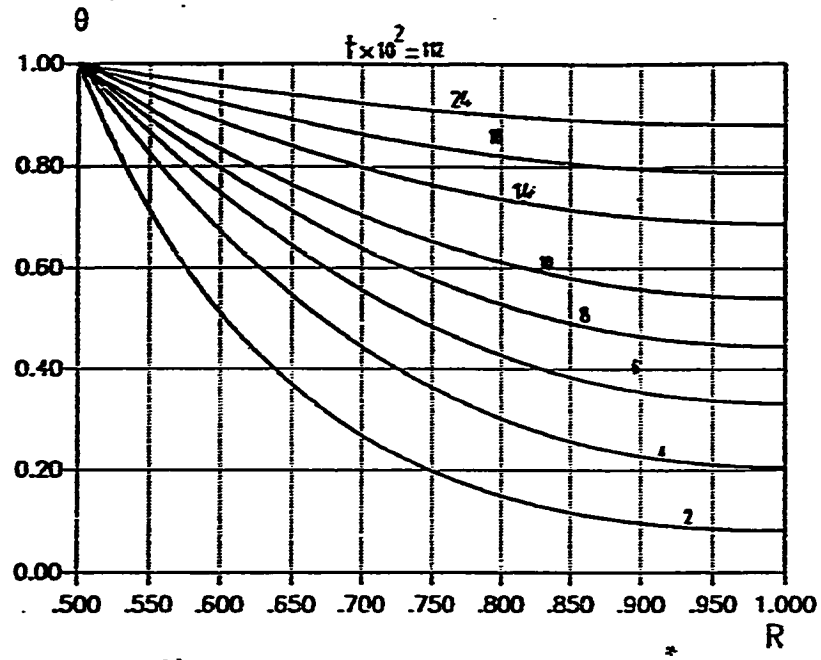

FIG. 54 Mid-height θ versus R for different t*,case(I) Gr=4,N=0.5

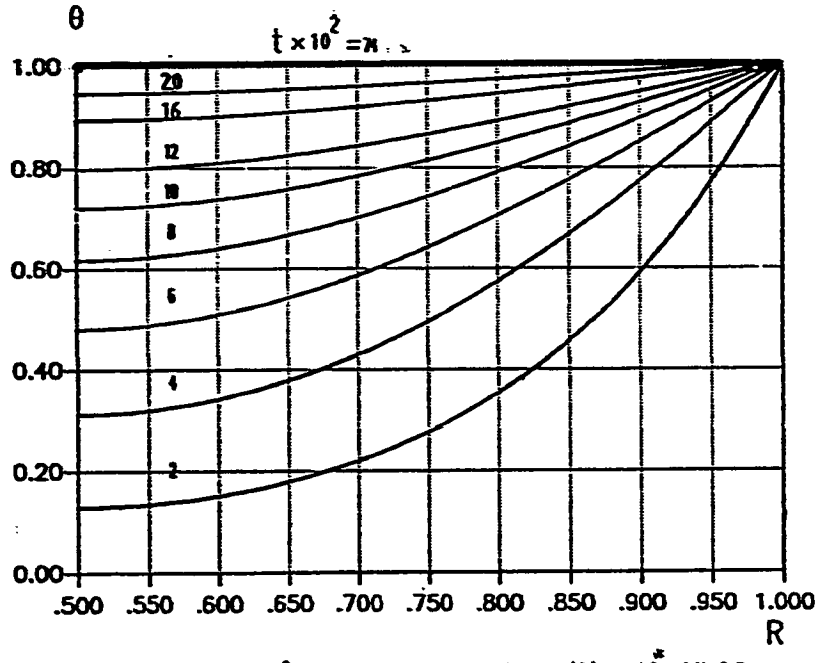

FIG 55 Mid-height θ versus R for different t*,case(0), Gr=4,N=0.5

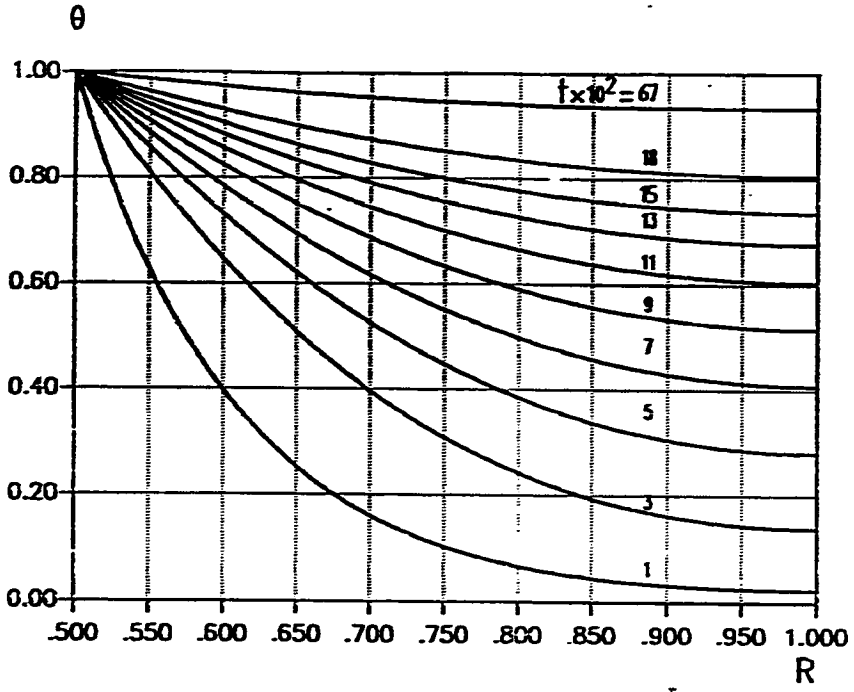

FIG. 56 Mid-height θ versus R for different t ,case(I) ,Gr=100,N=0.5

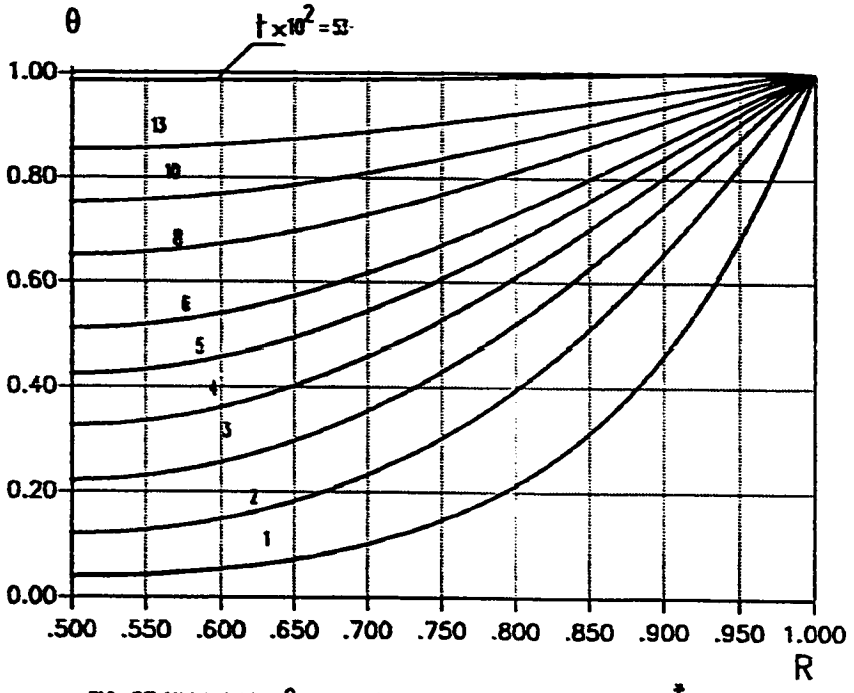

FIG. 57 Mid-height θ versus R for different t ,case(O) ,Gr=100,N=0.5

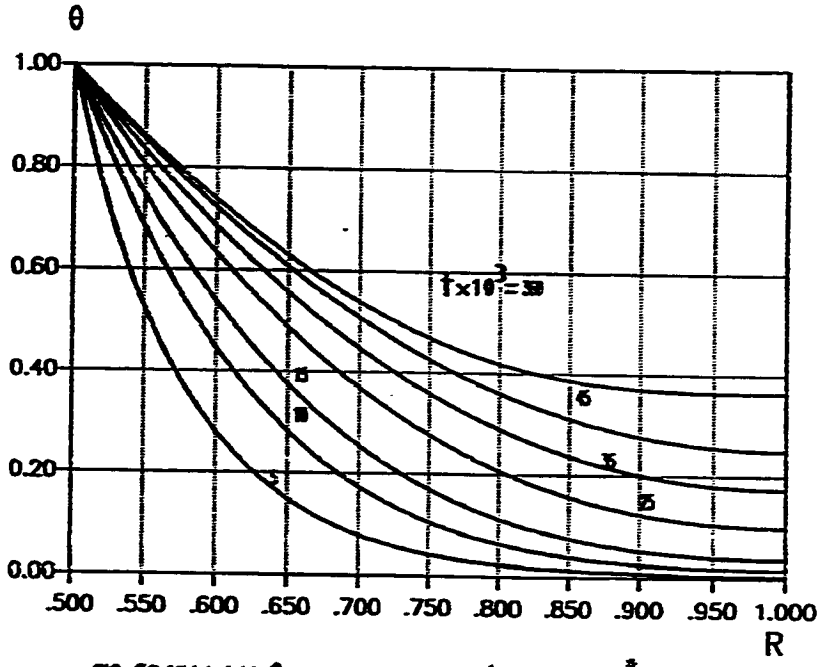

FIG. 58 Mid-height θ versus R for different † ,case(I) ,$\overset{*}{Gr}$=1000,N=0.5

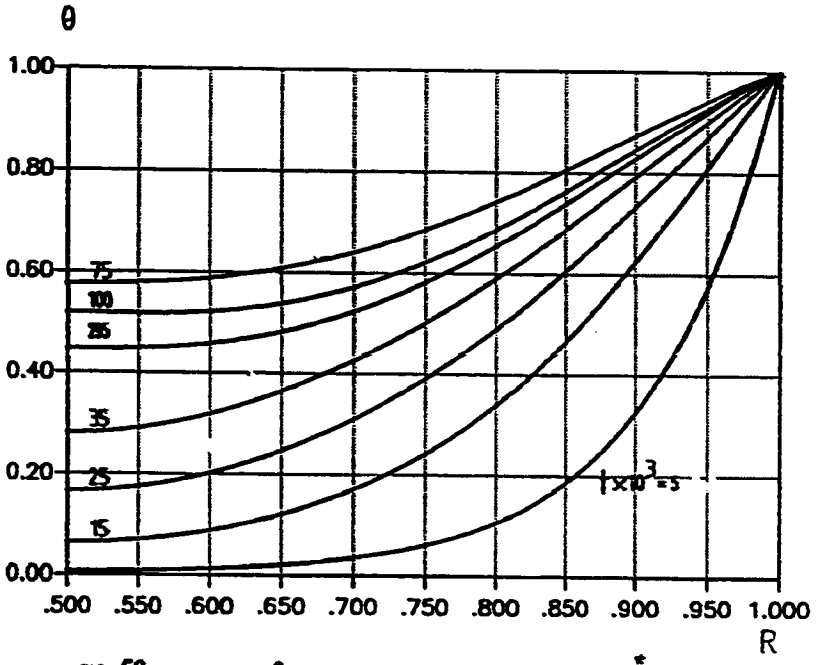

FIG. 59 Mid-height θ versus R for different t ,case(0) ,$\overset{*}{Gr}$=1000,N=0.5

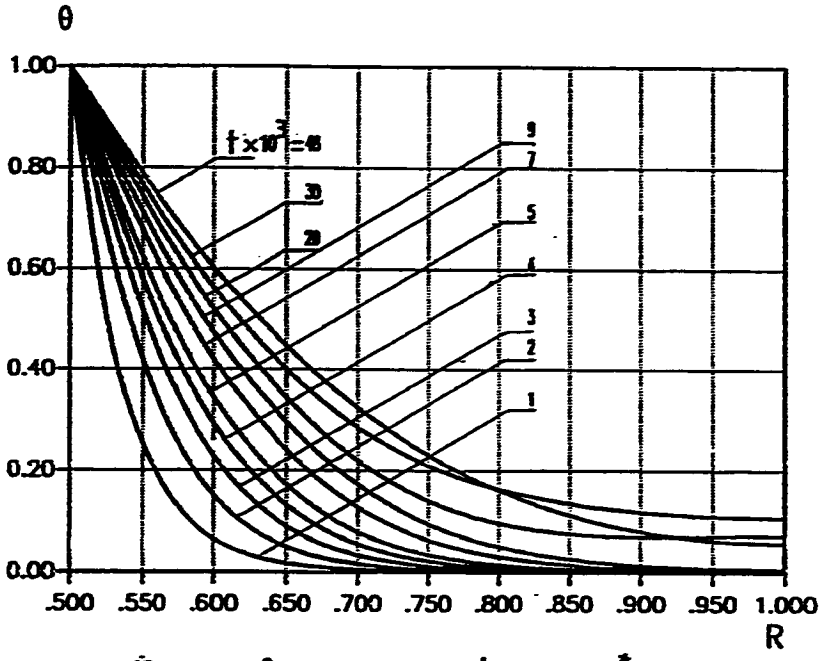

FIG. 6 Mid-height θ versus R for different τ ,case(i) Gr^*=10,000,N=0.5

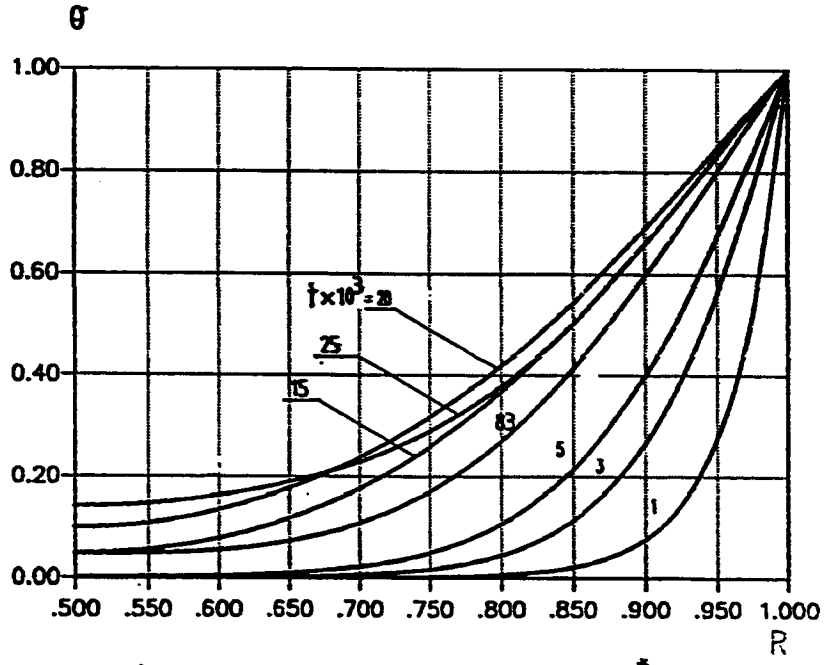

FIG. 7 Mid-height θ versus R for different τ ,case(ii) Gr^*=10,000,N=0.5

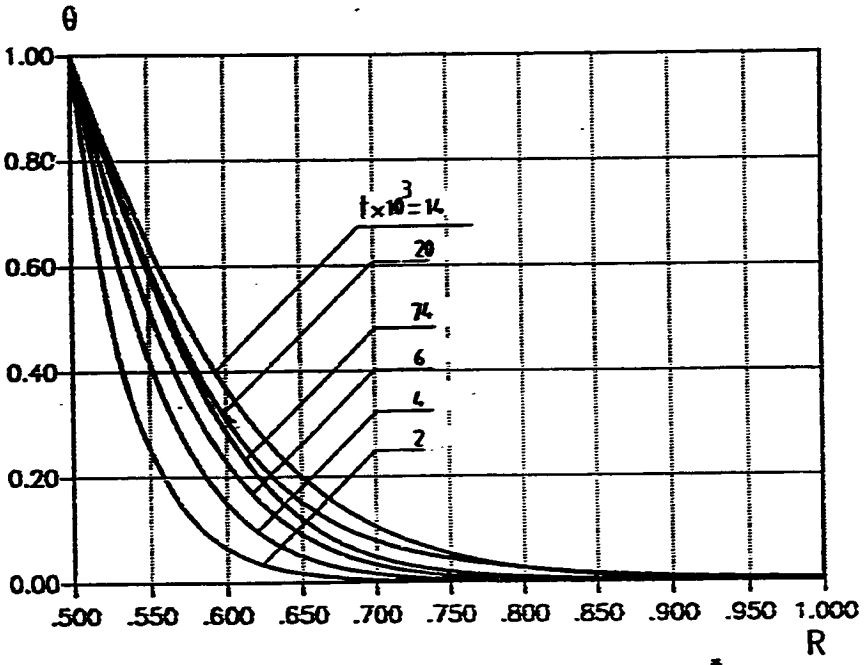

FIG. 62 Mid-height θ versus R for different t ,case(I) .,Gr^*=100,000,N=0.5

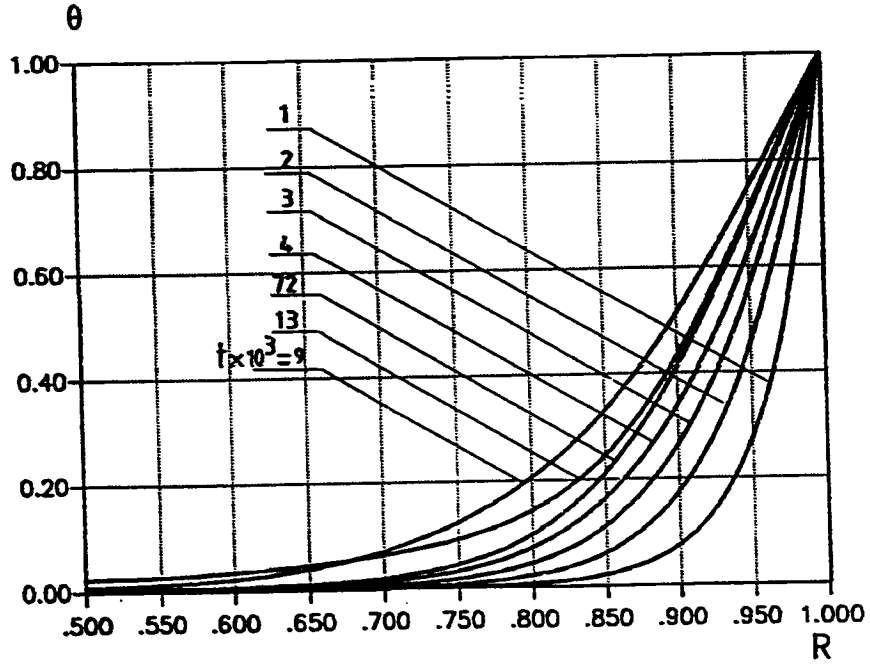

FIG. 63 Mid-height θ versus R for different t,case(0) ,Gr^*=60,000,N=0.5

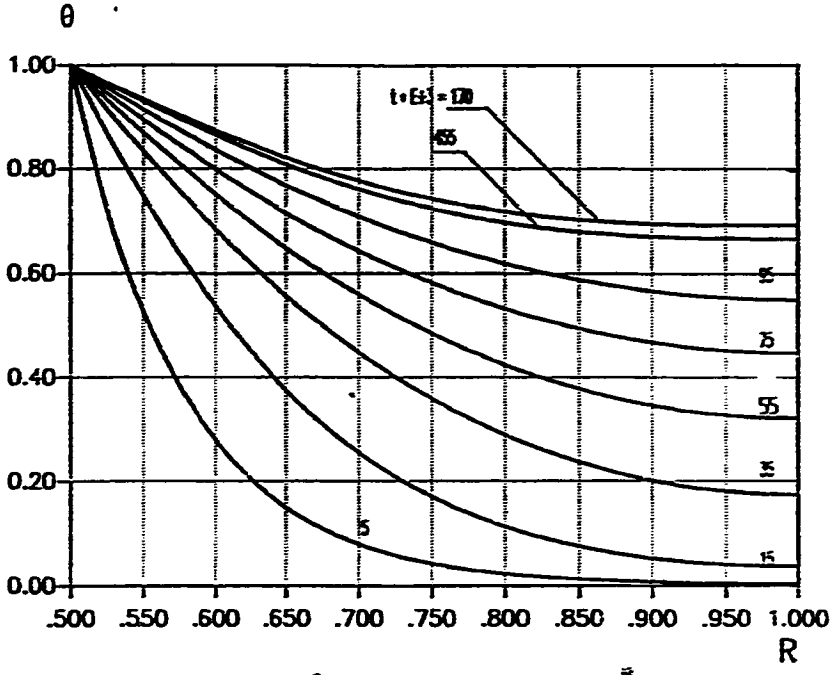

FIG. 64 Exit θ versus R for different t,case(I),$\overset{*}{Gr}$=1000,N=0.5

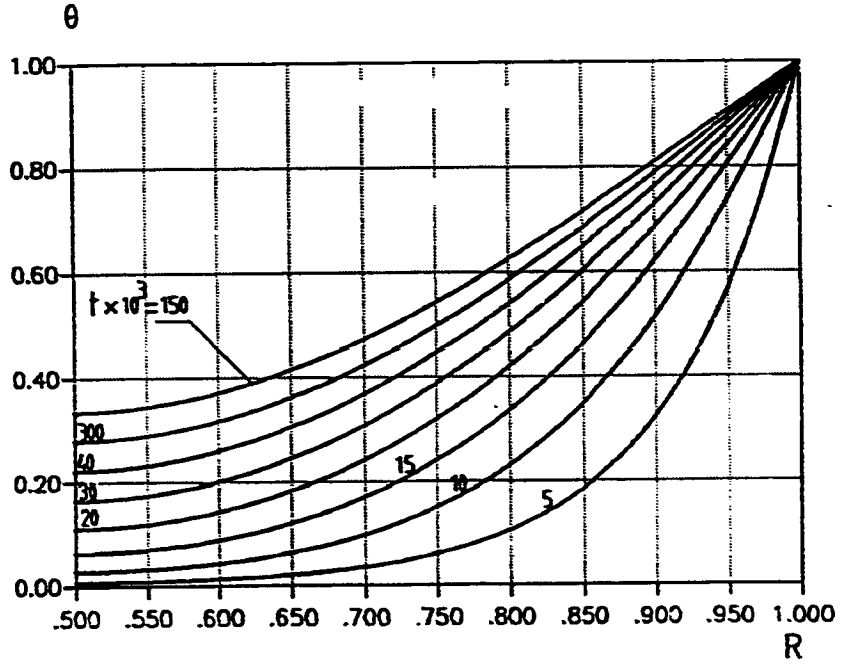

FIG. 65 Exit θ versus R for different t,case(O),$\overset{*}{Gr}$=1000,N=0.5

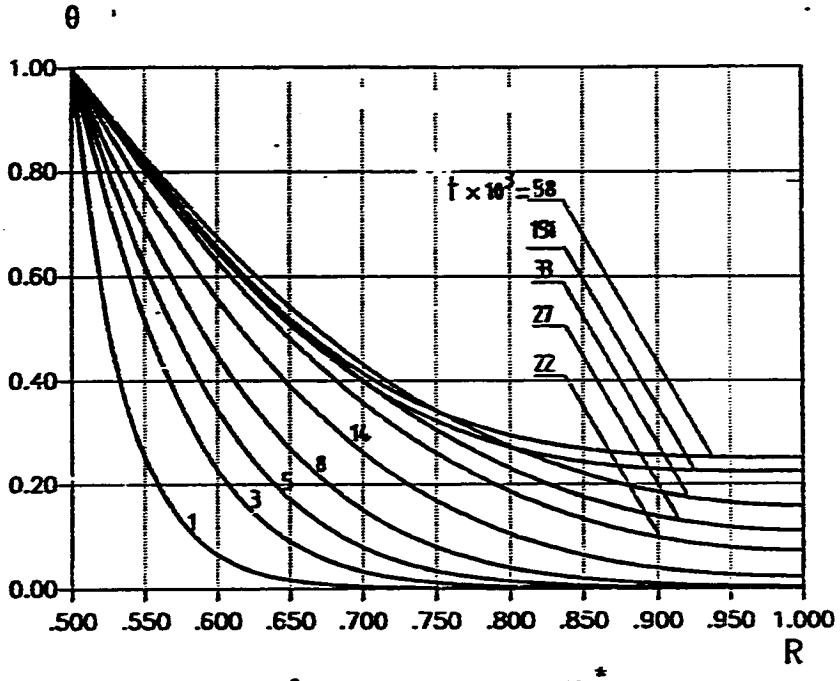

FIG. 66 Exit θ versus R for different t,case(1),Gr^*=10,000,N=0.5

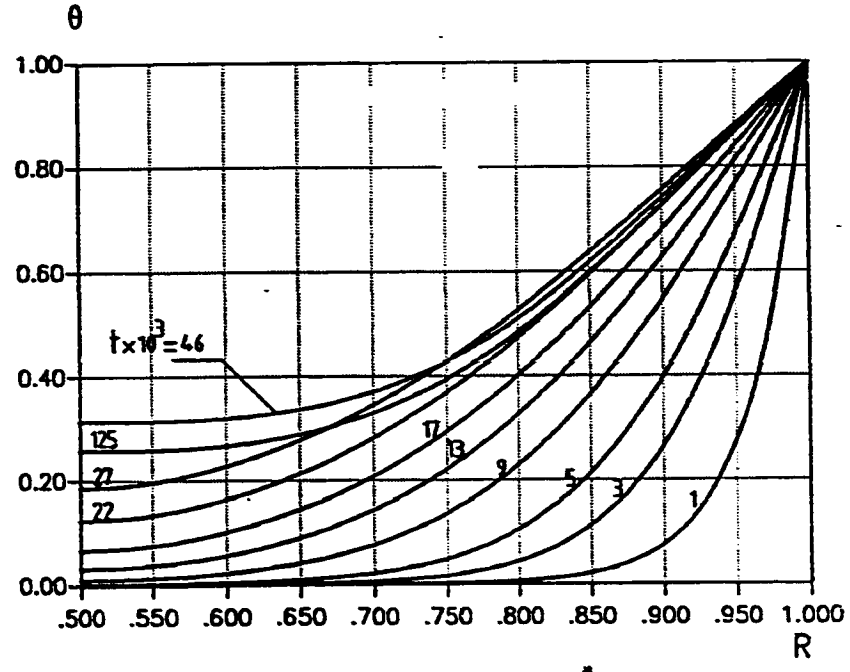

FIG. 67 Exit θ versus R for different t,case(0),Gr^*=10,000,N=0.5

5.3.4 Pressure Distribution Along the Annulus

Figures 68 through 77 present the time variation of the dimensionless pressure defect (P) with the dimensionless axial distance (Z) for the investigated values of Grashof number (Gr^*) in both cases (I) and (O) . In accordance with the definition of the dimensionless annulus height L,any P-Z curve intersects the Z-axis at Z = L . For a given time ,the pressure decreases with axial distance ,from the entrance value of $(-U_o^2/2)$, to a minimum and then it increases to reach zero at the exit cross-section . This phenomenon may be explained by the fact that P is affected by two variables ,the buoyancy force and the wall and fluid friction (viscous force). In the entrance region ,buoyancy is small compared to friction and as a result P decreases with Z. As the fluid moves upwards and absorbs heat from the heated boundary, buoyancy develops until it becomes equal to the friction force at the axial distance where the pressure is minimum . Then the buoyancy force becomes larger than the friction force and hence the pressure increases.

On the other hand,it can be seen from these figures that, as Grashof number decreases, the axial locations at which the minimum pressures occur shift towards the entrance, i.e. at smaller values of Z/L., This is because for low values of Gr^* there is larger temperature differences and hence buoyancy develops faster. Moreover, the figures show that the pressure is decreasing with

time for any specific value of Z . This is because as time elapses the axial velocity increases causing the friction force to increase and this reduces the pressure for the same axial position.

For $Gr^* = 100{,}000$ in case(I) and $Gr^* = 50{,}000$ in case(O), respectively, Figs. 76 and 77 show that the axial pressure distribution for such high Grashof numbers become almost flat over part of the channel height.This is attributed to the backflows occurring in these cases.

Comparing the figures corresponding to cases (I) and (O), it can be seen seen that the steady state profiles are reached faster in case (O) than in case (I). So, at the same time and for the same value of Grashof number, the value of the minimum pressure for case (O) is always less than that in case (I) .

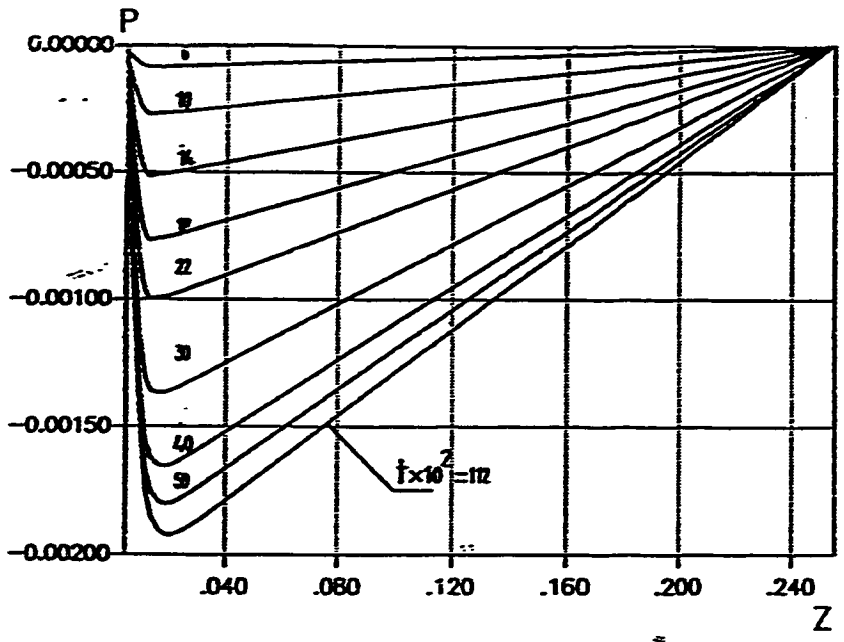

FIG. 68 P versus Z for different $\frac{t}{}$,case(i). ,Gr=4,N=0.5

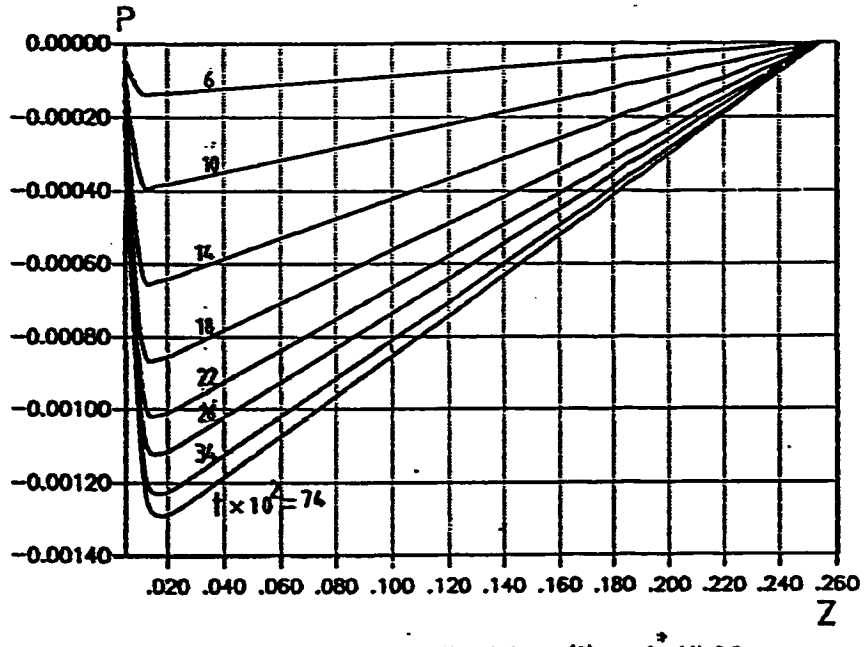

FIG. 69 P versus Z for different t ,case(i) . ,Gr=4,N=0.5

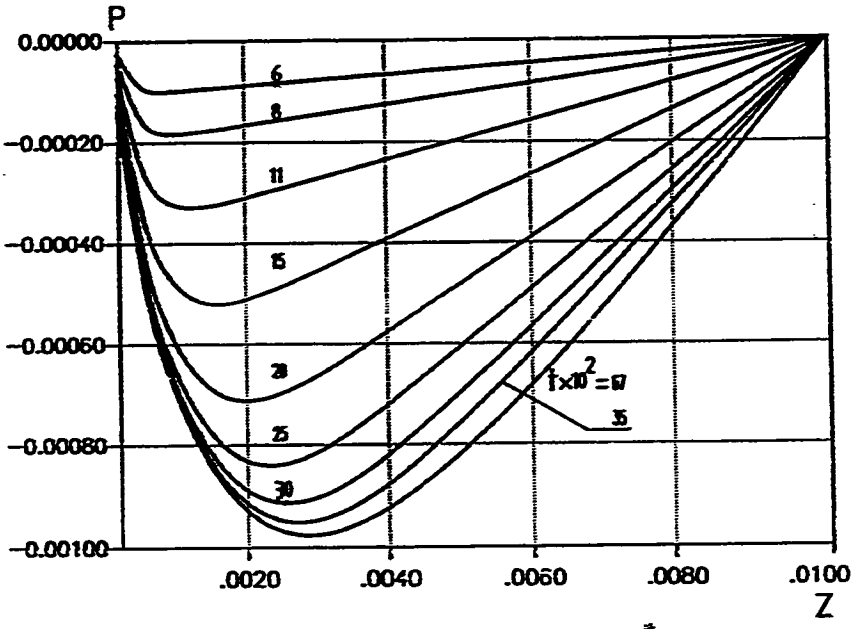

FIG. 70 P versus Z for different t ,case(1) ,$\overset{*}{Gr}$=100,N=0.5

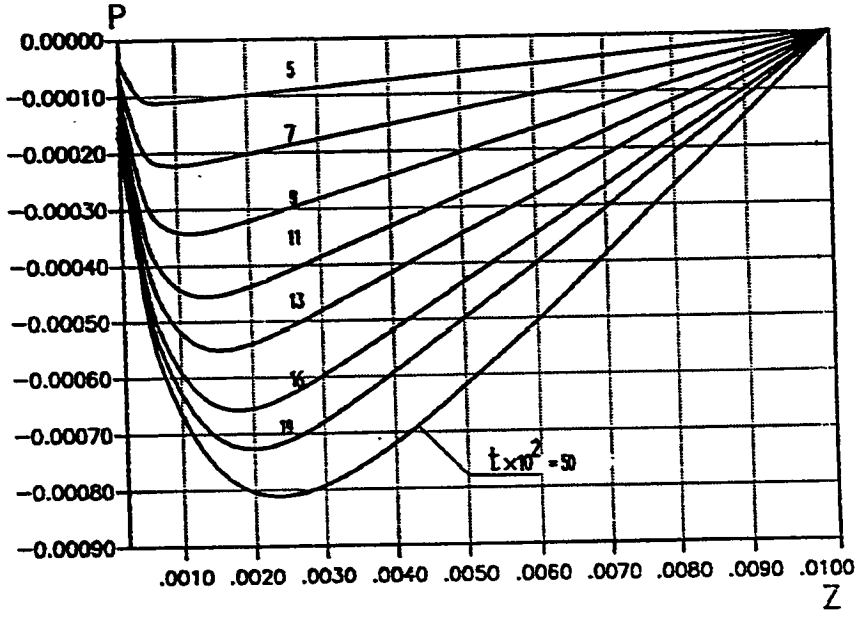

FIG. 71 P versus Z for different t ,case(0) ,$\overset{*}{Gr}$=100,N=0.5

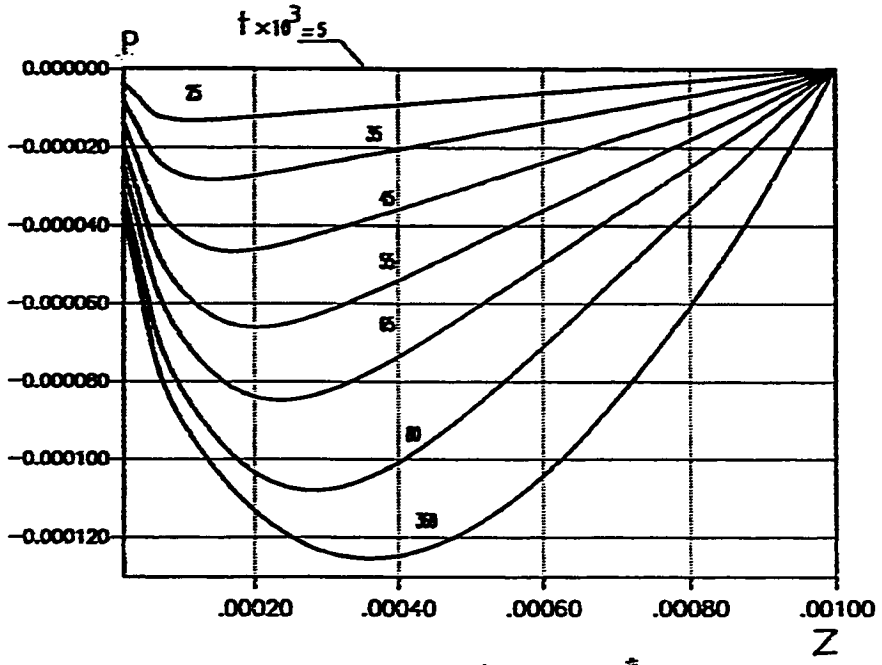

FIG. 72 P versus Z for different t ,case(I) $\overset{*}{Gr}$=1000,N=0.5

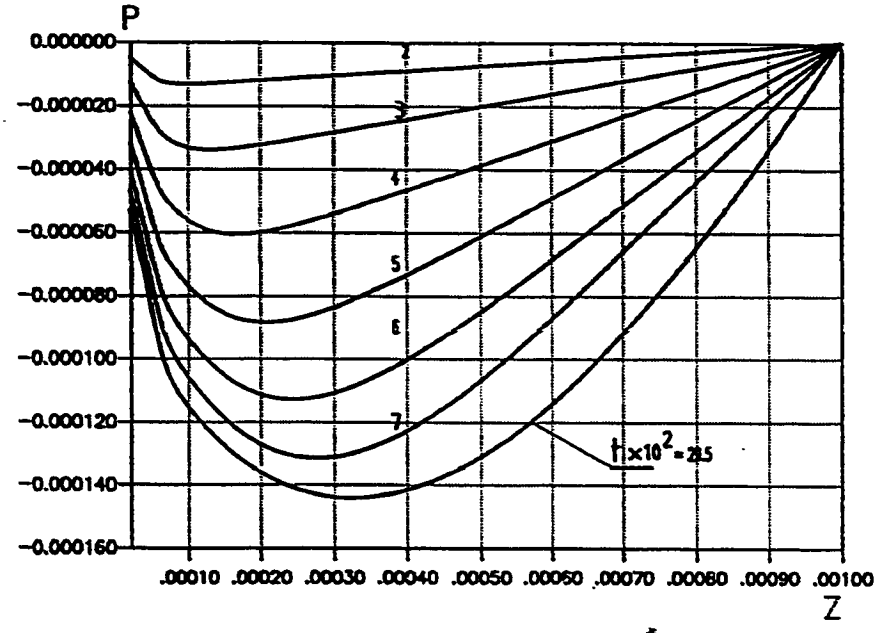

FIG. 73 P versus Z for different t ,case(0) $\overset{*}{Gr}$=1000,N=0.5

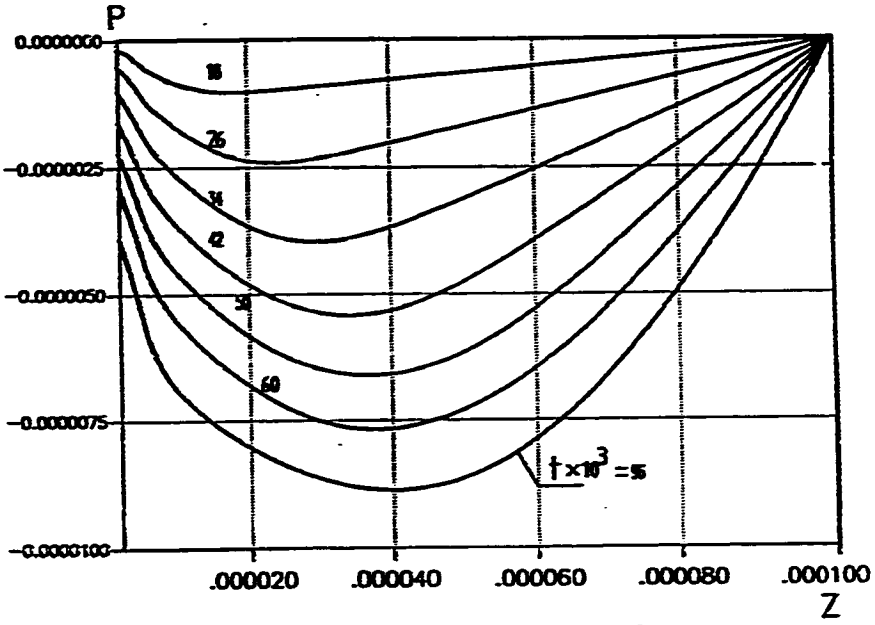

FIG. 74 P versus Z for different t ,case(I) $\overset{*}{Gr}$=10,000,N=0.5

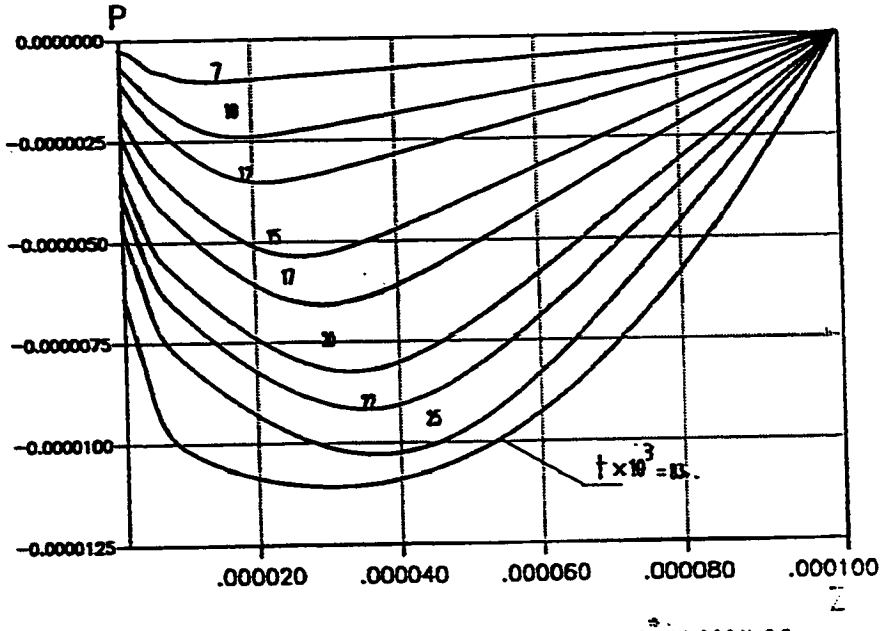

FIG. 75 P versus Z for different t ,case(C) $\overset{*}{Gr}$=10,000,N=0.5

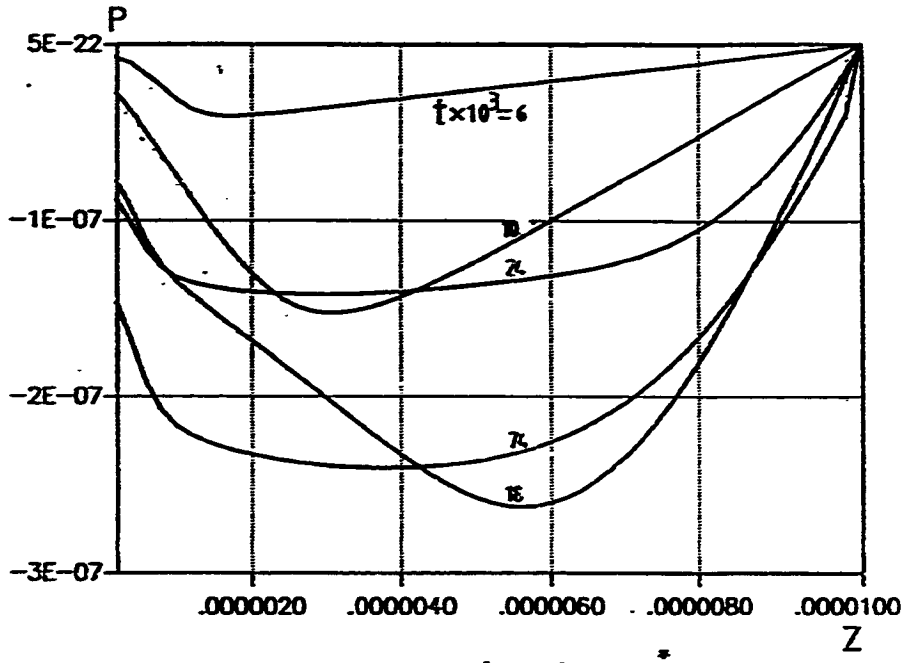

FIG. 76 P versus Z for different t ,case(i) ,Gr=100,000,N=0.5

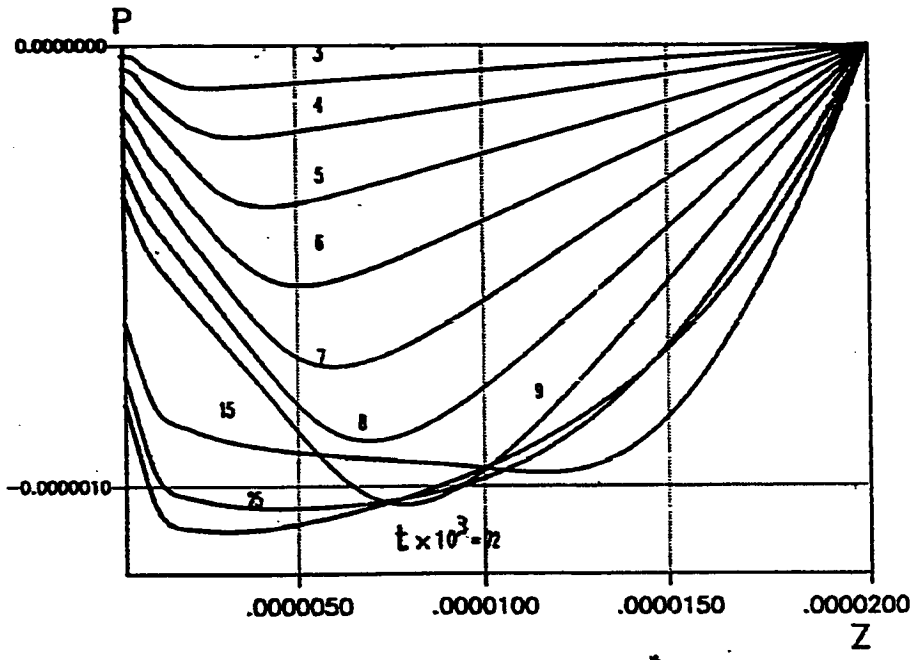

FIG. 77 P versusZ for different t ,case(0) ,Gr=50,000,N=0.5

5.3.5 Mixing Cup Temperature

One of the important engineering parameters is the mixing cup temperature at a cross section.Such a temperature can be used to calculate the amount of heat absorbed by the fluid from the entrance to the cross-section under consideration . The mixing cup temperature substitutes the local heat transfer coefficient (a) and the local Nusselt number (Nu), which require the calculation of the temperature-gradient at the wall and therefore are not so accurate in numerical solutions (particularly at early times after the step change in wall temperature). Similarly, knowing $\bar{\theta}_m$ the total heat absorbed ($\overline{H}$) can be computed without need of computing the average heat transfer coefficient $\bar{a}$ or the average Nusselt number $\overline{Nu}$.

Figures 78 through 87 present the variation of the dimensionless mixing cup temperature with the dimensionless axial distance for different Grashof numbers in both cases (I) and (O). For each given time shown in Fig. 78, which represents a case of low Grashof number ($Gr^* = 4$) ,the mixing cup temperature reaches a constant value at small values of Z/l . On the other hand,in Figs. 82 through 87, which are for larger values of Gr^* ,the mixing cup temperature becomes constant for small values of Z/L at early times but it has a continuously increasing profile at later times . This due to the fact that at early times the induced flow velocity is considerably low and hence the heat transfer

by conduction is the dominant factor. It is important to mention that the overlaps and intersections of the longitudinal distribution of θ_m at various times as shown in Figs. 78-87 are in fact due to the phenomenon of temperature overshoot, which has been discussed before.For example,in Fig. 82 at Z = 0.0004 the overshoot phenomenon in θ_m is clear. At this particular value of Z,the figure shows that the mixing cup temperature increases to a maximum value and then it decreases to the steady-state value.The other figures show the same trend .

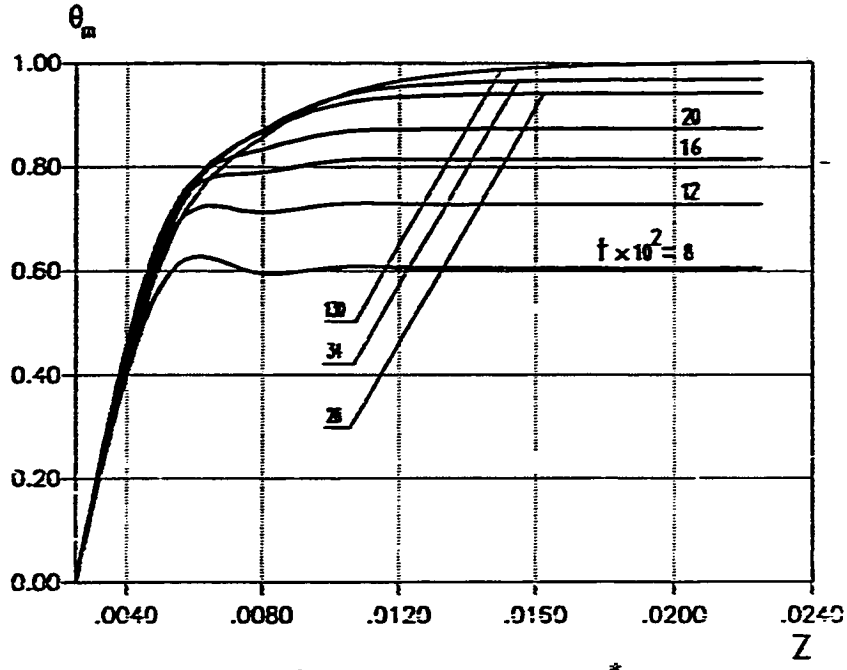

FIG. 78 θ_m versus Z for different t,case(I),Gr^*=4,N=0.5

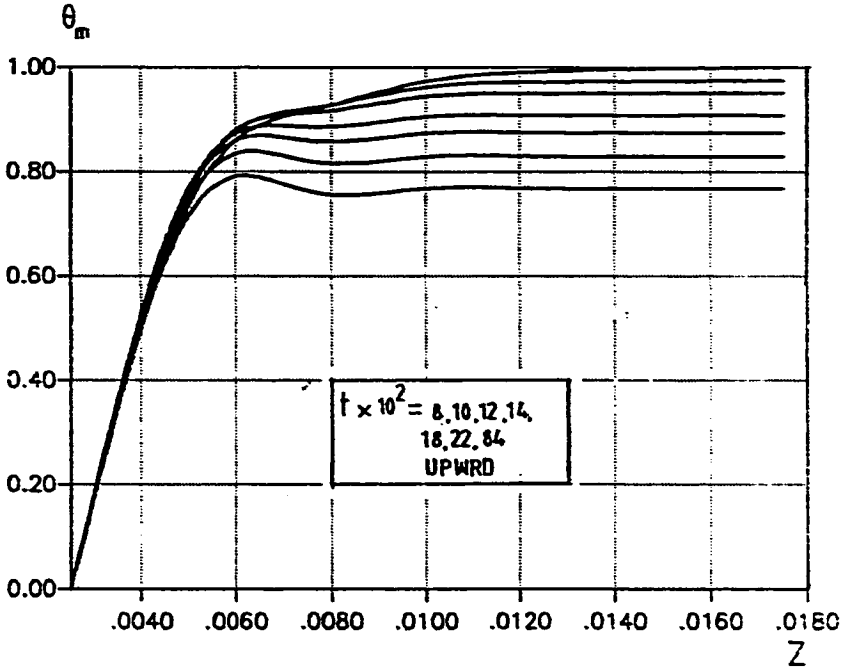

FIG. 79 θ_m versus Z for different t ,case(O),Gr^*=4,N=0.5

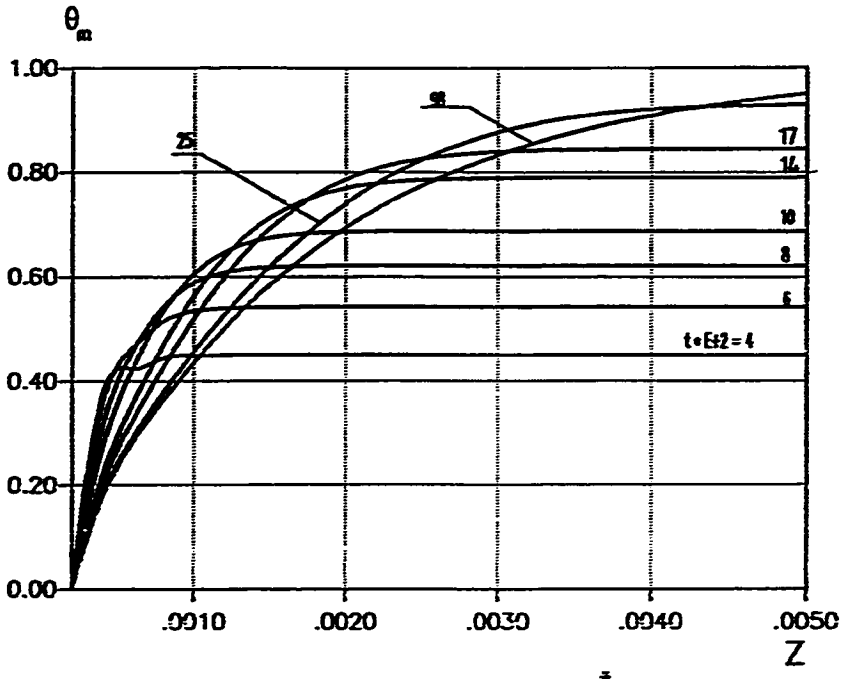

FIG. 80 θ_m versus Z for different t,case(1),$\overset{*}{Gr}$=100,N=0.5

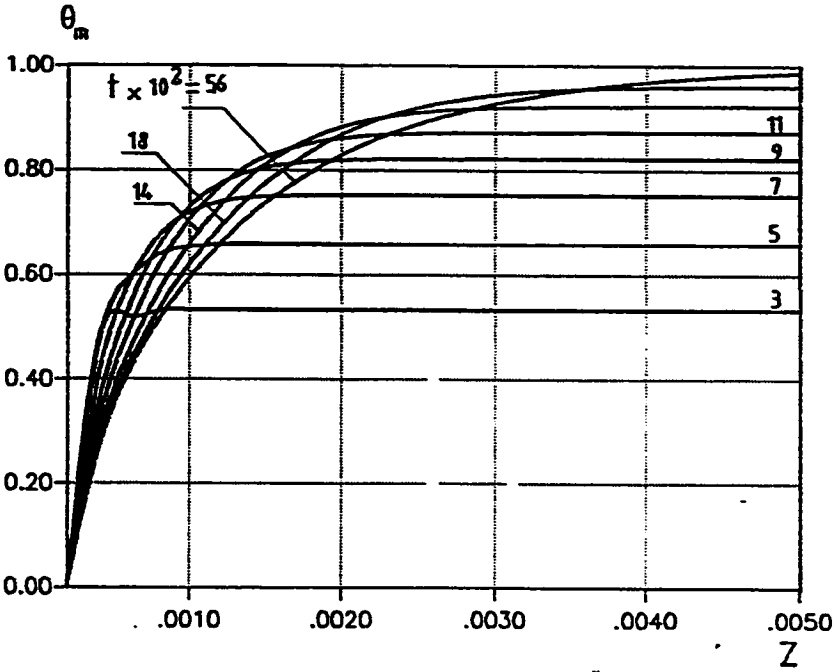

FIG. 81 θ_m versus Z for different t,case(0),$\overset{*}{Gr}$=100,N=0.5

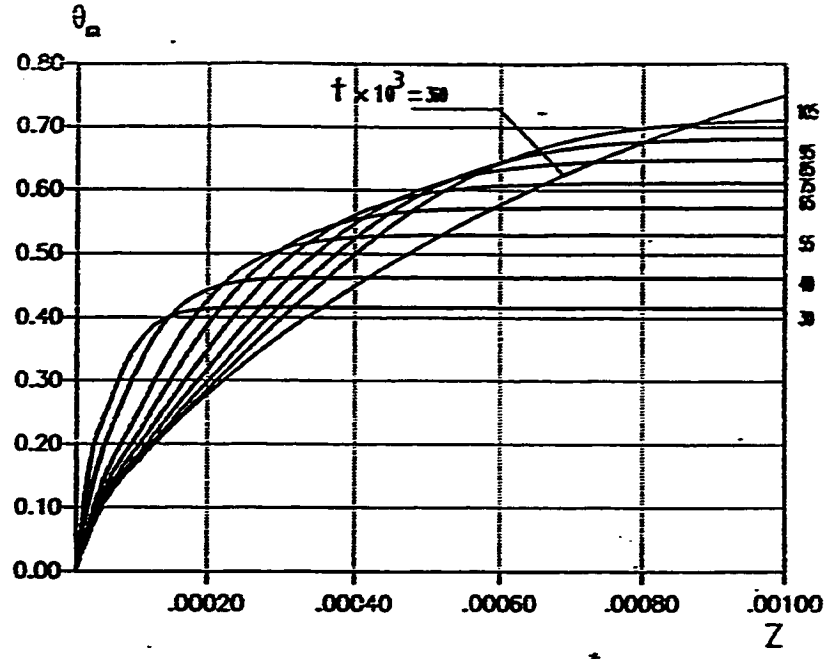

FIG. 82 θ_m versus Z for different t^* ,case(i) . ,Gr=1000,N=0.5

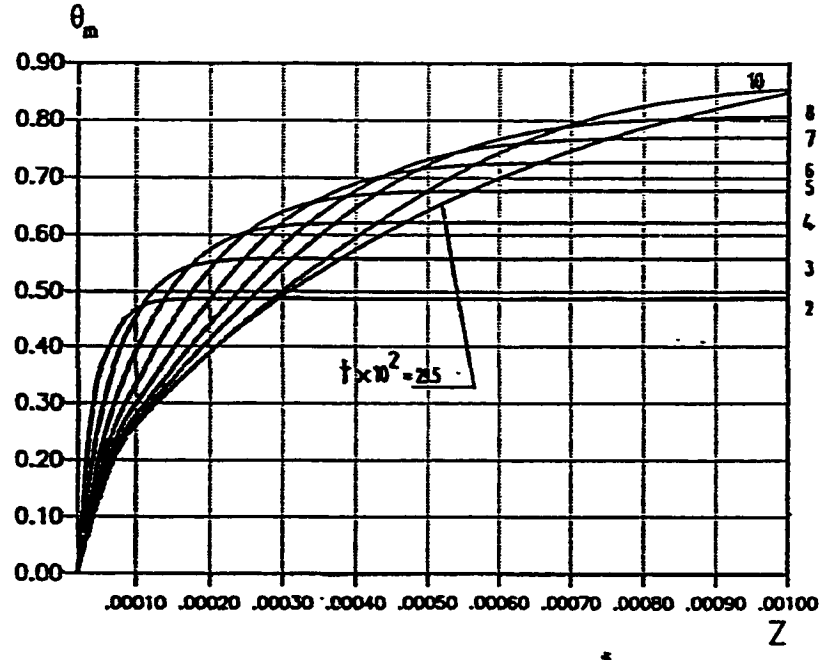

FIG. 83 θ_m versus Z for different t^* ,case(ii) . ,Gr=1000,N=0.6

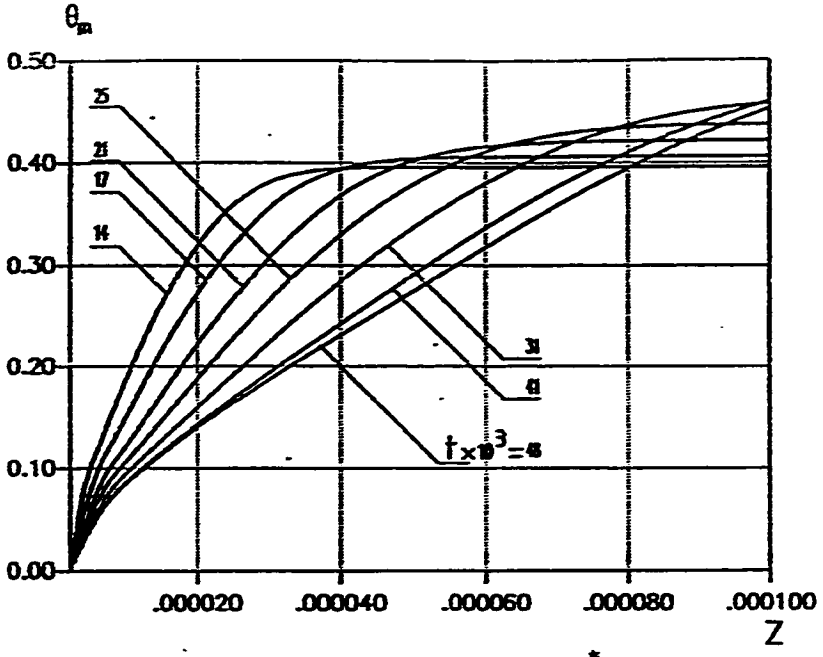

FIG. 84 θ_m versus Z for different t ,case(1) Gr^*=10,000,N=0.5

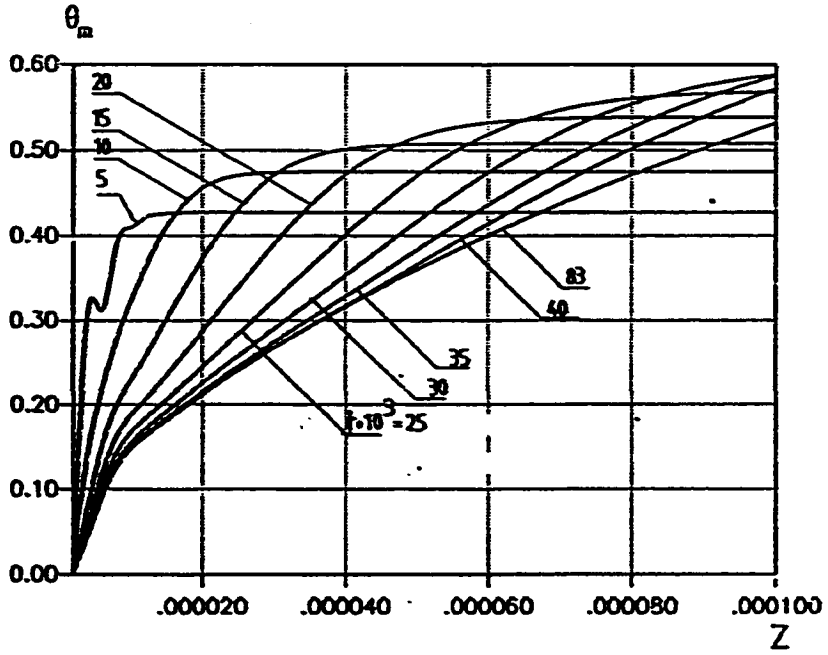

FIG. 85 θ_m versus Z for different t ,case(0) Gr^*=10,000,N=0.5

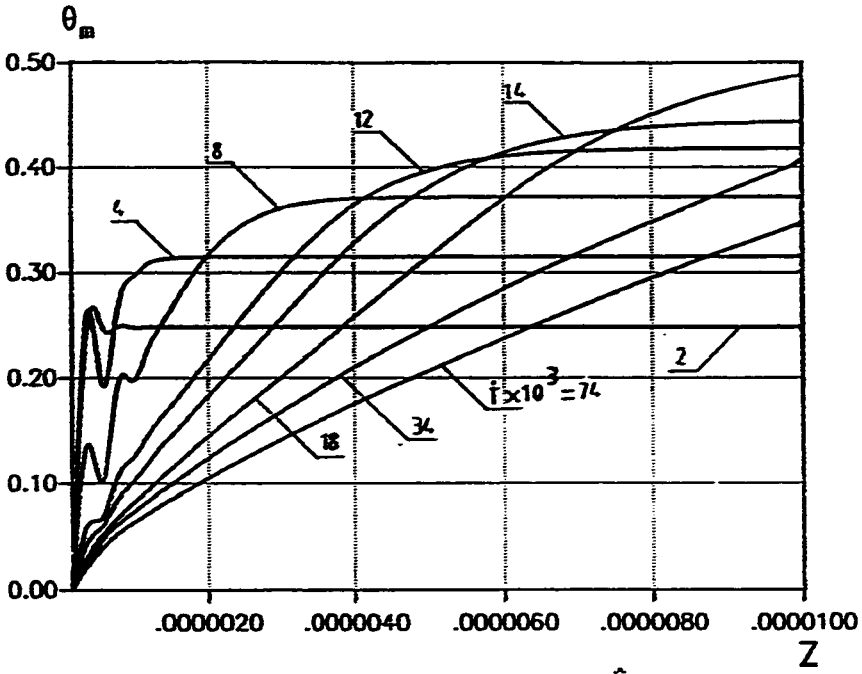

FIG.86 θ_m versus Z at different $\dot{t}$,case(I)· · · ,$\dot{Gr}$=100,000,N=0.5

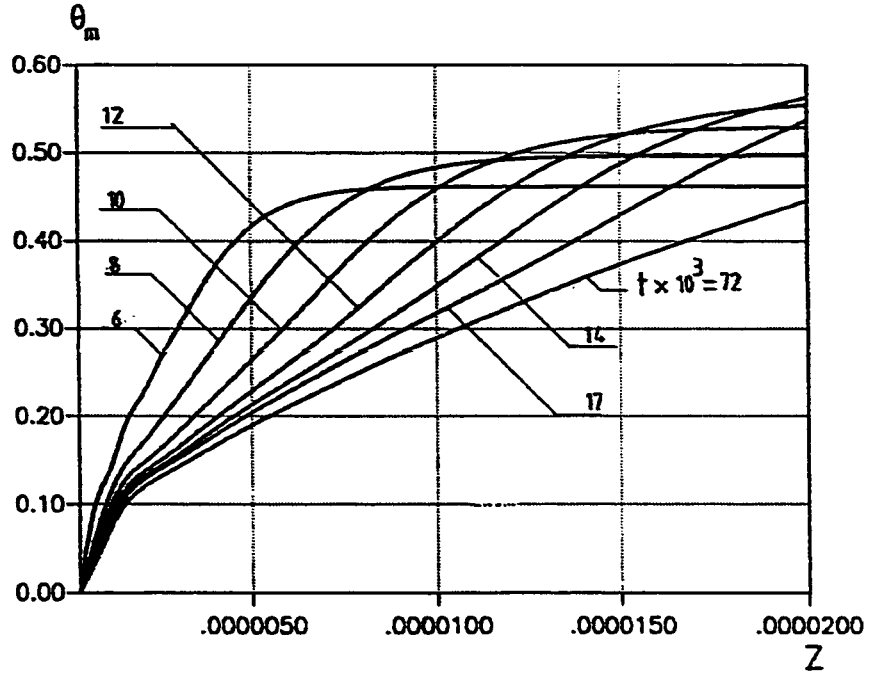

FIG. 87 θ_m versus Z for different t ,case(O) $\dot{Gr}$=50,000,N=0.5

5.3.6 Adiabatic Wall Temperature

Figures 88 through 97 present the time variation of the dimensionless adiabatic wall temperature against the dimensionless axial distance. The behavior of the adiabatic wall temperature is similar to that of the mixing cup temperature.

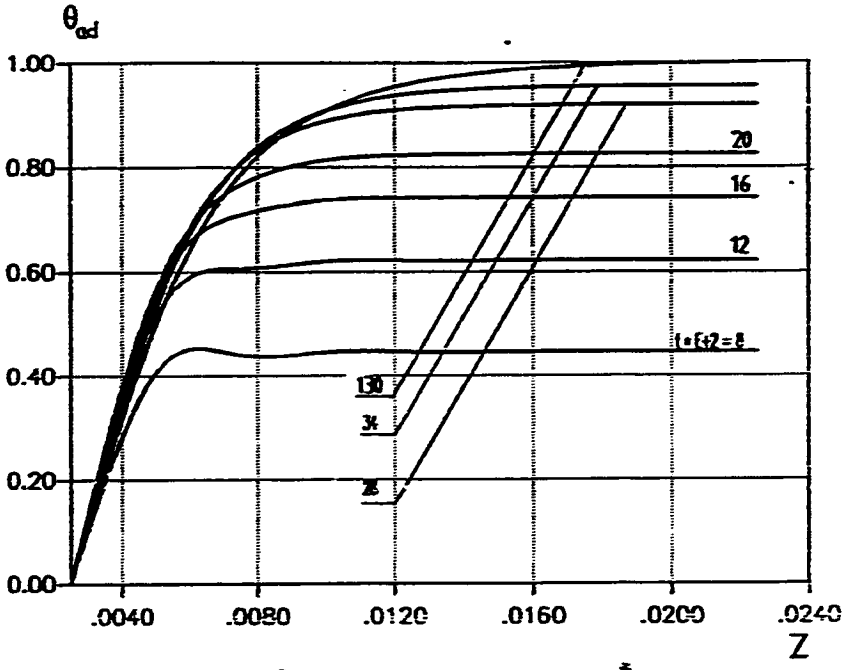

FIG. 88 θ_{ad} versus Z for different t,case(I),$\tilde{Gr}$=4,N=0.5

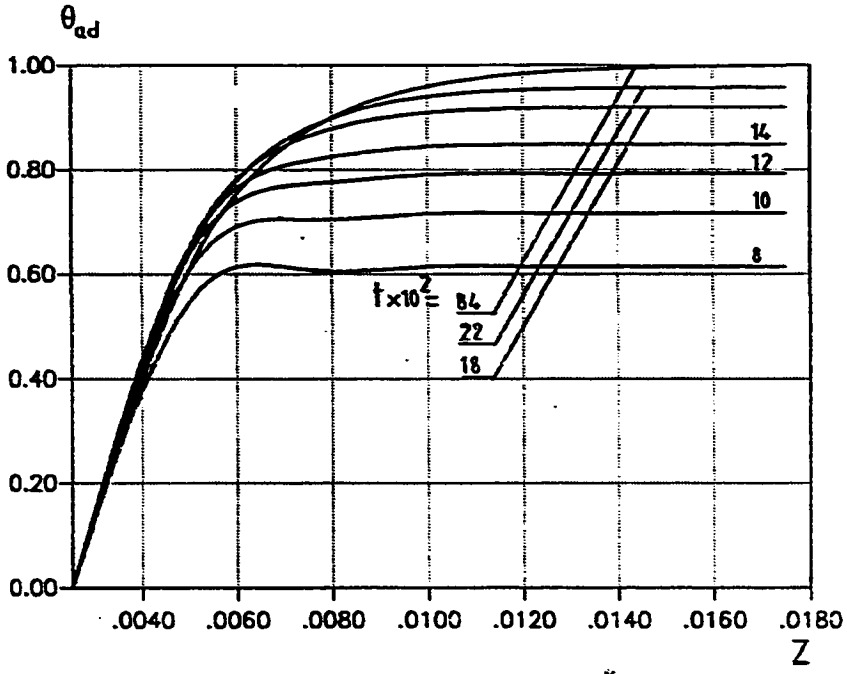

FIG. 89 θ_{ad} versus Z for different t,case(0),$\tilde{Gr}$=4,N=0.5

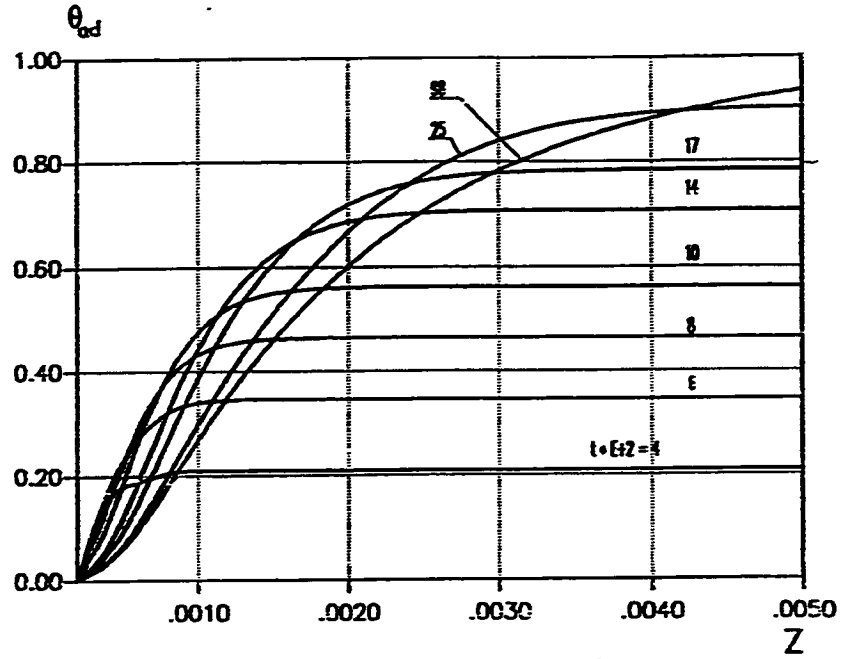

FIG. 90 θ_{ad} versus Z for different t,case(0),$\overset{*}{Gr}$=100,N=0.5

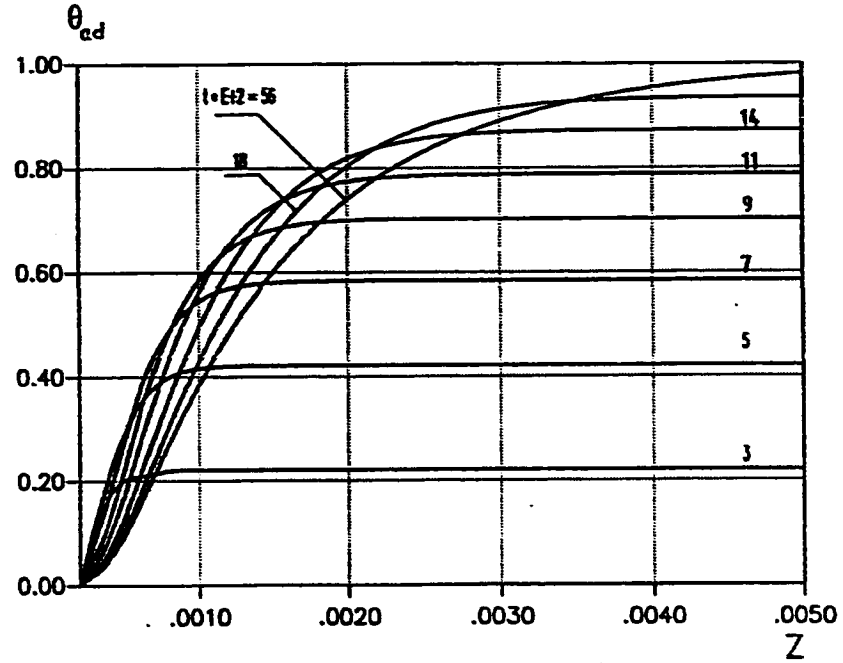

FIG. 91 θ_{ad} versus Z for different t,case(0),$\overset{*}{Gr}$=100,N=0.5

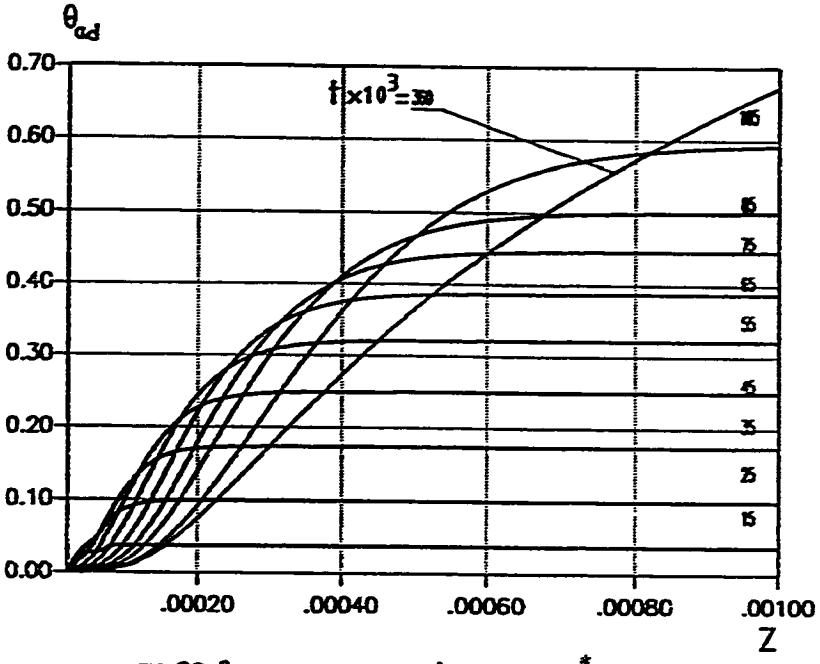

FIG. 92 θ_{ad} versus Z for different t ,case(I) ,Gr^*=1000,N=0.5

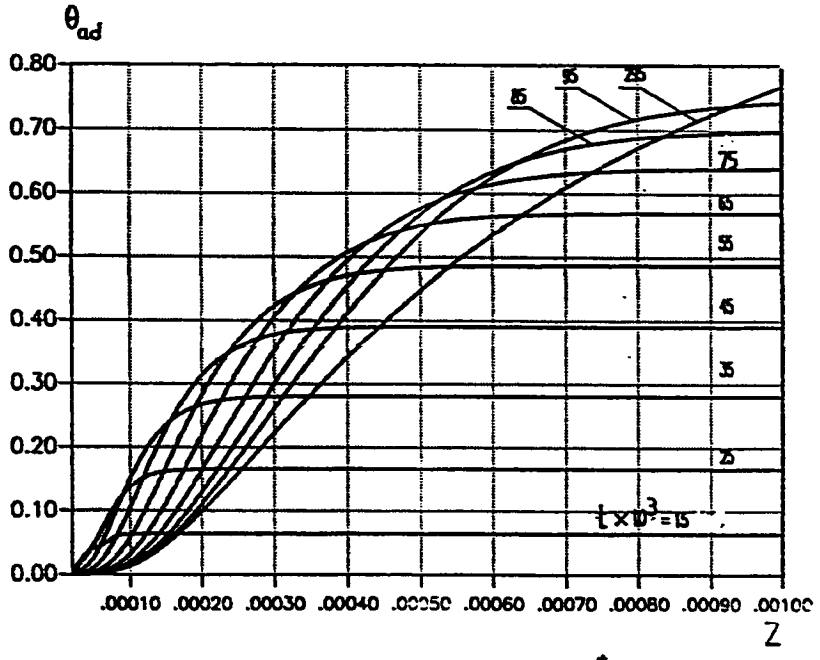

FIG. 93 θ_{ad} versus Z for different t ,case(0) ,Gr^*=1000,N=0.5

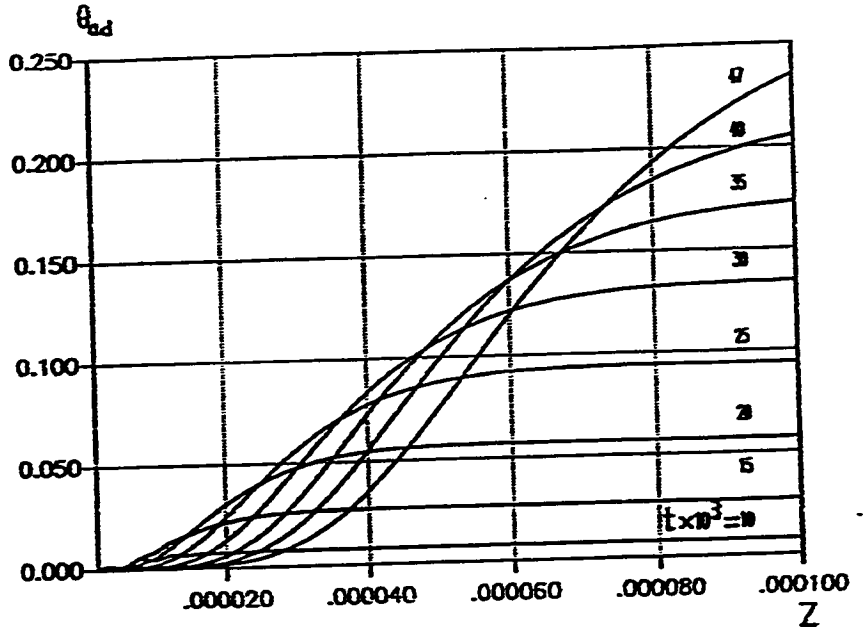

FIG. 94 θ_{ad} versus Z for different t ,case(I) ,Gr^{*}=10,000,N=0.5

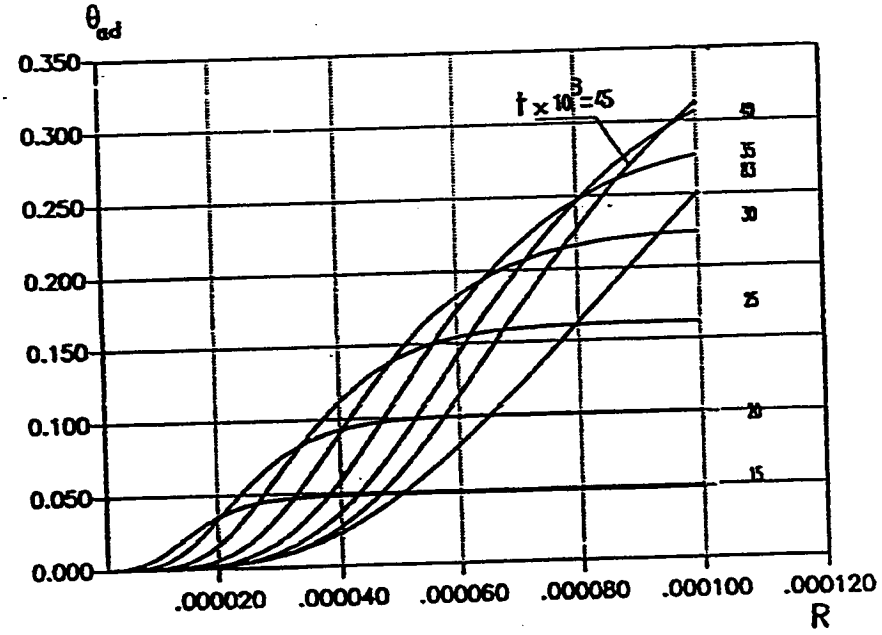

FIG. 95 θ_{ad} versus Z for different t,case(I) ,Gr^{*}=10,000,N=0.5

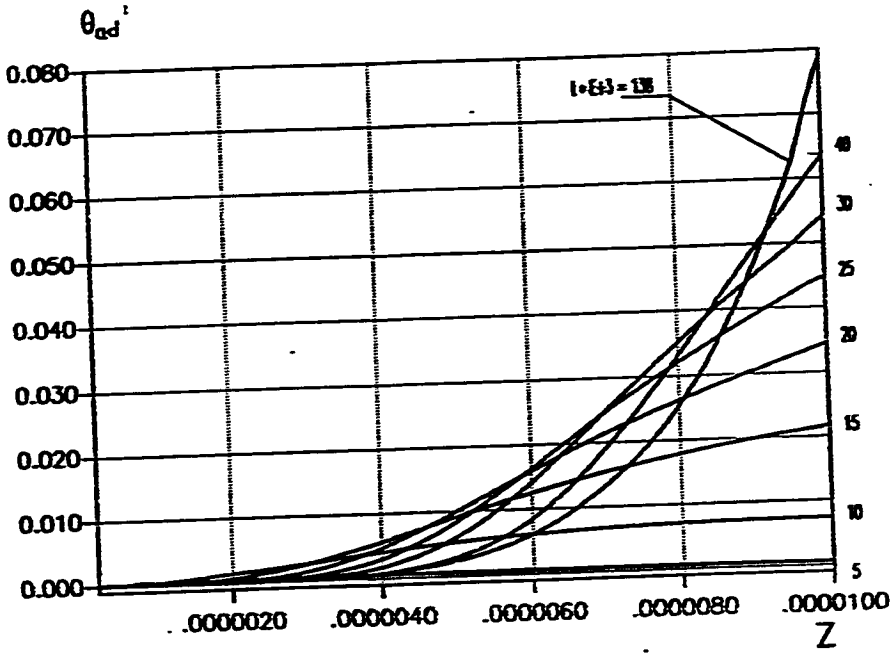

FIG. 96 θ_{ad} versus Z for different t,case(I),Gr^*=100,000,N=0.5

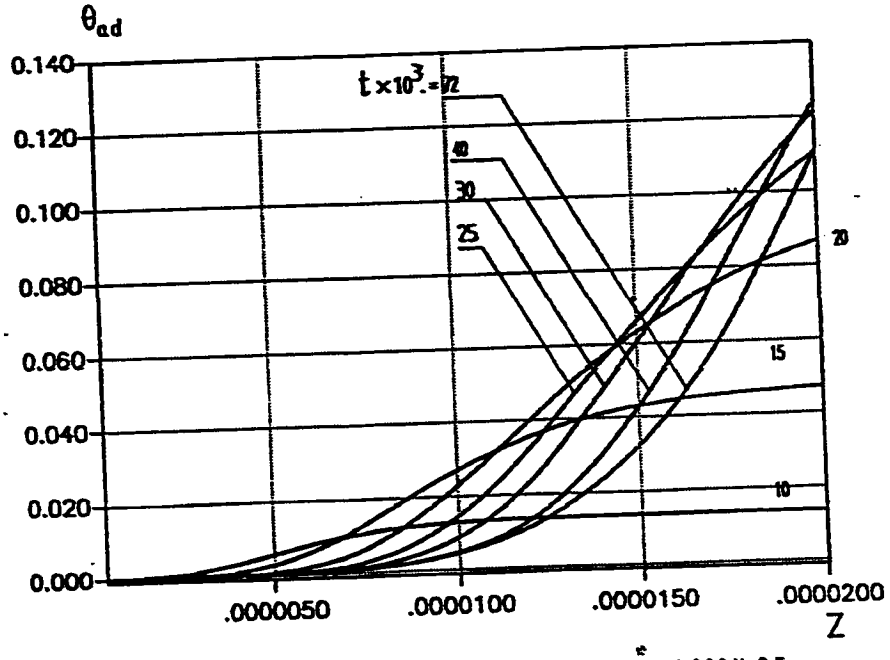

FIG. 97 θ_{ad} versus Z for different t ,case(I) Gr^*=50,000,N=0.5

5.3.7 Total Heat Absorbed

Figures 98 through 101 show the total heat absorbed ($\overline{H}$) versus time for the investigated values of the dimensionless annulus height (modified Grashof number) .As can be seen from these figures, the total heat, at a specific instant, is directly proportional to the annulus height (L). Thus it is inversely proportional to Gr^* . This is because as Gr^* (GrD/L) decreases ,the annulus height increases,more flow is sucked by the annulus by the chimney effect and hence more heat is absorbed by the fluid. The overshoot phenomenon is also clear in these figures of the total heat absorbed.This is a consequence of the presence of such a phenomenon in the corresponding curves which represent the mixing cup temperature θ_m . Such a phenomenon was attributed in a previous section to the domination of the conduction heat transfer mode at early time stages.It is worth mentioning that Joshi [22] and Chang and Lin [23] noticed the same phenomenon.

Comparing the results for cases (I) and (O), it can be seen from the above mentioned figures that, for a given dimensionless height ($L = \frac{1}{Gr^*}$) and a given time (t), the heat absorbed in case (O) is larger than that in case (I) . This is because the heat transfer area in the former case is larger than that in the latter.

Figures 102 through 105 present the variation of the total heat absorbed versus dimensionless height L for different time steps. It can be noticed from these figures that, as might be expected, the total heat absorbed increases with time for a given Grashof number.

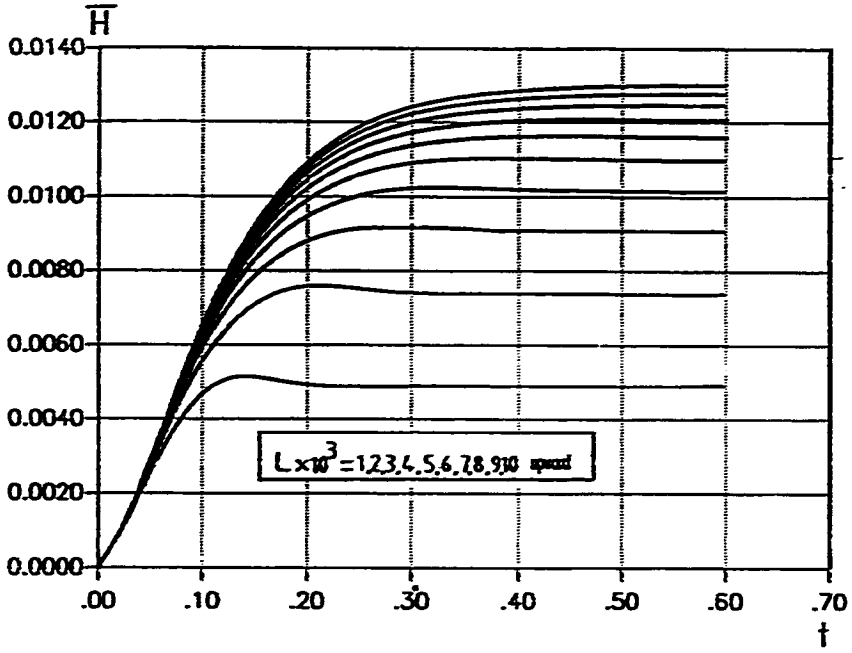

Fig. 98 Total heat absorbed $\overline{H}$ versus t for $0.001 < L < 0.01$, case(I), $N = 0.5$

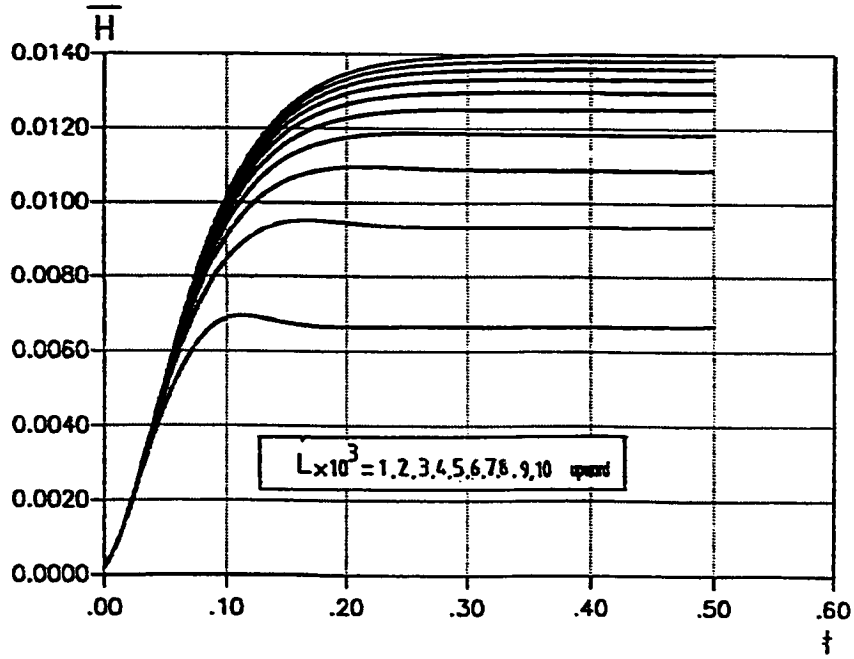

Fig. 99 Total heat absorbed $\overline{H}$ versus t for $0.001 < L < 0.01$, case(O), $N = 0.5$

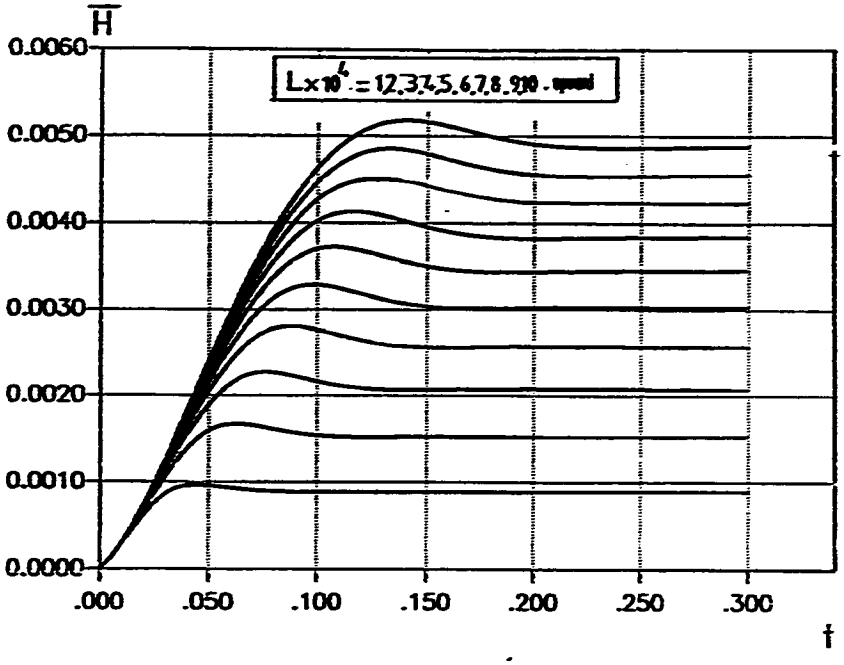

Fig. 100 Total heat absorbed $\overline{H}$ versus t for $0.0001 < L < 0.001$,case(I)N = 0.5

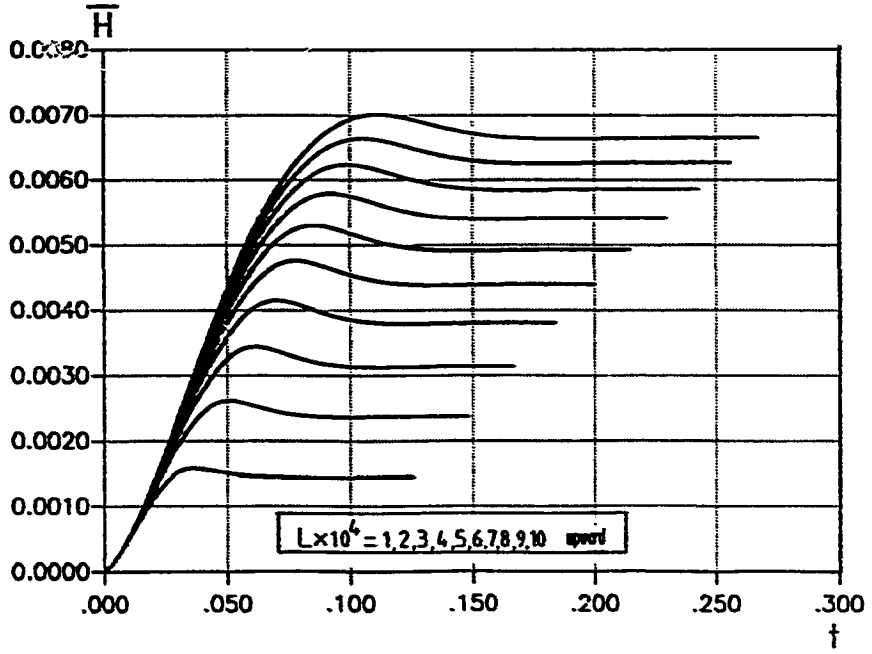

Fig. 101 Total heat absorbed $\overline{H}$ versus t for $0.0001 < L < 0.001$,case(O),N = 0.5

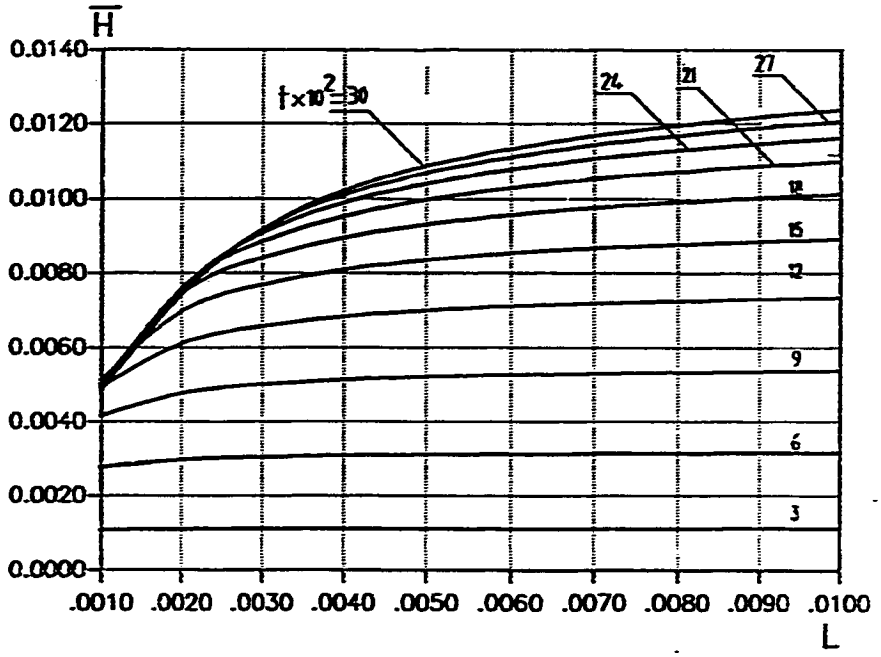

Fig. 102 Total heat absorbed $\overline{H}$ versus L for $0.001 < L < 0.01$ for different t ,case(I),N = 0.5

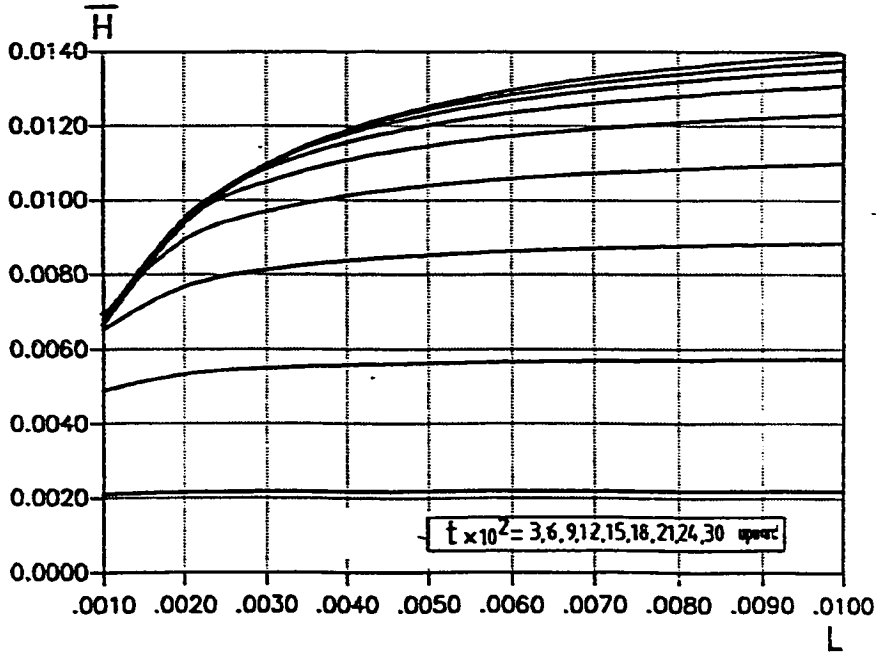

Fig .103 Total heat absorbed $\overline{H}$ versus L for $0.001 < L < 0.01$ for different t ,case(O),N = 0.5

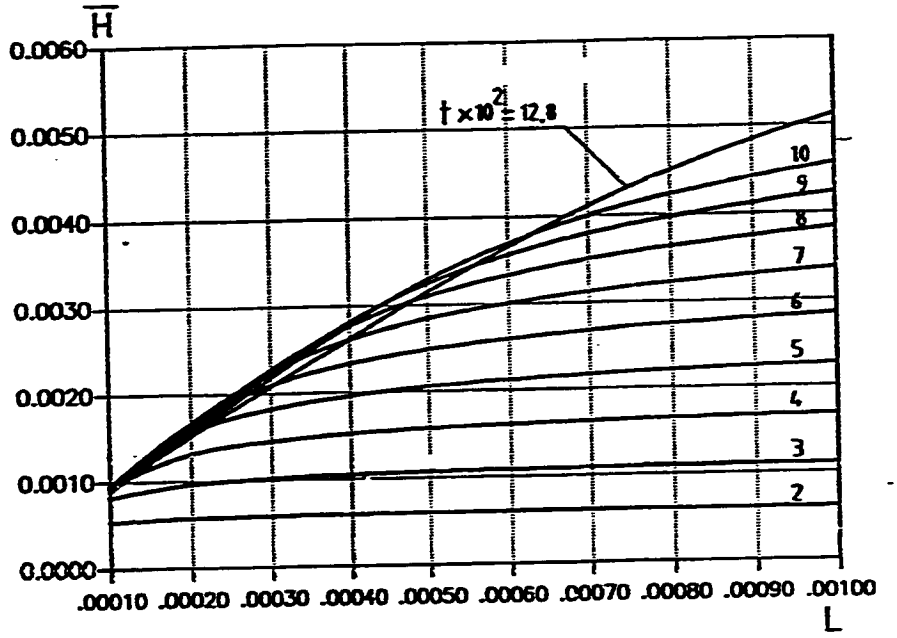

Fig. 104 Total heat absorbed $\overline{H}$ versus L for $0.0001 < L < 0.001$ for different t ,case(I),N = 0.5

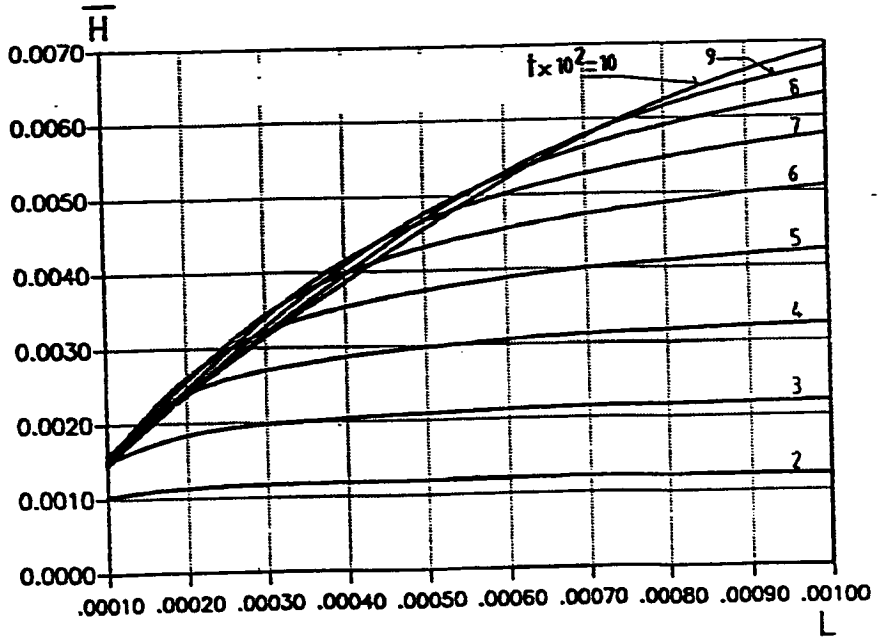

Fig. 105 Total heat absorbed $\overline{H}$ versus L for $0.0001 < L < 0.001$ for different t ,case(I),N = 0.5

5.3.8 Volumetric Flow Rate

Figures 106 through 109, present the dimensionless volumetric flow rate versus time for the investigated dimensionless annulus heights ($L=\frac{1}{Gr^*}$). For a given time, the volumetric flow rate increases with the dimensionless height ($L=\frac{1}{Gr^*}$). Moreover, for a given annulus height (i.e. modified Grashof number) it increases with time and have an overshoot which is clearer for shorter annuli (small values of L or high values of Gr^*). Figs. 110 through 113 present the time variation of the flow versus the dimensionless height. It can be seen from the figures that for a given dimensionless height L and a given time, the flow rate (F) for case (O) is larger than that for case (I).Again, this is because the amount of heat absorbed in case(O) is larger than that in case(I) due to the larger heat transfer surface area in the former case than in the latter.

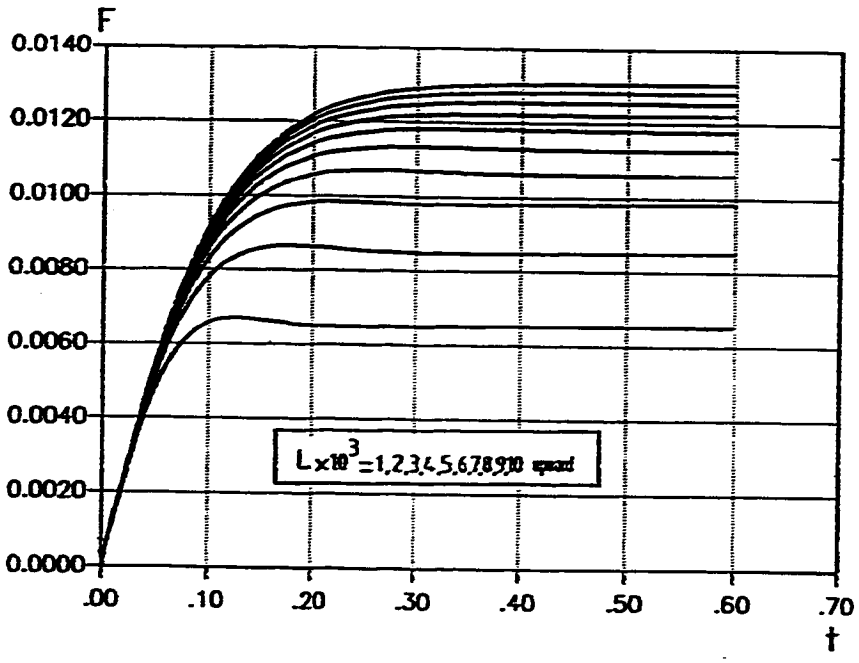

Fig. 106 Flow rate (F) versus time for $0.001 < L < 0.01$, case(I), $N = 0.5$

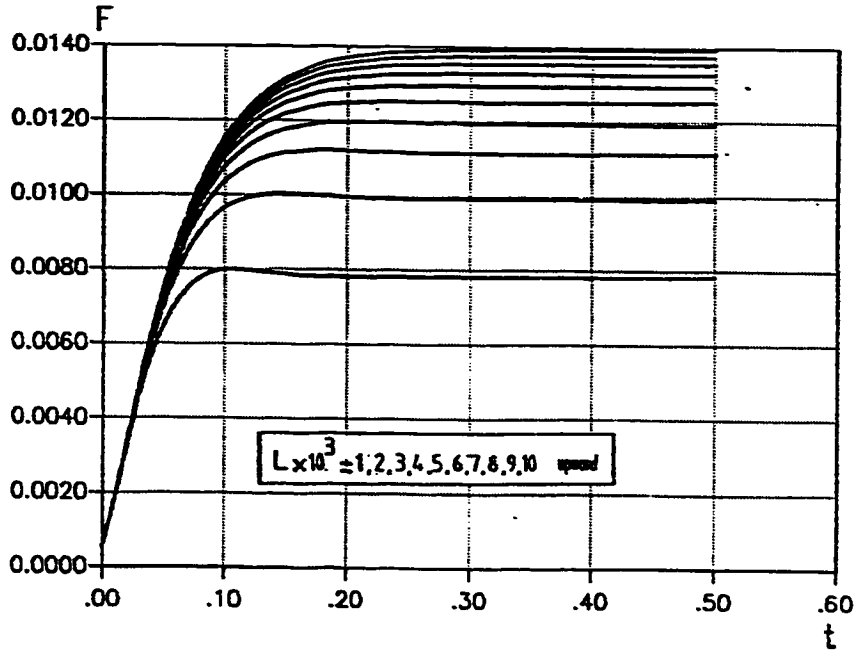

Fig. 107 Flow rate (F) versus time for $0.001 < L < 0.01$, case(O), $N = 0.5$

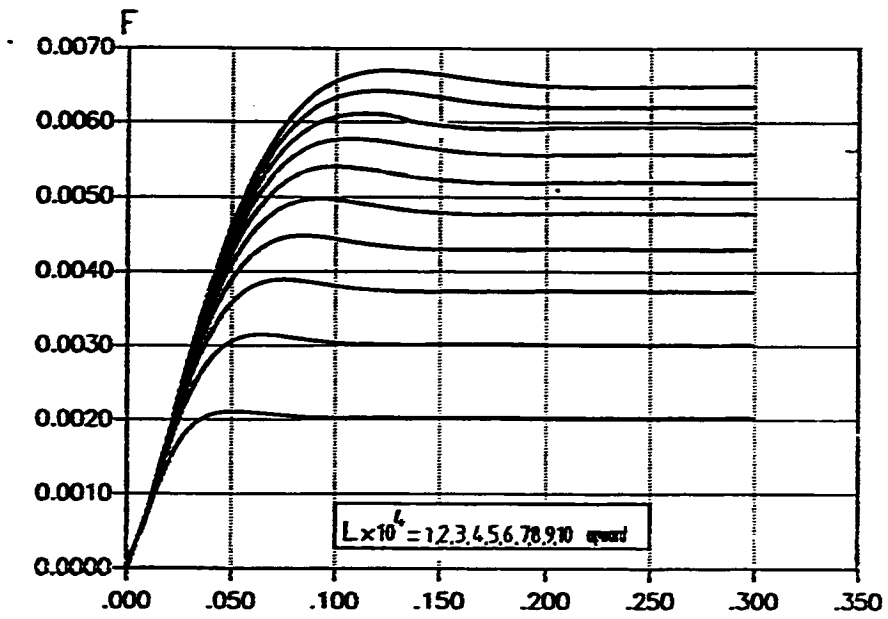

Fig. 108 Flow rate (F) versus time for $0.0001 < L < 0.001$, case(I), $N = 0.5$

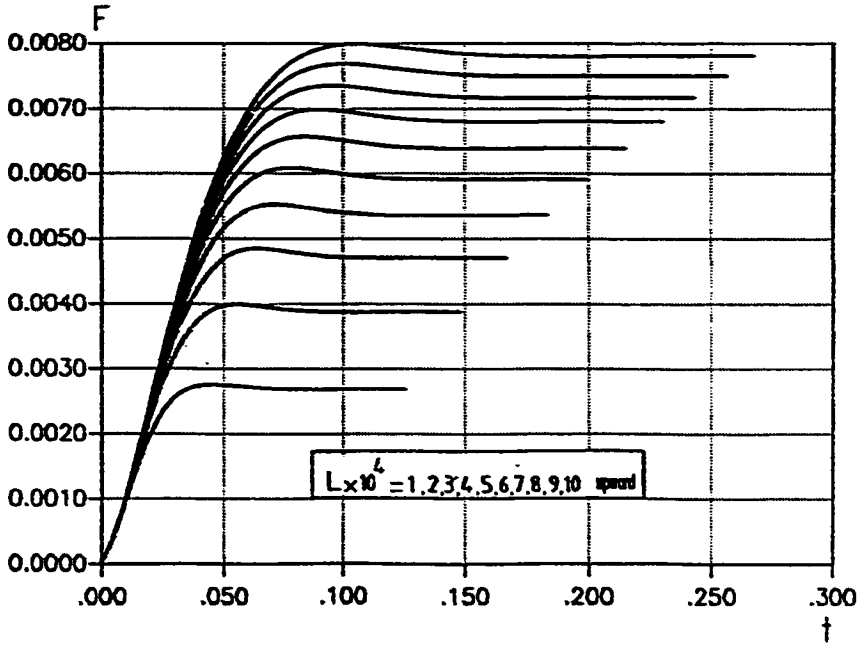

Fig. 109 Flow rate (F) versus time for $0.0001 < L < 0.001$, case(O), $N = 0.5$

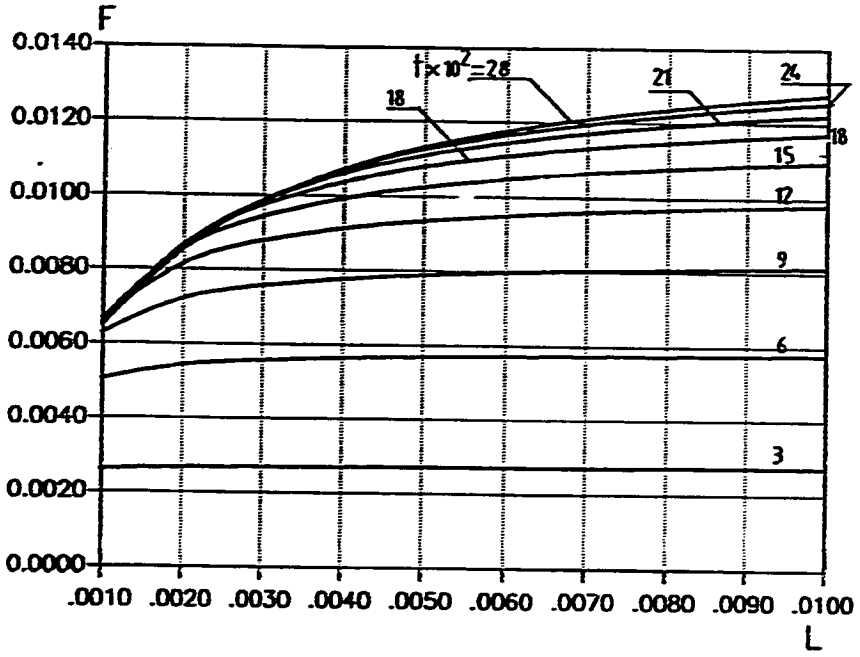

Fig. 110 Flow rate (F) versus L for $0.001 < L < 0.01$ for different time ,case(I),N = 0.5

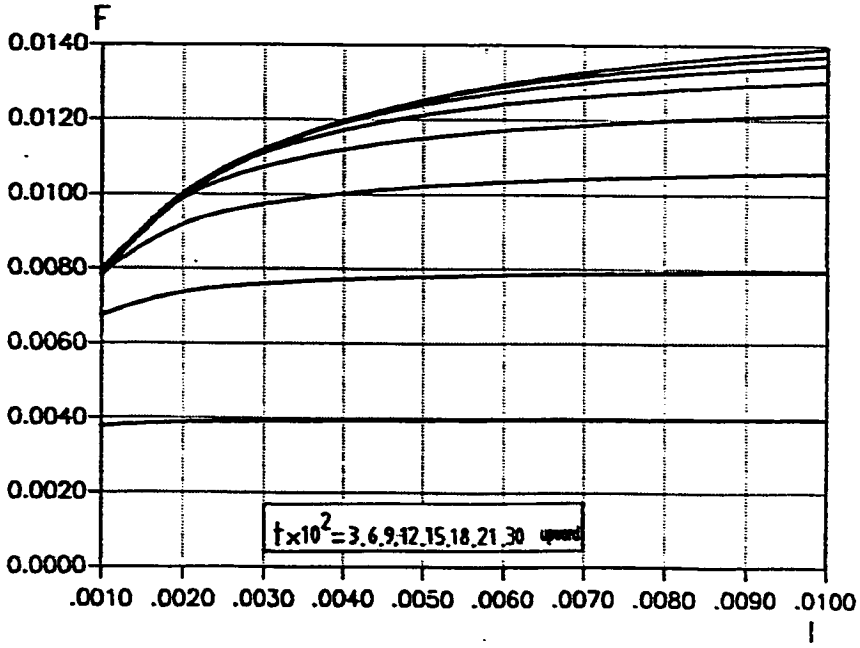

Fig. 111 Flow rate versus L for $0.001 < L < 0.01$ for different time ,case(O),N = 0.5

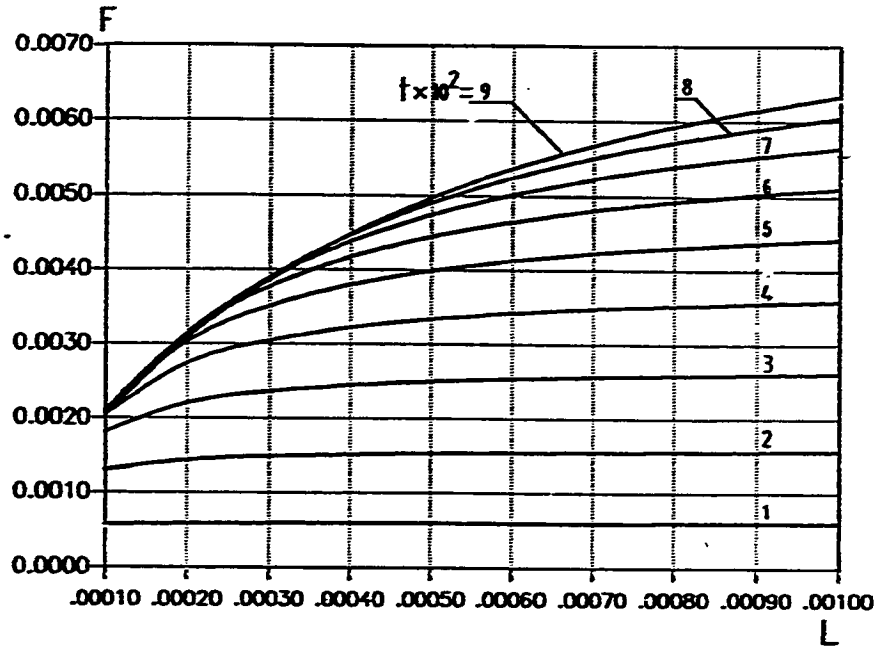

Fig. 112 Flow rate versus L for $0.0001 < L < 0.001$ for different time ,case(I),N = 0.5

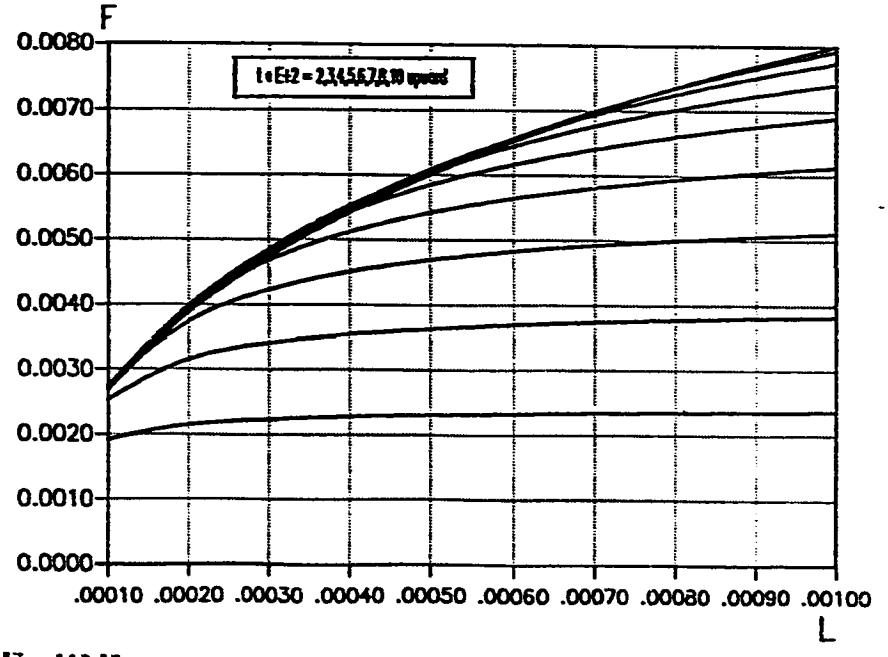

Fig. 113 Flow rate versus L for $0.0001 < L < 0.001$ for different time ,case(I),N = 0.5

5.3.9 Steady-State Time

The time needed to achieve the steady state conditions is computed based on the criterion given in section 4.6 .It is plotted against the dimensionless annulus height for both the investigated boundary conditions.For both cases, the steady state time (t_{ss}) increases with the annulus height. For a given height, t_{ss} is larger in case(I) than in case(O).This is attributed to the larger heat transfer occurring in case(O) due to the larger heat transfer area.

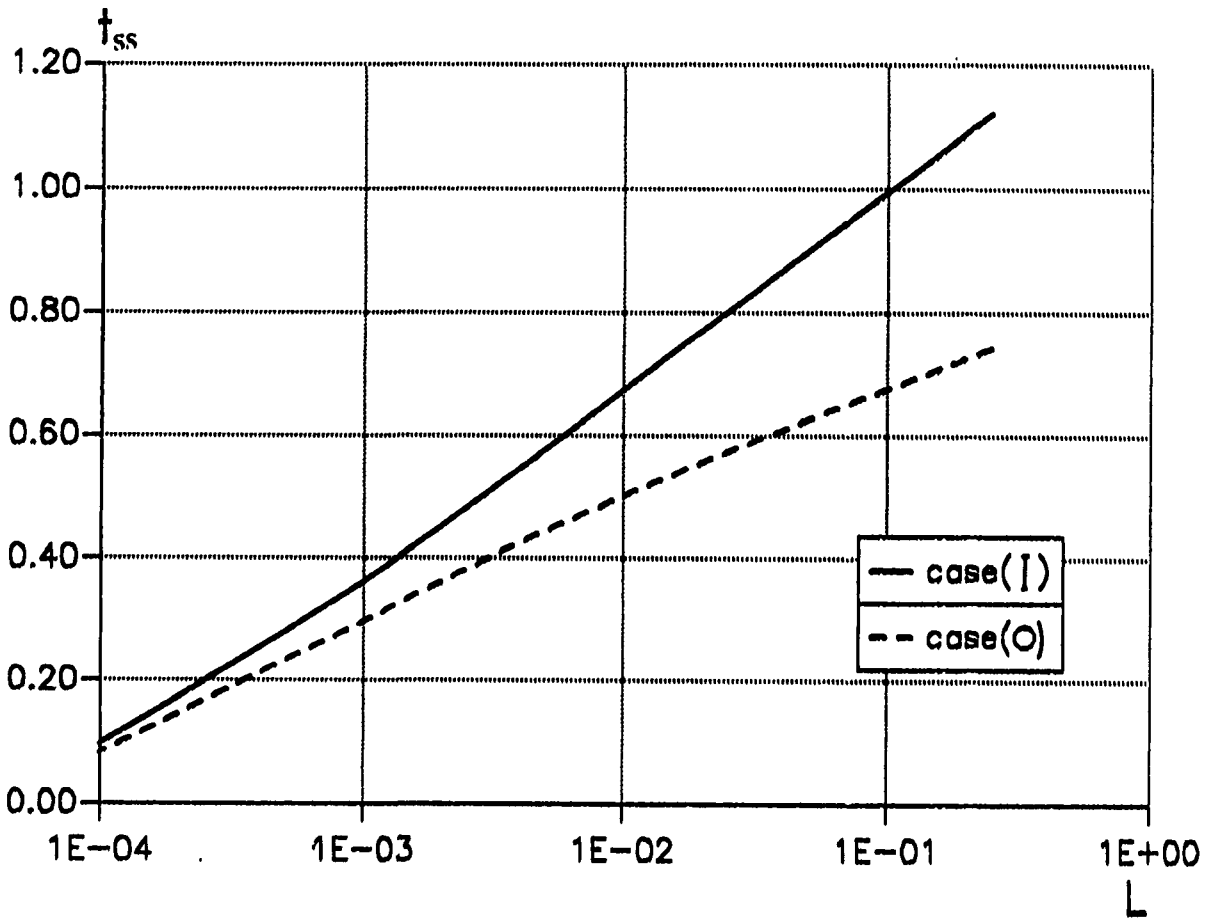

FIG. 114 t_{ss} versus L for case(I) and case(O),N=0.5

5.4 COMPARISONS WITH OTHER WORKS

To check the adequacy of the present results, a computer run with a value of N very close to 1 (N = 0.99) was made to obtain an asymptotic solution representing the case of free convection in the developing region of a vertical flat plate duct, with symmetric step change in temperature at both walls. Also, the program was modified to take into consideration a zero inlet dimensionless pressure defect as Joshi [22]. Moreover,it was taken into consideration that U_e is defined as $U_e=\frac{b^2u}{lvGr}$ hence $U_e=16(1-N)^2U_o$ which for N = 0.99 gives $U_e=16x10^{-4}U_o$.

Also it should be mentioned that Joshi defined his modified Grashof number as $Gr=\frac{g\beta(T-T_o)b^4}{lv^2}$. Hence, $Gr^*/Gr_j^*=16$. From which the corresponding ratio for the dimensionless annulus height $L_j/L=16$, where L_j is the dimensionless height as defined by Joshi.

The obtained entrance-velocity (U_e) values for different values of L are presented and compared in Fig. 115 with some selected points read from Joshi's corresponding figure. As can be seen from this figure,the comparison shows good agreement.

Moreover, the steady-state results of this work at the exit cross section of a

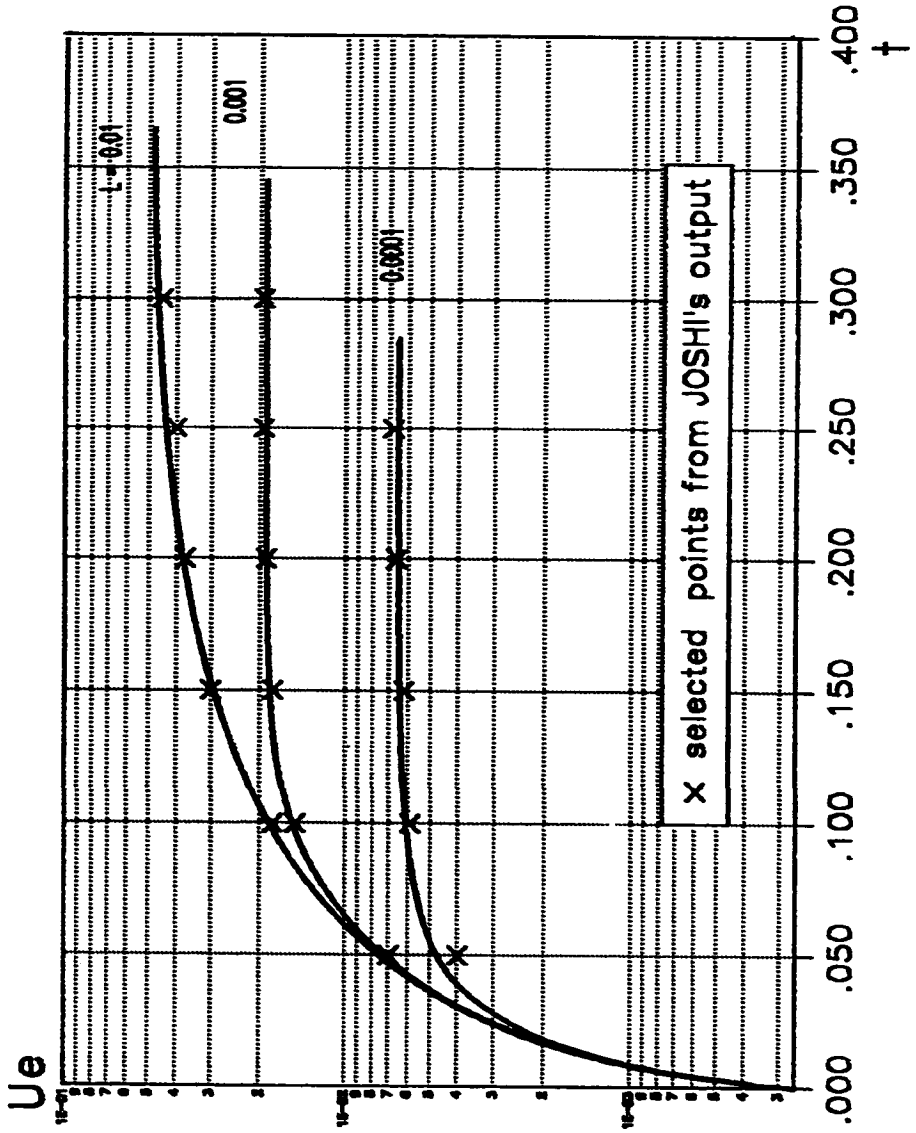

FIG. 115 U versus t for different L for JOSHI B.C.

sufficiently high annulus (large value of L or small value of Gr^*) are compared in Tables 1 and 2 with the fully developed analytical solution of the third kind given by El-Shaarawi and Al-Nimr [30]. The program results were taken after long period of time (large values of t) at the exit section in the case with $Gr^*=4$. The following equations represent the fully developed analytical solution of the third kind ,which corresponds to the present thermal boundary conditions,as given by El-Shaarawi and Al-Nimr [30].

$$F_{fd}=\overline{H}_{fd}=\frac{1-N^2}{128(1-N)^4}\left[1+N^2+\frac{1-N^2}{\ln(N)}\right]$$

$$U_{fd}=\frac{[1-R^2-(1-N^2)(\ln R/\ln N)]}{64(1-N)^4}$$

The comparison presented in Tables 1-2 shows an excellent agreement.

Finally , the steady state values of the flow rate and the total heat absorbed by the fluid are compared, for three values of Grashof number ($Gr^*=$ 100 , 1000 ,and 100,00), with El-Shaarawi and Sarhan results [24] in Table 3. Again, the comparison shows a very good agreement.

Table 1 Comparison of the present steady state F & $\overline{H}$ results for a sufficiently high annulus ($Gr^{*} = 4$,L = 0.25) with the corresponding fully developed analytical values of [30]

Qnt.	Case	Present Results	Ref. [30]	%differance
F	I	0.0156066	0.015748	0.898
	O	0.0156508	0.015748	0.618
$\overline{H}$	I	0.0156066	0.015748	0.899
	O	0.0156494	0.015748	0.626

Table 2 Comparison of the present steady state values of U at the exit of a sufficiently high annulus ($Gr^{*} = 4$,L = 0.25) with the corresponding fully developed analytical solution of [30]

R	Present Results	Ref. [30]
0.50	0.000000	0.000000
0.55	0.012621	0.012657
0.60	0.021757	0.021819
0.65	0.027767	0.027846
0.70	0.030932	0.031018
0.75	0.031472	0.031555
0.80	0.029565	0.029639
0.85	0.025354	0.025413
0.90	0.018959	0.018999
0.95	0.010480	0.010499
1.00	0.000000	0.000000

Table 3 Comparison of the present steady state F & $\overline{H}$ values with the corresponding results of Reference [24]

	Gr^*	100			1000			10,000		
Qnt.	Case	Ref.[24]	Present	% diff	Ref.[24]	Present	% diff	Ref.[24]	Present	%diff
F	I	13.0	13.0	0.00	6.4	6.5	1.56	2.0	2.0	0.00
	O	13.7	13.9	1.46	7.9	7.8	1.26	2.6	2.7	3.85
$\overline{H}$	I	13.0	13.0	0.00	4.8	4.9	2.08	0.9	0.9	0.00
	O	13.7	13.9	1.46	6.4	6.65	3.91	1.4	1.4	0.00

CHAPTER SIX

CONCLUSIONS

In this work an iterative implicit finite-difference scheme has been developed to solve the transient free convection problem in the developing region of a vertical concentric annulus. The problem was solved under the following two thermal boundary conditions.

Under the first condition, CASE(I), the inner wall is subjected to a step change in temperature, while the outer wall is maintained adiabatic. Under the second condition, CASE(O), the outer wall is isothermal while the inner wall is adiabatic.

From the results, the following important conclusions are drawn.

1. For a given time, the amount of induced flow and the total heat absorbed in a given annulus are larger for case (O) than for case(I).

2. For a given Gr^* ,if fully developed conditions are achieved in a given annulus, they are reached earlier in case(O) than in case(I).

3. Steady state conditions are reached faster for case (O) than case (I).

4. Flow rate variation with time is sensitive for the variation of the total heat absorbed with time.Consequently ,an overshoot is found in the flow rate variation with time which is a result of that overshoot occurring in the total heat value.This latter overshoot is due to the temperature overshoot occurring because of the domination of conduction heat transfer mode at early times.

5. Reversed flow is observed for large values of Gr^{*} .

APPENDIX (1)

BOUNDARY LAYER FORMULATION

To obtain the boundary layer equations, equations (1), (2), (4), (5) are transformed into dimensionless forms using a group of dimensionless parameters. Then, an order of magnitude analysis is done on each equation; terms of small order of magnitude will be neglected.

The following traditional dimensionless parameters are used in this appendix.

$$U=\frac{u}{u_*} \quad , \qquad V=\frac{v}{u_*} \quad ,$$

$$Z=\frac{z}{l} \quad , \qquad R=\frac{r}{l} \quad ,$$

$$t=\frac{u_*\tau}{l} \quad , \qquad P=\frac{p}{\rho u_*^2} \quad ,$$

$$\theta = \frac{T-T_o}{T_w - T_o} \quad \text{,and} \quad Re = \frac{u_o l}{\nu}$$

In above parameters, the reference length l and the reference velocity u_o are selected so that R, Z, t ,U and θ are of order 1, also $\partial u/\partial z$ and $\partial T/\partial z$ are of order 1 . For simplicity, velocity and thermal boundary layers are assumed to be of the same order of magnitude δ , i.e. the value of Prandtl number is near unity.

As discussed by El-Shaarawi [32] the governing complete equations should not be expanded to their elementary terms. This is to prevent neglecting some important elementary terms when compared with some other terms in an equation.

Substituting the above dimensionless parameters in the continuity equation (1) gives the following dimensionless continuity equation :

$$\frac{\partial}{\partial R}(RV) + \frac{\partial U}{\partial Z} = 0$$

$$\left(\frac{l\delta}{\delta}\right) \qquad \left(\frac{l}{l}\right)$$

The order of magnitude of each term is written under it , and they are estimated as follows.Since $\partial U/\partial Z$ is of order (1), the second term in the above equation should also be of order (1), so that both terms add to zero. Furthermore, since R is of order (1), ∂R is of order δ, and $(\partial(RV)/\partial R)$ is of order (1), then V is of order (δ)

Secondly, substituting the nondimensional parameters in the axial momentum equation (9) gives

$$\rho(\frac{u^{*2}}{l})[\frac{\partial U}{\partial \tau}+V\frac{\partial U}{\partial R}+U\frac{\partial U}{\partial Z}]=\rho(\frac{u^{*2}}{l})[-\frac{\partial P}{\partial Z}+\frac{Gr\theta}{Re^2}+\frac{1}{Re}[\frac{\partial^2 U}{\partial Z^2}+\frac{1}{R}\frac{\partial}{\partial R}[R(\frac{\partial U}{\partial R})]]$$

Dividing both sides over the common term $\rho(u^{*2}/l)$ gives the following dimensionless axial momentum equation.

$$\frac{\partial U}{\partial t}+V\frac{\partial U}{\partial R}+U\frac{\partial U}{\partial Z}=-\frac{\partial P}{\partial Z}+\frac{Gr\theta}{Re^2}+\frac{1}{Re}[\frac{\partial^2 U}{\partial Z^2}+\frac{1}{R}\frac{\partial}{\partial R}[R(\frac{\partial U}{\partial R})]]$$

$$(\frac{1}{l})+(\delta)(\frac{1}{\delta})+(1)(\frac{1}{l})=-\frac{\partial P}{\partial Z}+\frac{Gr}{Re^2}(1)+\frac{1}{Re}[(\frac{1}{l})+(\frac{1}{l})(\frac{1}{\delta})][(1)(\frac{1}{\delta})]$$

$$1 \qquad 1 \qquad 1 \qquad \frac{\partial P}{\partial Z} \qquad \frac{Gr}{Re^2} \qquad \delta^2\,[\quad 1 \qquad\quad \frac{1}{\delta^2}\ ]$$

From the above orders of magnitude ,it can be deduced that Re must be of order $1/\delta^2$ in order that the viscous terms on the RHS of the equation can balance, with the buoyancy term, the inertia terms on it's LHS.Moreover, the buoyancy term can not be neglected in the present case because it is establishing the flow field. This implies that the coefficient of (θ) , which is Gr/Re^2 , should be of order (1) and consequently Gr is of order $1/\delta^4$. Furthermore, $\partial P/\partial Z$ can not be dropped because it balances the inertia forces, which means that it is of order (1). Thus after dropping all the terms of order δ and higher powers of delta, the axial momentum equation reduces to

$$\frac{\partial U}{\partial t}+V\frac{\partial U}{\partial R}+U\frac{\partial U}{\partial Z}=-\frac{\partial P}{\partial Z}+\frac{Gr\theta}{Re^2}+\frac{1}{Re}[\frac{1}{R}\frac{\partial}{\partial R}[R(\frac{\partial U}{\partial R})]]$$

Thirdly, substituting the dimensionless parameters in equation (2) gives the following dimensionless radial momentum equation

$$\rho(\frac{u^{*2}}{l})[\frac{\partial V}{\partial t}+V\frac{\partial V}{\partial R}+U\frac{\partial V}{\partial Z}]=\rho(\frac{u^{*2}}{l})[-\frac{\partial P}{\partial R}+\frac{1}{Re}[\frac{\partial^2 V}{\partial Z^2}+\frac{\partial}{\partial R}(\frac{1}{R}\frac{\partial(RV)}{\partial R})]]$$

After dropping the common term $\rho u^{*2}/l$ the dimensionless radial momentum equation will be

$$\frac{\partial V}{\partial t}+V\frac{\partial V}{\partial R}+U\frac{\partial V}{\partial Z}=-\frac{\partial P}{\partial R}+\frac{1}{Re}[\frac{\partial^2 V}{\partial Z^2}+\frac{\partial}{\partial R}(\frac{1}{R}\frac{\partial (RV)}{\partial R})]$$

$$(\frac{\delta}{1}) \quad (\delta)(\frac{\delta}{\delta}) \quad (1)(\frac{\delta}{1})=-\frac{\partial P}{\partial R} \quad (\delta^2)](\frac{\delta}{1}) \qquad \frac{1.\delta}{\delta.1.\delta})]$$

$$(\delta) \quad (\delta) \quad (\delta) \quad = \quad -\frac{\partial P}{\partial R} \qquad [(\delta^3) \qquad (\delta)]$$

Dropping the terms of order δ or higher powers of δ , the radial momentum equation will reduce to

$$\frac{\partial P}{\partial R}=0 \quad ,$$

which means that the variation of pressure in the transverse direction is negligible. Thus the pressure in the annulus is a function of time and the streamwise direction only.

Finally, substituting the dimensionless parameters in the energy equation (4) gives

$$(\frac{u^*}{(T_w-T_o)l})[\frac{\partial \theta}{\partial t}+V\frac{\partial \theta}{\partial R}+U\frac{\partial \theta}{\partial Z}]=(\frac{u^*}{(T_w-T_o)l})[\frac{1}{PrRe}[\frac{1}{R}\frac{\partial}{\partial R}(R\frac{\partial \theta}{\partial R})+\frac{\partial^2 \theta}{\partial Z^2}]]$$

dividing both sides of the equation over the common term $u^*/(T_w-T_o)l$ gives the

following

$$\frac{\partial\theta}{\partial t}+V\frac{\partial\theta}{\partial R}+U\frac{\partial\theta}{\partial Z}=\frac{1}{PrRe}[\frac{1}{R}\frac{\partial}{\partial R}(R\frac{\partial\theta}{\partial R})+\frac{\partial^2\theta}{\partial Z^2}]$$

$$(\frac{1}{1})\ (\delta)(\frac{1}{\delta})\ (1)(\frac{1}{1})=(\delta^2)[(\frac{1}{1})(\frac{1}{\delta})((1)(\frac{1}{\delta}))\ (\frac{1}{1})]$$

$$1 \quad 1 \quad 1 = \quad 1 \quad \delta^2$$

Thus the equation reduces to the following

$$\frac{\partial\theta}{\partial t}+V\frac{\partial\theta}{\partial R}+U\frac{\partial\theta}{\partial Z}=\frac{1}{PrRe}[\frac{1}{R}\frac{\partial}{\partial R}(R\frac{\partial\theta}{\partial R})]$$

The dropped term ,$1/PrRe[\partial^2\theta/\partial Z^2]$, represents the axial diffusion of heat which is very small as compared with the radial heat diffusion.

APPENDIX 2

NUMERICAL STABILITY AND CONVERGENCE

In this Appendix, the finite difference equations corresponding to the governing partial differential equations will be analyzed to find the conditions under which the numerical solution of the former equations converges to the exact solution of the latter equations as the grid spacings approach zero. To find such conditions , a convergence analysis, which consists of two tests, consistency and stability, is done.

I. Consistency

A finite difference equation is a consistent representation of the corresponding partial differential equation if the truncation error resulting from this representation tend to zero as the numerical grid spacings tend to zero. The consistency analysis of the present continuity and energy equations is discussed in detail by Alkam [31]. But the consistency analysis of the axial momentum equation is discussed hereunder.

The axial momentum equation and it's corresponding finite difference equation are written below, respectively.

$$\frac{\partial U}{\partial t}+V\frac{\partial U}{\partial R}+U\frac{\partial U}{\partial Z}=-\frac{\partial P}{\partial z}+\frac{\theta}{16(1-N)^4}+\frac{1}{R}\frac{\partial}{\partial R}(R\frac{\partial U}{\partial R}) \qquad (10)$$

$$\frac{U_{i,j+1,k+1}-U_{i,j+1,k}}{\Delta t}+V_{i,j,k}\frac{U_{i+1,j+1,k+1}-U_{i-1,j+1,k+1}}{2\Delta R}+U_{i,j,k}\frac{U_{i,j+1,k+1}-U_{i,j,k+1}}{\Delta Z}$$

$$=\frac{P_{j,k+1}-P_{j+1,k+1}}{\Delta Z}+\frac{\theta_{i,j+1,k+1}}{16(1-N)^4}+\frac{U_{i+1,j+1,k+1}-U_{i-1,j+1,k+1}}{2\Delta R[N+(i-1)\Delta R]}$$

$$+\frac{U_{i+1,j+1,k+1}-2U_{i,j+1,k+1}+U_{i-1,j+1,k+1}}{(\Delta R^2)} \qquad (15)$$

By means of Taylor series expansion, U, V , θ can be expanded about the point $[i\Delta R,(j+1)\Delta Z,(k+1)\Delta t]$ as follows

$$U_{i,j+1,k}=U_{i,j+1,k+1}-\Delta t\frac{\partial U}{\partial t}+\frac{(\Delta t)^2}{2!}\frac{\partial^2 U}{\partial t^2}-\frac{(\Delta t)^3}{3!}\frac{\partial^3 U}{\partial t^3}+\ldots$$

$$U_{i+1,j+1,k+1}=U_{i,j+1,k+1}+\Delta R\frac{\partial U}{\partial R}+\frac{(\Delta R)^2}{2!}\frac{\partial^2 U}{\partial R^2}+\frac{(\Delta R)^3}{3!}\frac{\partial^3 U}{\partial R^3}+\ldots$$

$$U_{i-1,j+1,k+1}=U_{i,j+1,k+1}-\Delta R\frac{\partial U}{\partial R}+\frac{(\Delta R)^2}{2!}\frac{\partial^2 U}{\partial R^2}-\frac{(\Delta R)^3}{3!}\frac{\partial^3 U}{\partial R^3}+\ldots$$

$$U_{i,j,k+1}=U_{i,j+1,k+1}-\Delta Z\frac{\partial U}{\partial Z}+\frac{(\Delta Z)^2}{2!}\frac{\partial^2 U}{\partial Z^2}-\frac{(\Delta Z)^3}{3!}\frac{\partial^3 U}{\partial Z^3}+\quad\ldots$$

$$P_{j,k+1}=P_{j+1,k+1}-(\Delta Z)\frac{\partial p}{\partial Z}+\frac{(\Delta Z)^2}{2!}\frac{\partial^2 p}{\partial Z^2}-\frac{(\Delta Z)^3}{3!}\frac{\partial^3 p}{\partial Z^3}+\ldots.$$

$$U_{i,j,k} = U_{i,j+1,k+1} - \Delta t\frac{\partial U}{\partial t} - \Delta Z\frac{\partial U}{\partial Z} + \frac{(\Delta t)^2}{2!}\frac{\partial^2 U}{\partial t^2} + \frac{(\Delta Z)^2}{2!}\frac{\partial^2 U}{\partial Z^2} + \frac{2}{2!}\Delta t\Delta Z\frac{\partial^2 U}{\partial t\partial Z} + \quad \ldots$$

$$V_{i,j,k} = V_{i,j+1,k+1} - \Delta t\frac{\partial V}{\partial t} - \Delta Z\frac{\partial V}{\partial Z} + \frac{(\Delta t)^2}{2!}\frac{\partial^2 V}{\partial t^2} + \frac{(\Delta Z)^2}{2!}\frac{\partial^2 V}{\partial Z^2} + \frac{2}{2!}\Delta t\Delta Z\frac{\partial^2 V}{\partial t\partial Z} + \quad \ldots$$

All the variables with subscript $i,j+1,k+1$ are at the point under consideration, around which all other terms are expanded.

The truncation error is that due to the replacement of the partial differential equation by it's finite difference equation. Therefore, the truncation error in representing the axial momentum equation (10) by the finite difference equation (15), T_a, is

T_a = Equation (15) - Equation (10)

Hence

$$T_a = \frac{U_{i,j+1,k+1} - U_{i,j+1,k}}{\Delta t} - \frac{\partial U}{\partial t}\Big|_{i,j+1,k+1}$$

$$+ V_{i,j,k}\frac{U_{i+1,j+1,k+1} - U_{i-1,j+1,k+1}}{2\Delta R} - V\frac{\partial U}{\partial R}\Big|_{i,j+1,k+1}$$

$$+U_{i,j,k}\frac{U_{i,j+1,k+1}-U_{i,j,k+1}}{\Delta Z}-U\frac{\partial U}{\partial Z}\Big|_{i,j+1,k+1}$$

$$-\frac{P_{j,k+1}-P_{j+1,k+1}}{\Delta Z}+\frac{dP}{dZ}\Big|_{i,j+1,k+1}-\frac{1}{16(1-N)^4}\theta_{i,j+1,k+1}$$

$$+\frac{\theta}{16(1-N)^4}\Big|_{i,j+1,k+1}-[\frac{U_{i+1,j+1,k+1}-U_{i-1,j+1,k+1}}{2\Delta R[N+(i-1)\Delta R]}]$$

$$-[\frac{U_{i+1,j+1,k+1}-2U_{i,j+1,k+1}+U_{i-1,j+1,k+1}}{(\Delta R)^2}]+\frac{1}{R}\frac{\partial}{\partial R}(R(\frac{\partial U}{\partial R}))$$

Substituting the values of all the terms in the last equation and rearranging gives :

$$T_a=\{-\frac{(\Delta t)}{2!}\frac{\partial^2 U}{\partial t^2}+\frac{(\Delta t)^2}{3!}\frac{\partial^3 U}{\partial t^3}-\quad \ldots\ \}+$$

$$\{\frac{(\Delta R)^2}{3!}(\partial^3 U/\partial R^3)V_{i,j+1,k+1}-\Delta t\frac{\partial V}{\partial t}\frac{\partial U}{\partial R}-\Delta Z\frac{\partial V}{\partial Z}\frac{\partial U}{\partial R}+\frac{(\Delta t)^2}{2!}\frac{\partial^2 V}{\partial t^2}\frac{\partial U}{\partial R}+\quad \ldots\ \}+$$

$$\{-\frac{(\Delta Z)}{2!}\frac{\partial^2 U}{\partial Z^2}U_{i,j+1,k+1}-\Delta t\frac{\partial U}{\partial t}\frac{\partial U}{\partial Z}-\Delta Z(\frac{\partial U}{\partial Z})^2+\frac{(\Delta t)^2}{2!}\frac{\partial^2 U}{\partial t^2}\frac{\partial U}{\partial Z}+\quad \ldots\ \}+$$

$$+\{\frac{-\Delta Z}{2!}\frac{\partial^2 P}{\partial Z^2}-\quad \ldots\ \}+\{-2\frac{(\Delta R)^2}{4!}\frac{\partial^4 U}{\partial R^2}+\quad \ldots\ \}+$$

$$+\{-\frac{(\Delta R)^2}{3!R_i}\frac{\partial^3 U}{\partial R^3}+ \quad ... \}$$

Since, R_i is not zero in the domain of the solution, then

$$T_a = O[\Delta t + \Delta Z + (\Delta R)^2]$$

Thus $T_a \rightarrow 0$ as Δt, ΔZ and $\Delta R \rightarrow 0$

and therefore the finite difference equation (15) is a consistent representation of the axial momentum equation (10)

II. Stability Analysis

The numerical stability of the finite difference equations is examined by von Neumann's procedure.This type of analysis is done by introducing small perturbations into the finite difference equations and checking wether or not such small disturbance components amplify as computation proceeds in the marching direction .

The axial momentum equation and energy equation are rewritten below in finite difference forms where variables with prime represent their values at a new time step.

The axial momentum equation :

$$\frac{U'_{i,j+1}-U_{i,j+1}}{\Delta t}+V_{i,j}\frac{U'_{i+1,j+1}-U'_{i-1,j+1}}{2\Delta R}+U'_{i,j}\frac{U'_{i,j+1}-U'_{i,j}}{\Delta Z}$$

$$=\frac{P'_j-P'_{j+1}}{\Delta Z}+\frac{\theta'_{i,j+1}}{16(1-N)^4}+\frac{U'_{i+1,j+1}-U'_{i-1,j+1}}{2[N+(i-1)\Delta R]\Delta R}$$

$$+\frac{U'_{i+1,j+1}-2U'_{i,j+1}+U'_{i-1,j+1,k+1}}{(\Delta R)^2} \qquad (1)$$

The energy equation :

$$\frac{\theta'_{i,j+1}-\theta_{i,j+1}}{\Delta t}+V_{i,j}\frac{\theta'_{i+1,j+1}-\theta'_{i-1,j+1}}{2\Delta R}+U_{i,j}\frac{\theta'_{i,j+1}-\theta'_{i,j}}{\Delta Z}=$$

$$+\frac{1}{Pr}\left[\frac{1}{N+(i-1)\Delta R}\frac{\theta'_{i+1,j+1}-\theta'_{i-1,j+1}}{(2\Delta R)}+\frac{\theta'_{i+1,j+1}-2\theta'_{i,j+1}+\theta'_{i-1,j+1}}{(\Delta R)^2}\right] \qquad (2)$$

The continuity equation is not considered in the stability analysis because it is independent of time [34]. Similarly the pressure terms in the axial momentum equation do not affect the stability analysis, since they appear at one level of time. During any time step ,the coefficients $U_{i,j}$ and $V_{i,j}$ appearing in (1) and (2) are treated as constants.At the end of any time step Δt , the new temperatures θ' and the new velocity components U' and V' at all interior grid points may be obtained by solving equations (1) and (2) .This process is repeated in time , successive steps in time may be regarded as successive approximations towards the final steady state solution ,and provided the time step is sufficiently small U,V and θ should eventually converge to values which approximate the exact solutions .

The general terms of the Fourier expansion for the errors in U and θ (U^* and θ^*) at the point i,j and at a time arbitrarily called t = 0 are both $e^{i\alpha R}e^{i\beta Z}$. At a time t later ,these terms become

$U^* = f_1(t)e^{i\alpha R}e^{i\beta Z}$, $\theta^* = f_2(t)e^{i\alpha R}e^{i\beta Z}$, and $P^* = f_3e^{i\beta Z}$.

where $i=\sqrt{-1}$ and f_3 is assumed constant across one time step since the

pressure appears in the finite-difference equations at one level of time.

Substituting in (1) and(2) for one time step and denoting values after the time step by f_1' and f_2' gives upon simplification ,

$$\frac{(f_1'-f_1)e^{i\beta\Delta Z}}{\Delta t}+V\frac{f_1'(e^{i\alpha\Delta R}-e^{-i\alpha\Delta R})e^{i\beta\Delta Z}}{2\Delta R}+U\frac{f_1'(e^{i\beta\Delta Z}-1)}{\Delta Z}=\frac{f_3(1-e^{i\beta\Delta Z})}{\Delta Z e^{i\alpha R}}+\frac{f_2'e^{i\beta\Delta Z}}{16(1-N)^4}+$$

$$f_1'\frac{(e^{i\alpha\Delta R}-e^{-i\alpha\Delta R})e^{i\beta\Delta Z}}{2[N+(i-1)\Delta R]\Delta R}+f_1'(\frac{e^{i\alpha R}-2+e^{-i\alpha R})e^{i\beta\Delta Z}}{(\Delta R)^2} \quad \text{and} \qquad (3)$$

$$\frac{(f_2'-f_2)e^{i\beta\Delta Z}}{\Delta t}+V\frac{f_2'(e^{i\alpha\Delta R}-e^{-i\alpha\Delta R})e^{i\beta\Delta Z}}{2\Delta R}+U\frac{f_2'(e^{i\beta\Delta Z}-1)}{\Delta Z}=f_2'\frac{(e^{i\alpha\Delta R}-e^{-i\alpha\Delta R})e^{i\beta\Delta Z}}{2Pr[N+(i-1)\Delta R]\Delta R}+$$

$$f_2'\frac{(e^{i\alpha\Delta R}-2+e^{-i\alpha\Delta R})e^{i\beta\Delta Z}}{Pr.(\Delta R)^2} \qquad (4)$$

Multiplying (3) by $\Delta t/e^{i\beta\Delta Z}$, the axial momentum equation can be put in the following form

$$Af_1'=f_1+Cf_2'+D \quad , \qquad (5)$$

where

$$A=(1+\frac{V\Delta t}{2\Delta R}(e^{i\alpha\Delta R}-e^{-i\alpha\Delta R})+\frac{U\Delta t}{\Delta Z}(1-e^{-i\beta\Delta Z})-\frac{\Delta t(e^{i\alpha\Delta R}-e^{-i\alpha\Delta R})}{2[N+(i-1)\Delta R]\Delta R}-$$

$$\frac{\Delta t}{(\Delta R)^2}(e^{i\alpha\Delta R}-2+e^{-i\alpha\Delta R}) \quad ,$$

$$C=\frac{\Delta t}{16(1-N)^4} \quad \text{, and}$$

$$D=\frac{f_3\Delta t(e^{-i\beta\Delta Z}-1)}{e^{i\alpha R}}$$

It is worth mentioning that for a given time the term D is constant at the point under consideration .

The energy equation can be written in the following form

$$A^{*}f_2'=f_2, \qquad (6)$$

where

$$A^{*}=1+\frac{V\Delta t}{2\Delta R}(e^{i\alpha\Delta R}-e^{-i\alpha\Delta R})+\frac{U\Delta t}{\Delta Z}(1-e^{-i\beta\Delta Z})-\frac{\Delta t(e^{i\alpha\Delta R}-e^{-i\alpha\Delta R})}{2Pr[N+(i-1)\Delta R]\Delta R}-$$

$$\frac{\Delta t}{Pr(\Delta R)^2}(e^{i\alpha\Delta R}-2+e^{-i\alpha\Delta R})$$

and hence $A^{*} = A$, if $Pr = 1$.

In other form,

$$A^{*} = 1 + \frac{V\Delta t}{2\Delta R}[i2\sin(\alpha\Delta R)] + \frac{U\Delta t}{\Delta Z}[1-\cos(\beta\Delta Z) + i\sin(\beta\Delta Z)] - \frac{\Delta t[\, i\, 2\sin(\alpha\Delta R)]}{2Pr[N+(i-1)\Delta R]\Delta R} -$$

$$\frac{\Delta t}{Pr(\Delta R)^2}[2\cos(\alpha\Delta R) - 2]$$

$$= 1 + \Delta t\{\frac{U}{\Delta Z}[1-\cos(\beta\Delta Z)] - \frac{2\cos(\alpha\Delta R)}{Pr(\Delta R)^2} + \frac{2}{Pr(\Delta R)^2}\}$$

$$+ i\,\Delta t\{\sin(\alpha\Delta R)[\frac{V}{\Delta R} - \frac{1}{PrR_i\Delta R}] + \frac{U}{\Delta Z}\sin(\beta\Delta Z)\}$$

Equations (5) and (6) can be written in the following matrix form

$$\begin{pmatrix} f_1' \\ f_2' \end{pmatrix} = \begin{pmatrix} \frac{1}{A} & \frac{C}{AA^{*}} \\ 0 & \frac{1}{A^{*}} \end{pmatrix} \begin{pmatrix} f_1 \\ f_2 \end{pmatrix} + \begin{pmatrix} \frac{D}{A} \\ 0 \end{pmatrix}$$

$$= G \begin{pmatrix} f_1 \\ f_2 \end{pmatrix} + \begin{pmatrix} \frac{D}{A} \\ 0 \end{pmatrix}$$

where G is the amplification matrix. For stability each of the eigenvalues of the amplification matrix (λ_1 and λ_2) must not exceed unity in modulus. However, $\lambda_1 = 1/A$ and $\lambda_2 = 1/A^{*}$. Hence for stability the following conditions should be satisfied.

$|1/A| \le 1$ or $|A| \ge 1$ and

$|1/A^{\bullet}| \leq 1$ or $|A^{\bullet}| \geq 1$

First,the term $A^{\bullet}$, which consists of real and imaginary components, is investigated as follows

$$A^{\bullet} = RR + i\ II \tag{7}$$

where $RR = 1 + \frac{\Delta t\ U}{\Delta Z} + \frac{2\Delta t}{Pr(\Delta R)^2} + \Delta t(X + XX)\cos(\alpha\Delta R) + \Delta t(XXX)\cos(\beta\Delta Z)$,

$II = \Delta t(X\text{-}XX)\ \sin(\alpha\Delta R) - \Delta t(XXX)\ \sin(\beta\Delta Z)$,

$$X = \frac{V}{2\Delta R} - \frac{1}{Pr(\Delta R)^2} - \frac{1}{2R_i\Delta RPr},$$

$$XX = \frac{-V}{2\Delta R} - \frac{1}{Pr(\Delta R)^2} + \frac{1}{2R_i\Delta RPr}, \text{ and}$$

$$XXX = -\frac{U}{\Delta Z}$$

$R_i = N + (i\text{-}1)\Delta R$

Thus ,

$$X + XX = \frac{-2}{Pr(\Delta R)^2}$$

$$X\text{-}XX = \frac{V}{\Delta R} - \frac{1}{R_i\Delta RPr}$$

To satisfy the stability condition ,the amplitude of (RR+iII) [Eq(7)] should be greater than or equal to one .Thus, $\sqrt{RR^2+II^2}\geq 1$ or $RR^2+II^2\geq 1$.

However ,

$$RR^2=1+\frac{(\Delta t)^2\ U^2}{\Delta Z^2}+\frac{4(\Delta t)^2}{Pr^2(\Delta R)^4}+\frac{2(\Delta t)\ U}{\Delta Z}+\frac{4(\Delta t)}{Pr(\Delta R)^2}+\frac{4(\Delta t)^2}{Pr^2(\Delta R)^4}\cos^2(\alpha\Delta R)$$

$$+\cos(\alpha\Delta R)[-\frac{4(\Delta t)}{Pr(\Delta R)^2}-\frac{4(\Delta t)^2U}{Pr\Delta Z(\Delta R)^2}-\frac{8(\Delta t)^2}{Pr^2(\Delta R)^4}]+\frac{4(\Delta t)^2U}{Pr\Delta Z(\Delta R)^2}$$

$$+\frac{(\Delta t)^2U^2}{(\Delta Z)^2}\cos^2(\beta\Delta Z)+\cos(\beta\Delta Z)[-\frac{2(\Delta t)U}{\Delta Z}-\frac{2(\Delta t)^2U^2}{(\Delta Z)^2}-\frac{4(\Delta t)^2U}{Pr(\Delta R)^2\Delta Z}]$$

$$+\frac{4(\Delta t)^2U}{Pr(\Delta R)^2\Delta Z}\cos(\alpha\Delta R)\cos(\beta\Delta Z)$$

and,

$$II^2=[\frac{(\Delta t)V}{\Delta R}-\frac{(\Delta t)}{Pr(\Delta R)R_i}]^2\sin^2(\alpha\Delta R)+\frac{(\Delta t)^2\ U^2}{(\Delta Z)^2}\sin^2(\beta\Delta Z)+$$

$$[\frac{2(\Delta t)^2UV}{2\Delta Z\Delta R}-\frac{2(\Delta t)^2U}{Pr\Delta Z\Delta RR_i}]\sin(\alpha\Delta R)\sin(\beta\Delta Z).$$

Substituting the values of RR^2 and II^2 in equation (7) gives

$$1+\frac{(\Delta t)^2\ U^2}{\Delta Z^2}+\frac{4(\Delta t)^2}{Pr^2(\Delta R)sup4}+\frac{2(\Delta t)\ U}{\Delta Z}+\frac{4(\Delta t)}{Pr(\Delta R)^2}+\frac{4(\Delta t)^2}{Pr^2(\Delta R)^4}\cos^2(\alpha\Delta R)$$

$$+\cos(\alpha\Delta R)\left[-\frac{4(\Delta t)}{Pr(\Delta R)^2}-\frac{4(\Delta t)^2U}{Pr\Delta Z(\Delta R)^2}-\frac{8(\Delta t)^2}{Pr^2(\Delta R)^4}\right]+\frac{4(\Delta t)^2U}{Pr\Delta Z(\Delta R)^2}$$

$$+\frac{(\Delta t)^2U^2}{(\Delta Z)^2}\cos^2(\beta\Delta Z)+\cos(\beta\Delta Z)\left[-\frac{2(\Delta t)U}{(\Delta Z}-\frac{2(\Delta t)^2U^2}{(\Delta Z)^2}-\frac{4(\Delta t)^2U}{Pr(\Delta R)^2\Delta Z}\right]$$

$$+\frac{4(\Delta t)^2U}{Pr(\Delta R)^2\Delta Z}\cos(\alpha\Delta R)\cos(\beta\Delta Z)$$

$$\left[\frac{(\Delta t)V}{\Delta R}-\frac{(\Delta t)}{Pr(\Delta R)R_i}\right]^2\sin^2(\alpha\Delta R)+\frac{(\Delta t)^2\ U^2}{(\Delta Z)^2}\sin^2(\beta\Delta Z)+$$

$$\left[\frac{2(\Delta t)^2UV}{2\Delta Z\Delta R}-\frac{2(\Delta t)^2U}{Pr\Delta Z\Delta RR_i}\right]\sin(\alpha\Delta R)\sin(\beta\Delta Z)\geq 0 \qquad (8)$$

The condition under which the inequality (8) is satisfied can be investigated by inspection as follows.Taking into consideration that the present boundary layer model is applicable to cases without flow reversals.Then,assumed that U is always positive ,each term in the inequality (8) is positive except the following terms

$$\cos(\alpha\Delta R)\left[-\frac{4(\Delta t)}{Pr(\Delta R)^2}-\frac{4(\Delta t)^2U}{Pr\Delta Z(\Delta R)^2}-\frac{8(\Delta t)^2}{Pr^2(\Delta R)^4}\right]$$

$$\cos(\beta\Delta Z)\left[-\frac{2(\Delta t)U}{(\Delta Z}-\frac{2(\Delta t)^2U^2}{(\Delta Z)^2}-\frac{4(\Delta t)^2U}{Pr(\Delta R)^2\Delta Z}\right]$$

$$\frac{4(\Delta t)^2 U}{Pr(\Delta R)^2 \Delta Z}\cos(\alpha\Delta R)\ \cos(\beta\Delta Z)$$

$$[\frac{2(\Delta t)^2 U\ V}{\Delta R\Delta Z} - \frac{2(\Delta t^2)U}{\Delta Z Pr\Delta R R_i}]\sin(\alpha\Delta R)\ \sin(\beta\Delta Z)$$

By inspection ,the worst case occurs when both $\cos(\alpha\Delta R)$ and $\cos(\beta\Delta Z)$ are equal to unity ,because these two terms have ,in such a case their largest possible negative values.In this case , $\sin(\alpha\Delta R)$ and $\sin(\beta\Delta Z)$ will be zero.Substituting these values in the left side of inequality (8) shows that it vanishes. Thus ,under the worst conditions the inequality (8) is satisfied for all other values of $\cos(\alpha\Delta R)$, $\cos(\beta\Delta Z)$, $\sin(\alpha\Delta R)$,and $\sin(\beta\Delta Z)$

Using exactly the same procedure, it can be seen that the other inequality ($|A|\geq 1$) is also satisfied under the same condition that U is non-negative. This is because the only difference between the two eigenvalues is the Prandtl number (Pr) which does not have any effect on the above mentioned stability analysis.At the worst condition all the terms will be cancelled except the term (1),thus the stability condition is again satisfied.

In other words , the numerical stability condition is satisfied for all values of ΔR , ΔZ and Δt on condition that U is nonnegative.

APPENDIX (3)

COMPUTER PROGRAM

4.1 Introduction

The computer program is written in Fortran 77 and executed at King Fahd University of Petroleum and Minerals. The program was built to solve the problem of transient free convection in the developing region of a vertical concentric annulus under the investigated thermal boundary conditions (I) and (O).

The following are some important symbols used in the program.

A,B,C	Coefficients used for the energy equation matrix.
DR	The radial step, ΔR.
DT	The time step, Δt.
DZ	The axial step, ΔZ.
DZZ	The initial axial step .
EPS	Pressure tolerance (iteration criterion) at top exit.
FF(NC)	Dimensionless flow at any time .
G(I,J)	Coefficient of the Axial Momentum equation .
IC	Iteration Counter.

INT1	a numerical value of $\int_N^1 UR\theta dR$.
INT2	a numerical value of $\int_N^1 URdR$.
ISC	1 if the program is used for Case (I).
ISC	0 if the program is used for Case (O).
JC	Actual total number of axial increments.
M	Maximum possible number of axial increments allowed by the program.
N	Number of radial increments.
NC	Time Counter.
NK	Maximum number of time steps allowed by the program.
LZ	The dimensionless height, L .
PP(IC)	Exit dimensionless pressure at used in th iteration process at a specific time .
PR	Prandtl Number, Pr.
QF(NC)	Total Heat absorbed .
RAT	Radius ratio, N .
SS	Steady state criterion, $[\overline{H}(k+1)-\overline{H}(k)]/\overline{H}(k+1)$.
TIME	Time.
TM	Mixing Cup Temperature .
UE	UR .
UET	UR 0.

```
C=====================================================================  PR000010
C     THIS PROGRAM IS DEVELOPED TO SOLVE THE FREE NATURAL CONVECTION    PR000020
C     PROBLEM IN AN OPEN-ENDED VERTICAL ANNULUS FOR TWO DIFFERENT       PR000030
C     BOUNDARY CONDITIONS.                                              PR000040
C=====================================================================  PR000050
C                                                                       PR000060
C                                                                       PR000070
C---------------------------------------------------------------------  PR000080
                                                                        PR000090
      IMPLICIT REAL*8(A-H, O-Z)                                         PR000100
      INTEGER H,QH,Q,QQ,JM,JL,JO,JC,JH                                  PR000110
      REAL INT1,INT2,NULOCL,NU,LZ                                       PR000120
      DIMENSION  U(41,1002,2),V(41,1002,2),T(41,1002,2),P(1002,2),      PR000130
     * A(41),B(41),C(41),D(41),E(41),F(41),G(41,42),QF(1002,2),         PR000140
     * TM(1002,2),FF(200),PE(200),PP(100),FP(100),ZSS(200),             PR000150
     * UE(41),UET(41)                                                   PR000160
      OPEN(UNIT=1,FILE='OUT1')                                          PR000170
      OPEN(UNIT=2,FILE='OUT2')                                          PR000180
      OPEN(UNIT=3,FILE='OUT3')                                          PR000190
      OPEN(UNIT=4,FILE='OUT4')                                          PR000200
      OPEN(UNIT=5,FILE='OUT5')                                          PR000210
      OPEN(UNIT=7,FILE='OUT7')                                          PR000220
      OPEN(UNIT=8,FILE='OUT8')                                          PR000230
      OPEN(UNIT=9,FILE='OUT9')                                          PR000240
      OPEN(UNIT=10,FILE='OUT10')                                        PR000250
      OPEN(UNIT=11,FILE='OUT11')                                        PR000260
      OPEN(UNIT=12,FILE='OUT12')                                        PR000270
      OPEN(UNIT=13,FILE='OUT13')                                        PR000280
      OPEN(UNIT=14,FILE='OUT14')                                        PR000290
      OPEN(UNIT=15,FILE='OUT15')                                        PR000300
      OPEN(UNIT=16,FILE='OUT16')                                        PR000310
      OPEN(UNIT=17,FILE='OUT17')                                        PR000320
C---------------------------------------------------------------------  PR000330
C                                                                       PR000340
C---------------------------------------------------------------------  PR000350
      DATA FF(1)/.005/                                                  PR000360
      DATA DT/0.001/                                                    PR000370
      DATA DZZ/0.000002/                                                PR000380
      DATA RAT/0.5/                                                     PR000390
      DATA PR/0.7/                                                      PR000400
      DATA M/999/                                                       PR000410
      DATA N/40/                                                        PR000420
      DATA NK/100/                                                      PR000430
      DR=(1-RAT)/N                                                      PR000440
      ISC = 1                                                           PR000450
      NC= 1                                                             PR000460
      Z=0.0                                                             PR000470
      TIME = 0.0                                                        PR000480
      NC = 1                                                            PR000490
      IC = 1                                                            PR000500
      EPS=1.0E-15                                                       PR000510
      DZ=DZZ                                                            PR000520
      LZ = 0.0001                                                       PR000530
      JC=(LZ/DZZ)                                                       PR000540
C---------------------------------------------------------------------  PR000550
```

```
C                                                                       PR000560
C-----------------------------------------------------------------      PR000570
      K=1                                                               PR000580
      DO 1 J=1,M+1                                                      PR000590
         DO 2 I=1,N+1                                                   PR000600
            U(I,J,K) =0.0                                               PR000610
            V(I,J,K) =0.0                                               PR000620
            T(I,J,K) =0.0                                               PR000630
            P(J,K) =0.0                                                 PR000640
2     CONTINUE                                                          PR000650
1     CONTINUE                                                          PR000660
C-----------------------------------------------------------------      PR000670
C                                                                       PR000680
C-----------------------------------------------------------------      PR000690
22     DO 5 I=2,N                                                       PR000700
         V(I,1,2)=0.0                                                   PR000710
         T(I,1,2)=0.0                                                   PR000720
         U(I,1,2)=FF(NC)/(1-RAT**2)                                     PR000730
5     CONTINUE                                                          PR000740
      P(1,2)=-0.5*(FF(NC)/(1-RAT**2))**2                                PR000750
      T(1,1,2)   =0.0                                                   PR000760
      T(N+1,1,2) =0.0                                                   PR000770
        J=1                                                             PR000780
C-----------------------------------------------------------------      PR000790
C                                                                       PR000800
C-----------------------------------------------------------------      PR000810
                                                                        PR000820
33     IF (J .EQ. 1500)       THEN                                     PR000830
          DZ=2*DZ                                                       PR000840
       ELSEIF (J .EQ. 2000)   THEN                                      PR000850
          DZ=2*DZ                                                       PR000860
       ELSE IF (J .EQ. 3000)  THEN                                      PR000870
          DZ=5*DZ                                                       PR000880
       ELSE IF (J .EQ. 5000)  THEN                                      PR000890
          DZ=5*DZ                                                       PR000900
       ELSE IF (J .EQ. 10000) THEN                                      PR000910
          DZ=5*DZ                                                       PR000920
       ELSE IF (J .EQ. 15000) THEN                                      PR000930
          DZ=5*DZ                                                       PR000940
       ENDIF                                                            PR000950
       Z=Z+DZ                                                           PR000960
C      PRINT *,Z,LZ                                                     PR000970
C      IF (Z .EQ. LZ)  THEN                                             PR000980
C          JC=J                                                         PR000990
C       PRINT *,'JCJCJCJCJCJCJC',JC                                     PR001000
C      ENDIF                                                            PR001010
C-----------------------------------------------------------------      PR001020
C                                                                       PR001030
C-----------------------------------------------------------------      PR001040
         DO 7 L=J,J+1                                                   PR001050
           V(1,L,2)   = 0.0                                             PR001060
           V(N+1,L,2) = 0.0                                             PR001070
           U(1,L,2)   = 0.0                                             PR001080
           U(N+1,L,2) = 0.0                                             PR001090
         IF (ISC .EQ. 1) THEN                                           PR001100
```

```
          T(1,L,2)   = 1.0                                              PR001110
        ELSE                                                            PR001120
          T(N+1,L,2)   = 1.0                                            PR001130
        ENDIF                                                           PR001140
7       CONTINUE                                                        PR001150
        IF (ISC .EQ. 0) GOTO 2020                                       PR001160
                                                                        PR001170
C-------------------------------------------------------------------    PR001180
C                                                                       PR001190
C-------------------------------------------------------------------    PR001200
1010    DO 108 I=2,N+1                                                  PR001210
108       A(I) = U(I,J,K)/DZ+2/(PR*DR**2)+1/DT                          PR001220
        DO 109 I=2,N                                                    PR001230
109       B(I) = V(I,J,K)/(2*DR)-1/(PR*DR**2)-1/(2*PR*                  PR001240
     *              DR*(RAT+(I-1)*DR))                                 PR001250
        DO 110 I=3,N+1                                                  PR001260
110       C(I) = 1/(2*PR*DR*(RAT+(I-1)*DR))-V(I,J,K)                    PR001270
     *              /(2*DR)-1/(PR*DR**2)                               PR001280
         C(N+1) = -2/(PR*DR**2)                                         PR001290
        DO 113 I=2,N+1                                                  PR001300
113       D(I) = (T(I,J,K+1)*U(I,J,K))/DZ+T(I,J+1,K)/DT                 PR001310
          D(2) = D(2)+(1/(PR*DR**2)+V(2,J,K)/(2*DR)                     PR001320
     *    -1/(2*PR*DR*(RAT+DR)))                                        PR001330
C-------------------------------------------------------------------    PR001340
C                                                                       PR001350
C-------------------------------------------------------------------    PR001360
        E(2)=A(2)                                                       PR001370
        F(2)=D(2)/E(2)                                                  PR001380
        DO 300 I=3,N+1                                                  PR001390
          E(I)=A(I)-C(I)*B(I-1)/E(I-1)                                  PR001400
          F(I)=(D(I)-C(I)*F(I-1))/E(I)                                  PR001410
300     CONTINUE                                                        PR001420
        T(N+1,J+1,K+1)=F(N+1)                                           PR001430
        DO 310 JJ=1,N-1                                                 PR001440
          I=N+1-JJ                                                      PR001450
310     T(I,J+1,K+1)=F(I)-B(I)*T(I+1,J+1,K+1)/E(I)                      PR001460
        GOTO 3030                                                       PR001470
C-------------------------------------------------------------------    PR001480
C                                                                       PR001490
C-------------------------------------------------------------------    PR001500
2020    DO 311 I=1,N                                                    PR001510
311       A(I) = U(I,J,K)/DZ+2/(PR*DR**2)+1/DT                          PR001520
        DO 312 I=1,N-1                                                  PR001530
312       B(I) = V(I,J,K)/(2*DR)-1/(PR*DR**2)-1/(2*PR*                  PR001540
     *              DR*(RAT+(I-1)*DR))                                 PR001550
        DO 313 I=2,N                                                    PR001560
313       C(I) = 1/(2*PR*DR*(RAT+(I-1)*DR))-V(I,J,K)                    PR001570
     *              /(2*DR)-1/(PR*DR**2)                               PR001580
         B(1) = -2/(PR*DR**2)                                           PR001590
        DO 314 I=1,N                                                    PR001600
314       D(I) = (T(I,J,K+1)*U(I,J,K))/DZ+T(I,J+1,K)/DT                 PR001610
          D(N) = D(N)+(1/(PR*DR**2)-V(N,J,K)/(2*DR)                     PR001620
     *    +1/(2*PR*DR*(RAT+N*DR)))                                      PR001630
C-------------------------------------------------------------------    PR001640
C                                                                       PR001650
```

```
C-----------------------------------------------------------------      PR001660
      E(1)=A(1)                                                        PR001670
      F(1)=D(1)/E(1)                                                   PR001680
      DO 315 I=2,N                                                     PR001690
        E(I)=A(I)-C(I)*B(I-1)/E(I-1)                                   PR001700
        F(I)=(D(I)-C(I)*F(I-1))/E(I)                                   PR001710
315   CONTINUE                                                         PR001720
      T(N,J+1,K+1)=F(N)                                                PR001730
      DO 316 JJ=1,N-1                                                  PR001740
        I=N-JJ                                                         PR001750
316   T(I,J+1,K+1)=F(I)-B(I)*T(I+1,J+1,K+1)/E(I)                       PR001760
C-----------------------------------------------------------------      PR001770
C                                                                      PR001780
C-----------------------------------------------------------------      PR001790
3030  DO 116 Q=2,N+2                                                   PR001800
        DO 116 H=2,N+1                                                 PR001810
          G(H,Q)=0.0                                                   PR001820
116   CONTINUE                                                         PR001830
      G(2,N+2)=FF(NC)/(2*DR)                                           PR001840
      DO 117 I=2,N                                                     PR001850
        G(2,I) = RAT+(I-1)*DR                                          PR001860
117     G(I+1,N+1)=1.0                                                 PR001870
      DO 119 Q=2,N                                                     PR001880
119     G(Q+1,N+2)=U(Q,J+1,K)*(DZ/DT)+U(Q,J,K+1)*U(Q,J,K)              PR001890
     *    +P(J,K+1)+(DZ/(16*(1-RAT)**4))*T(Q,J+1,K+1)                 PR001900
      DO 120 I=2,N-1                                                   PR001910
        G(I+1,I+1)=(DZ/DR)*(V(I,J,K)/2-1/DR-1/(2*(RAT+(I-1)*DR)))      PR001920
        G(I+1,I)=DZ/DT+U(I,J,K)+(2*DZ)/(DR**2)                         PR001930
120     G(I+2,I)  =(DZ/DR)*(1/(2*(RAT+(I)*DR))-V(I+1,J,K)/2-1/DR)      PR001940
        G(N+1,N)=DZ/DT+U(N,J,K)+(2*DZ)/(DR**2)                         PR001950
C-----------------------------------------------------------------      PR001960
C                                                                      PR001970
C-----------------------------------------------------------------      PR001980
      DO 121 H=2,N+1                                                   PR001990
      DO 122 QH=H,N+2                                                  PR002000
      Q=N+2-QH+H                                                       PR002010
122   G(H,Q)=G(H,Q)/G(H,H)                                             PR002020
      I=1                                                              PR002030
      DO 150 I=I+1,H+2                                                 PR002040
      IF(I.EQ.H) GOTO 150                                              PR002050
      IF(I.GE.N+2)GOTO 121                                             PR002060
      DO 160 QQ=H,N+2                                                  PR002070
      Q=N+2-QQ+H                                                       PR002080
160   G(I,Q)=G(I,Q)-G(I,H)*G(H,Q)                                      PR002090
150   CONTINUE                                                         PR002100
121   CONTINUE                                                         PR002110
      P(J+1,K+1)=G(N+1,N+2)                                            PR002120
      DO 123 I=2,N                                                     PR002130
123   U(I,J+1,K+1)=G(I,N+2)                                            PR002140
C-----------------------------------------------------------------      PR002150
C                                                                      PR002160
C-----------------------------------------------------------------      PR002170
      IF (ICS .EQ. 0) GOTO 851                                         PR002180
      LC=N-3                                                           PR002190
      LD=N-1                                                           PR002200
```

```
        GOTO 852                                                        PR002210
851     LC=2                                                            PR002220
        LD=5                                                            PR002230
852     DO 853 I=LC,LD                                                  PR002240
          IF (U(I+1,J+1,K+1).GT.0.0) GOTO 853                           PR002250
C         PRINT *,Z,U(I+1,J+1,K+1)                                      PR002260
853     CONTINUE                                                        PR002270
                                                                        PR002280
C-------------------------------------------------------------------    PR002290
C                                                                       PR002300
C-------------------------------------------------------------------    PR002310
        DO 450 I=1,N-1                                                  PR002320
450     V(I+1,J+1,K+1)=V(I,J+1,K+1)*(RAT+(I-1)*DR)/(RAT+I*DR)-          PR002330
     *  ((2*RAT+(2*I-1)*DR)*(DR/(4*DZ))/(RAT+I*DR))*                    PR002340
     *  (U(I+1,J+1,K+1)+U(I,J+1,K+1)-U(I+1,J,K+1)-U(I,J,K+1))           PR002350
C-------------------------------------------------------------------    PR002360
C                                                                       PR002370
C-------------------------------------------------------------------    PR002380
      IF (IC .NE. 1) GOTO 560                                           PR002390
      IF (NC .NE. 1) GOTO 560                                           PR002400
      IF (P(J+1,K+1).GT.0.0) THEN                                       PR002410
          FF(NC)=1.3*FF(NC)                                             PR002420
          GOTO 910                                                      PR002430
      ELSE                                                              PR002440
        IF (Z.GT.LZ) THEN                                               PR002450
          PRINT *,NC,IC,P(JC,2),FF(NC)                                  PR002460
          IC=IC+1                                                       PR002470
          PP(1)=P(JC,K+1)                                               PR002480
          FP(1)=FF(NC)                                                  PR002490
          FF(NC)=1.05*FF(NC)                                            PR002500
          QF(JC,K)=0.0                                                  PR002510
          GOTO 910                                                      PR002520
        ENDIF                                                           PR002530
         J=J+1                                                          PR002540
         PRINT *,' ---------',J,P(J,K+1)                                PR002550
         GOTO  33                                                       PR002560
      ENDIF                                                             PR002570
C-------------------------------------------------------------------    PR002580
C                                                                       PR002590
C-------------------------------------------------------------------    PR002600
560   IF (Z .GT. LZ) GOTO 570                                           PR002610
      IF (P(J+1,K+1).GE.0.0) THEN                                       PR002620
        IF (IC.EQ.1) THEN                                               PR002630
          FF(NC)=10.3 * FF(NC-1)                                        PR002640
          PRINT *,'PRESSURE IS POSITIVE EARLY         11111'            PR002650
        ELSE                                                            PR002660
          GOTO 569                                                      PR002670
        ENDIF                                                           PR002680
        GOTO 910                                                        PR002690
      ELSE                                                              PR002700
569     J=J+1                                                           PR002710
       GOTO 33                                                          PR002720
      ENDIF                                                             PR002730
C-------------------------------------------------------------------    PR002740
570    PP(IC)=P(JC,K+1)                                                 PR002750
```

```
      FP(IC)=FF(NC)                                                     PR002760
      PRINT *,NC,IC,PP(IC),FP(IC)                                       PR002770
      IC=IC+1                                                           PR002780
      IF (IC .NE. 2) GOTO 610                                           PR002790
      FF(NC)=1.1 * FF(NC-1)                                             PR002800
      GOTO 910                                                          PR002810
610   FP(IC)=FP(IC-2)-PP(IC-2)*(FP(IC-2)-FP(IC-1))/(PP(IC-2)-PP(IC-1)) PR002820
      FF(NC)=FP(IC)                                                     PR002830
      IF((P(JC,K+1).GT.-EPS).AND.(P(JC,K+1).LT.EPS)) THEN               PR002840
      IC =1                                                             PR002850
      GOTO 705                                                          PR002860
     ELSE                                                               PR002870
      GOTO 910                                                          PR002880
     ENDIF                                                              PR002890
C-----------------------------------------------------------------------PR002900
C                                                                       PR002910
C-----------------------------------------------------------------------PR002920
705   Z=0.0                                                             PR002930
      DZ=DZZ                                                            PR002940
      DO 1700 J=1,JC                                                    PR002950
C      PRINT *,J,J,J                                                    PR002960
C-----------------------------------------------------------------------PR002970
C                                                                       PR002980
C-----------------------------------------------------------------------PR002990
1555  IF (J .EQ. 1500)       THEN                                       PR003000
         DZ=2*DZ                                                        PR003010
      ELSEIF (J .EQ. 2000)   THEN                                       PR003020
         DZ=2*DZ                                                        PR003030
      ELSE IF (J .EQ. 3000)  THEN                                       PR003040
         DZ=5*DZ                                                        PR003050
      ELSE IF (J .EQ. 5000)  THEN                                       PR003060
         DZ=5*DZ                                                        PR003070
      ELSE IF (J .EQ. 10000) THEN                                       PR003080
         DZ=5*DZ                                                        PR003090
      ELSE IF (J .EQ. 15000) THEN                                       PR003100
         DZ=5*DZ                                                        PR003110
      ENDIF                                                             PR003120
      Z=Z+DZ                                                            PR003130
                                                                        PR003140
C-----------------------------------------------------------------------PR003150
1556     IF (NC.NE. 5) GOTO 711                                         PR003160
C         IF ((J.GT.30).OR.(J.NE.JC)) GOTO 711                          PR003170
          DO 710 I=1,41,2                                               PR003180
             DR1=RAT+(I-1)*DR                                           PR003190
             WRITE (1,*) DR1,U(I,J,2),J,NC                              PR003200
             WRITE (2,*) DR1,V(I,J,2),J,NC                              PR003210
             WRITE (3,*) DR1,T(I,J,2),J,NC                              PR003220
710       CONTINUE                                                      PR003230
C-----------------------------------------------------------------------PR003240
C                                                                       PR003250
C                                                                       PR003260
C-----------------------------------------------------------------------PR003270
711     DO 970 I=1,N+1                                                  PR003280
          UE(I)=(RAT+(I-1)*DR)*U(I,J,K+1)                               PR003290
970       UET(I)=UE(I)*T(I,J,K+1)                                       PR003300
```

```
        INT1 = 0.0                                                      PR003310
        INT2 = 0.0                                                      PR003320
       DO 971 I=2,N                                                     PR003330
        INT1=INT1+2*UET(I)                                              PR003340
971     INT2=INT2+2*UE(I)                                               PR003350
       TM(J,K+1)=INT1/INT2                                              PR003360
       QF(J,K+1)=INT1*DR                                                PR003370
       WRITE(4,*)Z,P(J,K+1),J,NC                                        PR003380
       WRITE(5,*)Z,TM(J,K+1),J,NC                                       PR003390
       WRITE(8,*)Z,T(N+1,J,K+1),J,NC                                    PR003400
       WRITE(9,*)Z,T(20,J,K+1),J,NC                                     PR003410
        IF (J.NE.(JC/2))GOTO 972                                        PR003420
          DO 973 I=1,41,2                                               PR003430
             DR1=RAT+(I-1)*DR                                           PR003440
             WRITE (10,*) DR1,U(I,J,2),J,NC                             PR003450
             WRITE (11,*) DR1,V(I,J,2),J,NC                             PR003460
             WRITE (12,*) DR1,T(I,J,2),J,NC                             PR003470
 973        CONTINUE                                                    PR003480
972      IF (J.NE. JC) GOTO 712                                         PR003490
                                                                        PR003500
                                                                        PR003510
712     IF (J.EQ.JC) GOTO 888                                           PR003520
1700   CONTINUE                                                         PR003530
       IF (J .NE. JC) THEN                                              PR003540
         PRINT *,'HERE J=JC    !!!!!!!!!!!!!!!!!!!'                     PR003550
         J=JC                                                           PR003560
         GOTO 1555                                                      PR003570
       ENDIF                                                            PR003580
888     SS=(QF(JC,2)-QF(JC,1))/QF(JC,2)                                 PR003590
        PRINT *,NC,SS,QF(JC,1),QF(JC,2)                                 PR003600
         WRITE(14,*)TIME,FF(NC),J,NC                                    PR003610
         WRITE(15,*)TIME,QF(JC,2),J,NC                                  PR003620
        IF (ABS(SS) .LT. 1E-6) GOTO 6000                                PR003630
        DO 889 J=1,JC                                                   PR003640
             QF(J,1) = QF(J,2)                                          PR003650
             TM(J,1) = TM(J,2)                                          PR003660
889     CONTINUE                                                        PR003670
C-----------------------------------------------------------------------PR003680
C                                                                       PR003690
C-----------------------------------------------------------------------PR003700
       DO 903 J=1,JC                                                    PR003710
         DO 900  I=1,N+1                                                PR003720
             U(I,J,1)=U(I,J,2)                                          PR003730
             V(I,J,1)=V(I,J,2)                                          PR003740
             T(I,J,1)=T(I,J,2)                                          PR003750
900    CONTINUE                                                         PR003760
             P(J,1)  = P(J,2)                                           PR003770
903    CONTINUE                                                         PR003780
        NC=NC+1                                                         PR003790
        TIME = TIME + DT                                                PR003800
        IF (NC .EQ. 3) GOTO 6000                                        PR003810
        IC = 1                                                          PR003820
        RN = 1.05                                                       PR003830
        FF(NC)=  RN * FF(NC-1)                                          PR003840
910     Z=0.0                                                           PR003850
```

```
       J=1                                                          PR003860
       DZ=DZZ                                                       PR003870
       GOTO 22                                                      PR003880
6000   CLOSE(1)                                                     PR003890
       CLOSE(2)                                                     PR003900
       CLOSE(3)                                                     PR003910
       CLOSE(4)                                                     PR003920
       CLOSE(5)                                                     PR003930
       CLOSE(7)                                                     PR003940
       CLOSE(8)                                                     PR003950
       CLOSE(9)                                                     PR003960
       CLOSE(10)                                                    PR003970
       CLOSE(11)                                                    PR003980
       CLOSE(12)                                                    PR003990
       CLOSE(13)                                                    PR004000
       CLOSE(14)                                                    PR004010
       CLOSE(15)                                                    PR004020
       CLOSE(16)                                                    PR004030
       CLOSE(17)                                                    PR004040
       STOP                                                         PR004050
       END                                                          PR004060
```

REFERENCES

1. R. Siegel,"Transient Free Convection from a Vertical Flat Plate", Trans. ASME ,Vol. 80,pp. 347-359,1958.

2. E.M. Sparrow and J.L. Gregg, "Nearly Quasi-Steady Free Convection Heat Transfer in Gases", ASME J. Heat Transfer, Vol.82, pp. 258-260,1960.

3. P.M. Chung and A.D. Anderson,"Unsteady Laminar Free Convection", ASME J. Heat Transfer ,Vol. 83,pp. 473-478,1961.

4. B. Gebhart," Transient Natural Convection from Vertical Elements", ASME J. Heat Transfer,Vol 83, pp. 61-70, 1961.

5. J.D. Hellums and S.W. Churchill,"Computation of Natural Convection by Finite-Difference Methods",Proceedings of the Int. Heat Transfer Conference,Part V,pp. 985-994,1961.

6. J.D. Hellums and S.W. Churchill," Transient and Steady State, Free and Natural Convection, Numerical Solutions", A.I.Ch.E. Journal, Vol.8, pp. 690-692,1962.

7. J.A. Schetz and R. Eichhorn," Unsteady Natural Convection in the Vicinity of a Doubly Infinite Vertical Plate", ASME J. Heat Transfer, Vol. 84, pp. 334-338,1962.

8. E.R. Menold and K. Yang," Asymptotic Solutions for Unsteady Laminar Free Convection on a Vertical Plate", ASME J. Applied Mechanics, Vol. 84,pp. 124-126,1962.

9. B. Gebhart, and D.E. Adams," Measurement of Transient Natural Convection on Flat Vertical Surfaces", ASME J. Heat Transfer,Vol. 85, pp. 25-28,1963.

10. A.J. Ede,"Advances in Free Convection,in Advances in Heat Transfer" ,ed. T.F. Irvire and J.P. Hartnett,Vol. 4,pp. 1-64,Academic,NewYork ,1968.

11. K. Nanbu," Limit of Pure Conduction for Unsteady Free Convection on a Vertical Plate", Int. J. Heat Mass Transfer, Vol.14, pp. 1531-1534, 1971.

12. R. Nanda, and V. Sharma," Free-Convection Laminar Boundary Layers in Oscillatory Flow", AIAA Journal, Vol.1, pp. 937-938, 1963.

13. J.W. Yang, C. Scaccia, and J. Goodman," Laminar Natural Convection About Plates with Oscillatory Surface Temperatures", ASME J. of Heat Transfer,Vol. 96, pp. 9-14, 1974.

14. Y. Kawase and J. Ulbrecht," Approximate Solution to the Natural Convection Heat Transfer from a Vertical Plate", Int. Comm. Heat Mass transfer, Vol.11, pp. 143-155, 1984.

15. S. Haq ,C. Kleinstreuer and J.C.Mulligan,"Transient Free Convection of a Non-Newtonian Fluid a Long a Vertical Wall" ,ASME J. Heat Transfer ,Vol.110,pp. 604-607,1988.

16. J.R. Bodia and J.F. Osterle,"The Development of Free Convection Between Heated Vertical Plates",ASME J. Heat Transfer ,Vol. 84,pp. 40-44, 1962.

17. C. F. Kettleborough," Transient Laminar Free Convection Between Heated Vertical Plates Including Entrance Effects", Int. J. Heat Mass Transfer, Vol.15, pp. 883-896, 1972.

18. T.S. Lee, P.G. Parikh, A. Acrivos and D. Bershader," Natural Convection in Vertical Channel with Opposing Buoyancy Forces", Int. J. Heat Mass Transfer, Vol.25, pp. 499-511, 1982.

19. E.M. Sparrow, G.M. Chrysler and L.F. Azevedo," Observed Flow Reversals and Measured-Predicted Nusselt Numbers for Natural Convection in a One-Sided Heated Vertical Channel", ASME J. Heat Transfer, Vol.106, pp. 325-332, 1984.

20. T. Burch, T. Rhodes, and S. Acharya," Laminar Natural Convection Between Finitely Conducting Vertical Plates", Int. J. Heat Mass Transfer, Vol.28, pp. 1173-1186, 1985.

21. L.F.A. Azevedo and E.M. Sparrow," Natural Convection in Open-Ended Inclined Channels", ASME J. of Heat Transfer, Vol.107, pp. 893-901, 1985.

22. H.M. Joshi," Transient Effects in Natural Convection Cooling of Vertical Parallel Plates", Int. Comm. Heat Mass Transfer, Vol.15, pp. 227-238, 1988.

23. T.S. Chang, and T.F. Lin," Transient Buoyancy-Induced Flow Through a Heated Vertical Channel of Finite Height", Numerical Heat Transfer, part A, Vol.16, pp. 15-35, 1989.

24. M.A.I. El-Shaarawi and A. Sarhan,"Developing Laminar Free Convection in an Open-Ended Vertical Annulus with a Rotating Inner Cylinder",ASME J. Heat Transfer, Vol 103,pp. 552- 558,1981.

25. M.A.I. El-Shaarawi and A. Sarhan," Developing Laminar Free Convection in a Heated Vertical Open-Ended Concentric Annulus", Ind. Eng. Chem. Fundam, Vol.20, pp. 388-394, 1981.

26. A. Sarhan," Developing Laminar Convection in the Free and the Mixed Regimes in Vertical Concentric Annuli with Stationary or Rotating Inner Walls", Ph.D. Thesis, Mechanical Engineering Department, Al Azhar University, Nasr City, Cairo, Egypt. (1981).

27. M. Keyhani, F.S. Kulacki and R.N. Christensen," Free Convection in Vertical Annulus with Constant Heat Flux on The Inner Wall", ASME J. Heat Transfer, Vol.105, pp. 454-459,1983.

28. D. Littlefield, and P. Desai," Buoyant Laminar Convection in a Vertical Cylindrical Annulus", ASME J. Heat Transfer, Vol.108, pp. 814-8219, 1986.

29. M. Al-Arabi, M.A.I. El-Shaarawi and M. Khamis," Natural Convection in Uniformly Heated Vertical Annuli", Int. J. Heat Mass Transfer. Vol.30, pp. 1381-1389, 1987.

30. M.A.I. El-Shaarawi, and M.A.Al-Nimr," Fully Developed Laminar Natural Convection in Open-Ended Vertical Concentric Annuli", Int. J. Heat Mass Transfer, Vol.33, pp. 1873-1884, 1990.

31. M.K. Alkam," Transient Forced Convection in the Developing Region of a Concentric Annulus", M.S. Thesis, Mechanical Engineering Department, Jordan University of Science and Technology, Irbid,Jordan, 1990.

32. M.A.I. El-Shaarawi," Derivation of Boundary Layer Equations for Cases with Curved Boundaries", Int. J. of Engineering Fluid Mechanics, Vol. 3, pp. 113-128, 1990.

33. L. Lapidus,"Digital Computation for Chemical Engineers",pp. 254-255 ,McGraw Hill ,1962.

34. B. Carnahn, H.A. Luther and J.o. Wilkes,"Applied Numerical Methods" ,pp. 449-475,John Wiley,1969.